2008

Composite Membranes for Proton Exchange Membrane Fuel Cells

Jinjun Shi
Wright State University

Composite Membranes for Proton Exchange Membrane Fuel Cells

A dissertation submitted in partial fulfillment of the
requirements for the degree of
Doctor or Philosophy

By

Jinjun Shi
M.S., Tongji University, 2003

_____
(Signature of Student)

2008
Wright State University

WRIGHT STATE UNIVERSITY

SCHOOL OF GRADUATE STUDIES

February 27, 2008

I HEREBY RECOMMEND THAT THE DISSERTATION PREPARED UNDER MY SUPERVISION BY **Jinjun Shi** ENTITLED **Composite Membranes for Proton Exchange Membrane Fuel Cells** BE ACCEPTED IN PARTIAL FULFILLMENT OF THE REQUIREMENTS FOR THE DEGREE OF **Doctor of Philosophy.**

_____
Bor Z Jang, Ph.D.
Dissertation Director

_____
Ramana V. Grandhi, Ph.D.
Director, Ph.D. in Engineering Program

_____
Joseph F. Thomas Jr., Ph.D.
Dean, School of Graduate Studies

Committee on Final Examination

_____
Bor Z Jang, Ph.D.

_____
Sharmila M. Mukhopadhyay, Ph.D.

_____
Henry Daniel Young, Ph.D.

_____
Eric A. Fossum, Ph.D.

_____
Terry Murray, Ph.D.

Abstract

Jinjun Shi, Ph.D., Department of Mechanical and Materials Engineering, Wright State University, 2008. “Composite Membranes for Proton Exchange Membrane Fuel Cells.”

Proton exchange membrane fuel cells (PEMFCs), often regarded as a green energy source, have become a promising candidate to replace traditional power sources. One of the obstacles toward commercialization of PEM fuel cells is lack of high performance and low cost proton exchange membranes. The objective of this study was to develop and evaluate higher-performance, Nafion-based composite proton exchange membranes that are suitable for operating at higher temperatures (> 85ºC).

Proton exchange membranes were prepared by adding silica and heteropolyacids (HPAs) to a proton-conducting polymer matrix, Nafion. The added silica powder particles, either by direct mixing or sol-gel reaction, were found to enhance the thermal stability and lower thermal expansion of the composite membranes. Incorporating HPAs into Nafion greatly increased the proton conductivity of Nafion and the single cell performance was also greatly improved. In order to prevent HPA leaching, Y zeolite was used to encage HPA molecules inside its supercages. A templating mechanism was also used to trap HPAs with silica gels. Membranes and membrane-electrode assemblies (MEAs) with encaged HPAs were studied in light of HPA’s effects on the proton conductivity, thermal stability, thermal expansion coefficient, single cell performance, micro-morphology (SEM), and acid leaching. A nonelinear equation from fitted

experimental data was proposed to model the relationship between proton conductivity and the acid doping level. The results showed that Y zeolite and silica gel can be used to prevent HPA from leaching by water. In order to increase the mechanical properties and water uptake properties, hydrophilic, expanded PTFE (ePTFE) was used as the scaffold material for PEM.

TABLE OF CONTENTS

LIST OF FIGURES

LIST OF TABLES

1. Introduction

1.1 History of fuel cells

Fuel cells are electrochemical devices that can convert chemical energy into electrical energy. The concept of fuel cell was first proposed by Swiss scientist Christian Friedrich Schönbein in 1839 while the first fuel cell was designed by Sir William Grove in 1839[1]. Grove's fuel cell is shown in Fig 1-1. Grove's experiment was inspired by the idea of electrolyzing water to generate hydrogen and oxygen. By reversing the electrolysis setup, Grove was able to generate current flow between two platinum electrodes.

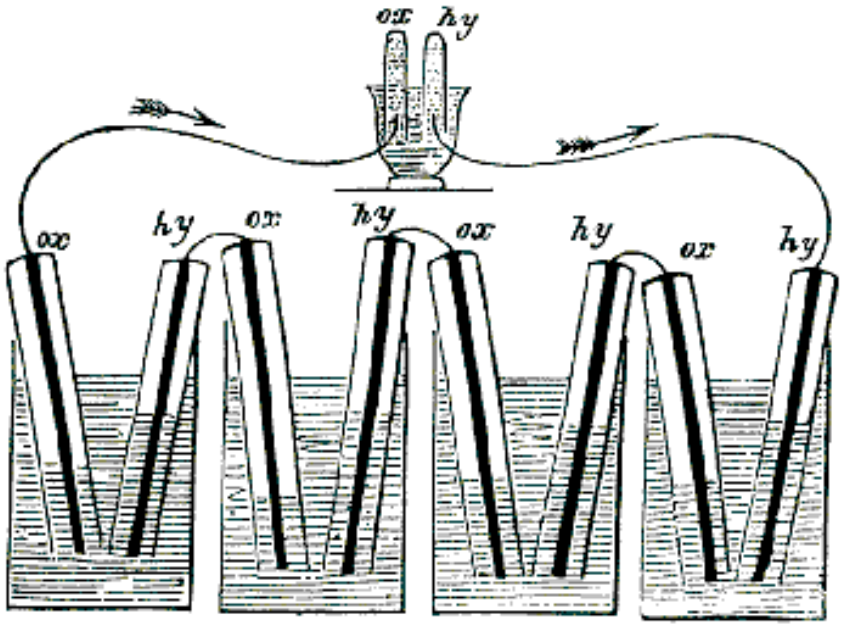

Fig 1-1. Grove's fuel cell [1]

The first practical fuel cell was developed by Charles Langer and Ludwig Mond in 1989 and coal gas and air were used as the reactant gases [2]. In 1939, Francis Thomas Bacon modified Langer & Mond's fuel cell design and used nickel to replace platinum as the electrode material. A 5 kW-fuel cell stack was demonstrated by Bacon in 1959 which had an efficiency of 60%. Bacon's fuel cell, which can be regarded as the first generation of alkaline fuel cell, was later on used for Apollo space vehicles of the United States.

1960s can be regarded as the starting time of the development of modern fuel cells. The National Aeronautics and Space Administration (NASA) was looking for a compact and light weight power source for its space missions. Batteries were not suitable for that application because of the weight and size restrictions. In order to solve this problem, Willard Thomas Grubb and Leonard Niedrach, two scientists from General Electric (GE), developed the first generation proton exchange membrane (PEM) fuel cell and used that for NASA's Project Gemini. After that, GE continued working on PEM fuel cells and GE's fuel cells was used by US Army and US Navy Bureau of Ships. At that time, the main difficulty for fuel cells was the membrane degradation problem.

The discovery of Nafion®, which was developed in 1960s by Walther Grot of DuPont de Nemours, was one of the milestones of fuel cell history. Nafion has excellent proton conductivity, thermal and chemical stability, and also high mechanical strength. Even after more than forty years from the birth of Nafion, it is still the material-of-choice for low temperature PEM fuel cells at this time[3, 4].

In the past 10-20 years, a lot of research work has been done on the materials development and system design for fuel cells. One of the noteworthy achievements was Ballard's first generation fuel cell powered vehicle in 1993. Nowadays most of the auto

makers are developing fuel cell powered cars and some of the prototypes have already been demonstrated on the road. Fuel cell systems targeted at portable applications have also been developed and commercialized.

1.2 Benefit of fuel cells

Fuel cells are called clean energy or green energy because of their low pollution, low emission, and quite operation. For PEM fuel cells, the reactants are hydrogen and oxygen, and water is the only product which is totally harmless to the environment.

Compared to traditional power sources such as combustion engines, the efficiency of fuel cells are much higher, especially at low temperature range [5]. The efficiency of combustion engines are limited by the Carnot's Law and a good amount of the energy is lost in the form of heat or friction during mechanical motion.

As it can be seen from *Table 1-1*, all fuel cells do not release harmful products to the environment. While one of the emission gases from internal combustion is NOx, which is the major source of photochemical smog. Using hydrogen fuel cells can greatly reduce the release of natural greenhouse gas into the atmosphere, which helps to relieve the atmosphere temperature increase on the earth [6].

Table 1-1. Comparison of emission between fuel cells and internal combustion engines

Type of power source	Emission content	Emission harmful?
SOFC	H_2O	No
MCFC	CO_2+H_2O	No
PAFC	H_2O	No
AFC	H_2O	No
PEMFC	H_2O	No
DMFC	CO_2+H_2O	No
Internal combustion engine	NOx+H_2O+CO_2	Yes

1.3 Types of fuel cells

There are several ways to classify the current available fuel cells. Based on the electrolyte material, fuel cells can be classified into solid oxide fuel cells, molten carbonate fuel cells, phosphoric acid fuel cells, alkaline fuel cells, proton exchange membrane fuel cells, and direct methanol fuel cells. When the working temperature is concerned, fuel cells can be classified into low-temperature fuel cells (PEMFC & DMFC), medium-temperature fuel cells (AFC & PAFC), and high-temperature fuel cells (SOFC & MCFC). The operating condition and application field of different fuel cell types are summarized in *Fig 1-2* and *Table 1-2*.

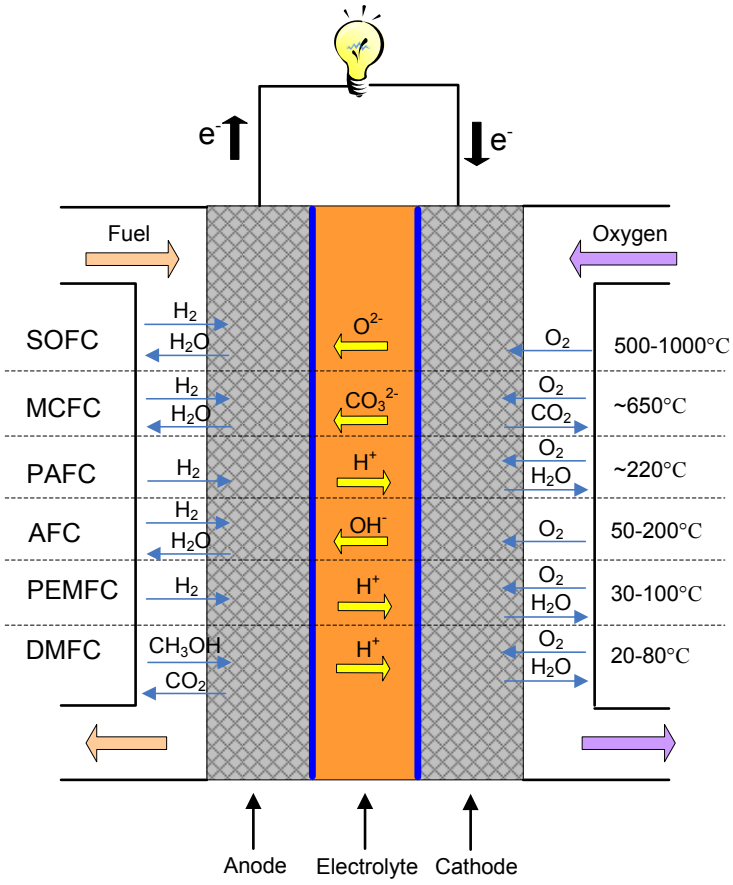

Fig 1-2. Major types of fuel cells

Table 1-2. Characteristics of different types of fuel cells [5, 7]

	Electrical Efficiency (%)	Power Density (mW/cm^2)	Internal Reforming	Power Range (kW)	Application Range
SOFC	50-60	250-350	Yes	10-100000	All sizes of CHP systems
MCFC	45-55	100-300	Yes	100-100000	Dedium to large-scale CHP systems
PAFC	40	150-300	No	50-1000	Stationary power source
AFC	50	150-400	No	1-100	Space and military applications
PEMFC	40-50	300-1000	No	0.001-1000	Mobile and portable applications
DMFC	15-25	30-160	No	<0.25	Portable applications

1.4 Proton exchange membrane fuel cells

Proton exchange membrane fuel cell, also called polymer electrolyte fuel cell, is a type of low temperature fuel cell aimed at mobile and portable applications because of the simplicity in structure and fast start up. For this type of fuel cell, a solid ionic polymer membrane is used as electrolyte material and carbon-supported platinum is usually used as catalyst. The proton exchange membrane separates the anode and cathode and conducts the protons generated at the anode side. Hydrogen fuel is fed into the anode side and split into protons and electrons, and electrons go through the external circuit and protons cross the PEM to the anode side. The oxidant, usually oxygen or air, is fed into the cathode size and reacts with protons and generates water. The reactions for PEM fuel cells are:

Anode: $H_2 \xrightarrow{Pt} 2H^+ + 2e^-$

Cathode: $\frac{1}{2}O_2 + 2H^+ + 2e^- \xrightarrow{Pt} H_2O$

Overall: $H_2 + \frac{1}{2}O_2 \xrightarrow{Pt} H_2O$

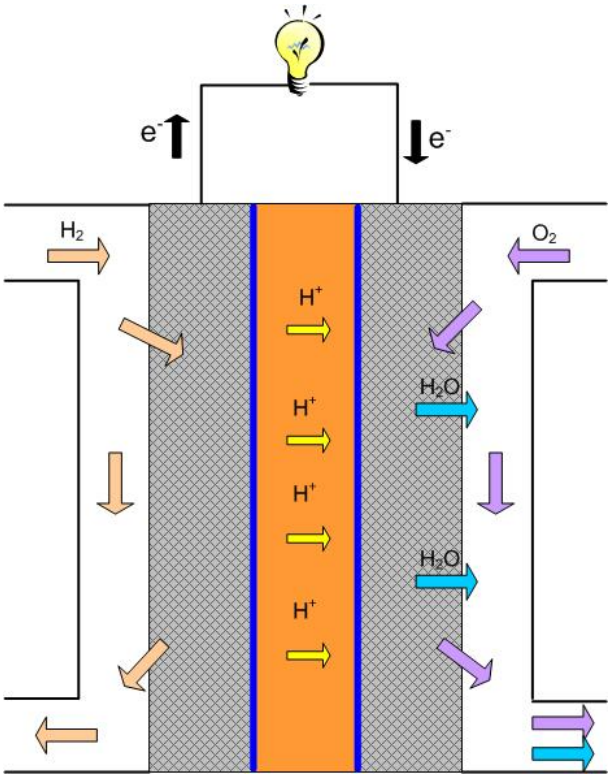

Fig 1-3. Schematic of proton exchange membrane (PEM) fuel cells

Currently PEM fuel cells are the most studied fuel cells because of the simple structure and wide application range. Many prototype PEM fuel cell based battery chargers, fuel cell engines, and portable power source are available, and the major auto makers are planning to release fuel cell powered hybrid vehicles into the markets. But there are still some barriers toward the commercialization of PEM fuel cells:

Cost. Cost is always the final factor for a product to enter the market. Currently the majority of the cost of PEM fuel cells comes from the platinum catalyst and proton exchange membrane.

Hydrogen storage. Hydrogen is a low density and combustible gas. Many new materials, such as carbon nanotubes, are reported to have hydrogen storage capability [8-10], and metal hydride can be used to storage hydrogen at low pressure [11-14]. But

when it comes to mobile applications, high-pressure hydrogen tank is still the only solution for hydrogen storage.

Water management. Water management is a very tricky process for PEM fuel cells. In order to better utilize the catalyst nano-particles on the electrode, the gas diffusion layer is expected to be hydrophobic so that the chemically generated water and humidity in the reactant gas won't block the micro-pores inside it. While on the other side, the proton conductivity of the PEM heavily relies on the water content inside the membrane. So keeping the water content in the PEM, especially near the anode side, at higher temperature and lower humidity level conditions is the most challenging task for PEM materials research.

There are some general requirements for PEMs:

High proton conductivity, which intends to reduce ohmic loss inside the fuel cells. Good water retention capability. As proton conductivity heavily relies on water molecules [15-17], the water content inside PEMs is essential for their proton conductivity.

Good mechanical strength. Generally speaking, PEMs do not take a lot of load during fuel cell operation so the requirement for their mechanical strength is not critical. But the bottom line is the ability to withstand the hot-pressing process during MEA fabrication.

Low fuel permeability in order to maximize coulombic efficiency[18].

Good dimensional stability. Compared to gas diffusion layers, the PEMs have much higher swelling ratio and the ratio changes along with the relative humidity

fluctuation. A high dimensional stability helps maintain the integral structure of the membrane electrode assembly (MEA).

Good chemical and thermal stability. The PEM should not degrade or lose performance under the normal fuel cell operating conditions.

Low cost. The cost of PEM is one of the key factors for fuel cell commercialization. Fuel cells won't take the place of traditional power sources until its price is comparable or even lower than internal combustion engines.

Environmental considerations. Fuel cells by themselves are called clean power sources, but it is important that there are no environmentally detrimental processes or byproducts generated during the manufacturing process of fuel cells.

1.5 Scope of research

The purpose of this study is to develop and study Nafion-based composite membranes for PEM fuel cell applications. The developed membranes will be studied and compared to recast Nafion in terms of proton conductivity, thermal stability, activation energy, micro-morphology, thermal expansion, and single cell performance. One important task of this study is to investigate the HPA trapping in Y zeolite and silica gel and their application to PEM. An experimental equation will be developed to study the relationship between acid doping level and proton conductivity.

2. Literature review

2.1 Benefits of higher working temperature

Recent research on PEM fuel cells has been more on working at higher temperatures (>85ºC) [19]. There are several benefits of running PEM fuel cells at higher temperatures: (1) higher proton conductivity at the same relative humidity level, (2) better water management, (3) improved catalyst tolerance to fuel impurities, (4) faster electrode kinetics, and (5) simpler cooling system structure.

The proton conductivity of PEM is closely related to temperature and most proton conductive materials follow Arrhenius behavior [20]. Fig 2-1 is the Arrhenius plot of composite Nafion membrane with 3% TEOS at 95% relative humidity level. In this aspect, it is preferable to have the fuel cells work at higher temperatures.

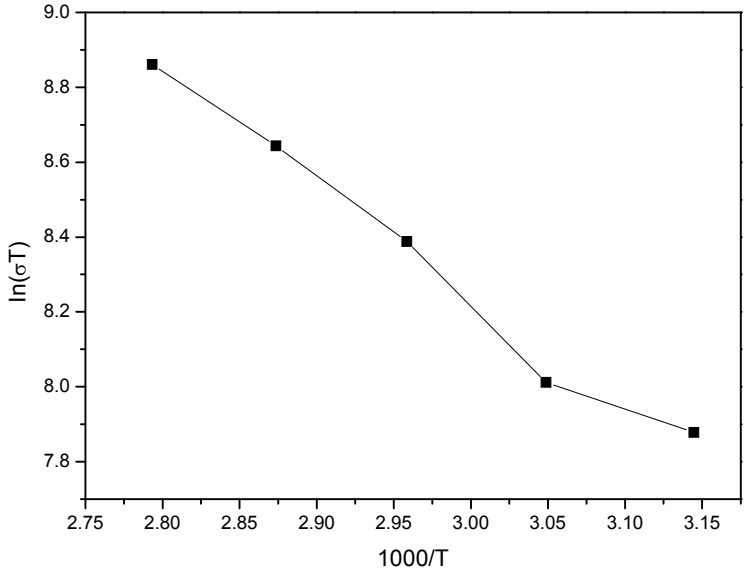

Fig 2-1. Arrhenius plot of Nafion with 3% TEOS at 95% relative humidity (this work)

The activation energy loss can be calculated by the following equation [5]

$$\Delta V_{act} = \frac{RT}{2\alpha F} \ln\left(\frac{i}{i_0}\right)$$

Where i_0 is exchange current density, R is universal gas constant, F is Faraday constant, and α is the charge transfer constant. With the increase in temperature, the effect of i_0 dominates so the activation energy is greatly reduced.

Water plays an important role in PEM fuel cells. Usually the reactant gas is humidified before reaching fuel cell electrodes. The water content in the reactant gas helps keep the moisture inside the fuel cell membrane and thus maintain good proton conductivity. But as proton migrate from anode to cathode, each proton will drag about 2.5 water molecules to the cathode side [21]. The cathode reaction will also generate water continuously at the cathode side during fuel cell operation. Too much water will block the pores inside the gas diffusion layer and decrease the fuel cell performance. This is called electrode flooding [22, 23]. The electrode flooding is more serious in fuel cell stacks as the high power output will generate more water at the cathode side. In order to avoid the flooding phenomena, a fuel cell stack needs to be well engineered so that water inside the fuel cell can reach a balanced state.

Ideally the effect of catalyst won't decrease with time if pure hydrogen and oxygen is used as the reactants. But pure hydrogen will be too expensive for fuel cell applications. From industrial point of view, fuel reforming is the way for large-scale low cost hydrogen production. If steam reforming is used to generate hydrogen, the reaction follows the equations below [5]:

$$C_nH_m + nH_2O \rightarrow nCO + (\frac{m}{2} + n)H_2$$
$$CO + H_2O \rightarrow CO_2 + H_2$$

The carbon monoxide/water reaction is called water-gas shift reaction. Thermodynamically the water-gas shift reaction can proceed in either direction and it leads to the result that certain carbon monoxide will be left in the final hydrogen gas. The carbon monoxide can have a poisonous effect on platinum catalyst as it can strongly adsorb on the surface of platinum and prevent hydrogen and oxygen from reaching the catalyst (Fig 2-2). To relieve this poisoning effect, either extra hydrogen purification or CO-tolerant electrocatalyst should be applied. Some research work has been done to study the poising effect of CO on Pt catalyst for fuel cell applications [24]. As the adsorption of CO on Pt has a negative enthalpy, so by elevating the temperature can greatly reduce the poisoning effect [25, 26]. If reformed hydrogen can be used for PEM fuel cells without the need of extra purification, the potential operating cost of fuel cells will be greatly reduced.

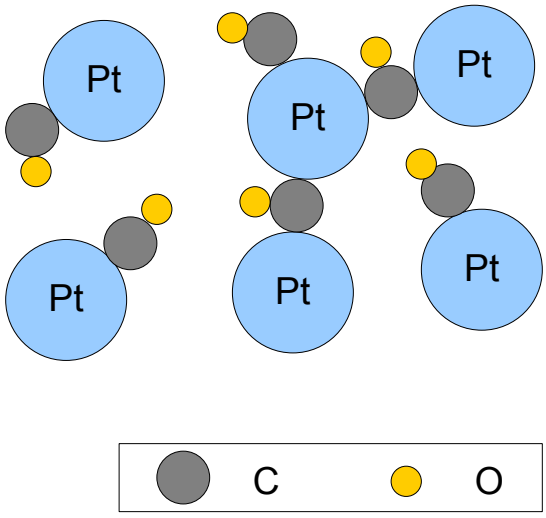

Fig 2-2. Schematic of Pt catalyst poisoning by carbon monoxide

2.2 Water management

It has been reported by Zawodzinski [21] that each transported proton can drag about 2.5 water molecules for fully hydrated Nafion 117 at room temperature. Based on the fact that water molecules dragged by other ions are much more than protons, Zawodzinski suggested that most proton conduction in proton exchange membrane can be contributed by Grotthuss mechanism [15, 16].

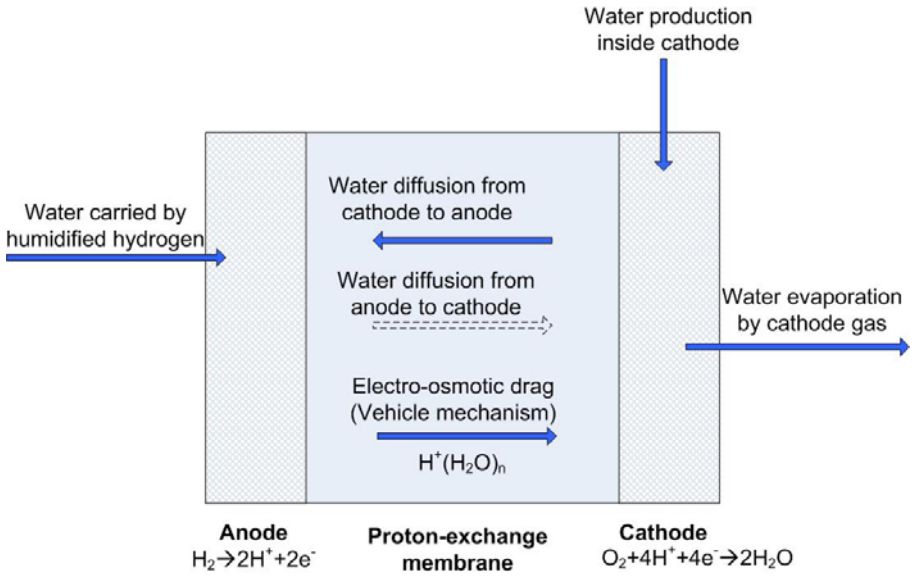

Fig 2-3. Schematic of water manage in PEM fuel cells [5]

The relationship of λ (ratio of the number of water molecules to the number of SO_3H^+) at 30 ºC was fitted from experimental data [27]:

$\lambda = 0.043 + 17.81a - 39.85a^2 + 36.0a^3$ for $0 < a \leq 1$, where a is the water vapor activity (P_w/P_{sat})

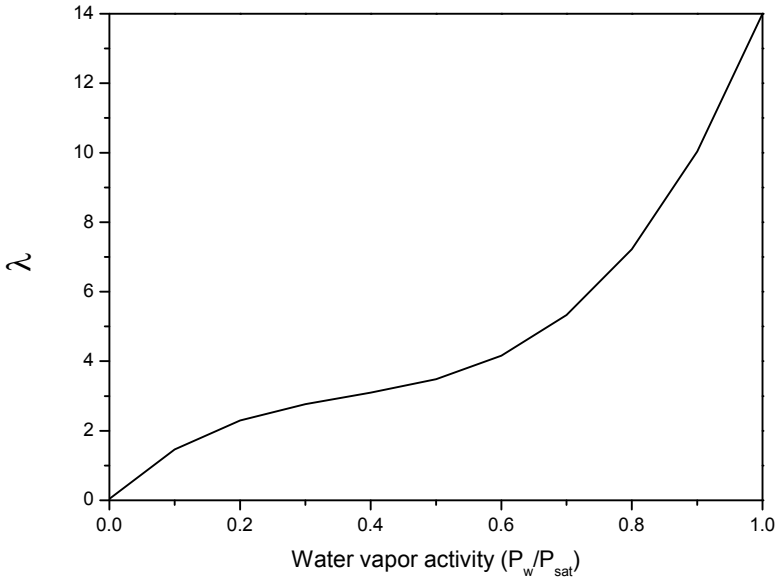

Fig 2-4. Water content vs. water activity of Nafion 117 at 30ºC [27]

2.3 Status of proton exchange membrane materials

2.3.1 PFSA membranes

Perfluorosulfonic acid (PFSA) is currently the most widely used membrane material for proton exchange membrane fuel cells. PFSA membranes have good mechanical strength, high proton conductivity, and chemical and thermal stability. The commercial PFSA membranes include DuPont's Nafion, Asahi Glass's Flemion, Asahi Chemical's Aciplex, Dow Chemical membrane, and Golden Energy's GEFC, etc.

Among all those PFSA membranes, Nafion is the most studied one. Nafion was developed by Dupont de Nemours in late 1960s and it showed surprisingly high ionic conductivity and durability. As almost the only commercial proton exchange membrane for decades, a lot of research work has been done to study Nafion's structure [28-34], proton conducting mechanism [35-41], physical and chemical properties [42-45], computational modeling [46-48], and composite membranes [49-55] as well. Currently

almost all the commercial PEM fuel cells and stacks are still using Nafion as the PEM material.

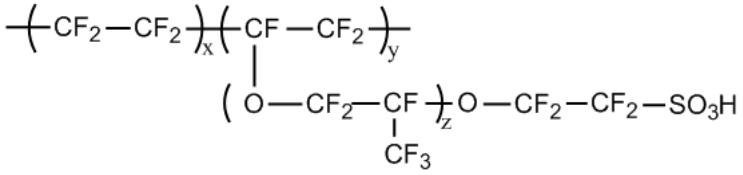

Fig 2-5. Structure of Nafion

To better understand the high proton conductivity of Nafion ionomer, researchers have done a lot of work on ion-exchange membrane models. Gierke et al. [28, 37, 56] proposed a famous Cluster-network model in early 1980s based on small-angle X-ray study. This widely accepted model describes the structure of Nafion as dispersed ionic clusters in a fluorocarbon matrix. The clusters are approximately spherical with a diameter of ~40Å, and connected by short channels. Water absorbed by the membrane only stays inside the ionic clusters and contributes to the proton conductivity. Gierke and Hsu [37] used percolation theroy to study the proton conduction mechanism with the cluster-network model: $\sigma = \sigma_0 (c - c_0)^n$, where c is the volume fraction of the aqueous phase, c_0 is the threshold volume fraction (15% for 3D, continuous and random structure), n is a constant (1.5 for 3-dimensional systems), and σ_0 is a prefactor. Choi [57] proposed a cylindrical pore model which divides the ionic pores into surface diffusion region and bulk diffusion region. The total proton conductivity is the combination of surface diffusion, Grotthuss mechanism, and *en mass* diffusion. The porosity, volume

fraction of water content, tortuosity, diffusion coefficients, and proton distributions are considered as the main factors that affect the total proton conductivity.

A lot of efforts have been made to improve Nafion's performance at high temperature and low humidity conditions. Watanabe [58-60] developed a series of self-humidifying PEMs by adding nanoscale Pt and metal oxide particles into Nafion. The Pt particles inside the membrane can promote the reaction between hydrogen and oxygen that diffuse into the membrane into water, which can humidify the membrane and help the cold start of the fuel cell. And the dispersed metal oxide nanoparticles (SiO_2, TiO_2) can absorb water molecules which also help to maintain the water content inside the membrane. Antonucci[51] studied the effect of incorporating silica nanoparicles into Nafion membrane to improve the water retention capability at higher temperatures. A DMFC with the silica-based composite membrane showed a peak power density output of 240 mW/cm^2 at 145ºC. As it is very hard to fully disperse nanoparticles into PEM, sol-gel technique [53, 54, 61, 62] has been used to incorporate oxide nanoparticles into PEM. By using the sol-gel method, the reaction parameters (pH level, temperature, duration, et al.) need to be well designed to avoid too much oxide particles covering the surface of the membrane.

One way of improving the high temperature performance of Nafion is to incorporate solid proton conductors. Heteropolyacids (HPAs) are the most solid proton conductive materials and a lot of effort has been applied on developing Nafion/HPA composite membranes. Tian [63] studied the effect of adding silicotungstic (STA) into Nafion and tested the fuel cell performance up to 110ºC. It was found that the

HPA/Nafion composite membrane showed better proton conductivity and thermal stability.

Microporous PTFE substrate has been used to increase the mechanical properties of Nafion membrane [64-66]. The expanded PTFE can have porosity up to 90% and the interconnected micro pores can form a continuous percolating pathway for Nafion ionomer. The PTFE reinforced composite membranes also show better thermal stability and dimensional stability. Thanks to the excellent mechanical strength of the expanded PTFE, the composite membranes can be made much thinner than pure Nafion membrane and the corresponding area conductivity (mS/cm^2) can be lower than that of Nafion. But because of the strong hydrophobicity of PTFE, it has been very difficult to fully impregnate Nafion resin into the micropores of ePTFE [65, 67]. The voids inside the composite membrane can cause lower proton conductivity and also form a continuous pathway for reactant crossover. To overcome this problem, the ePTFE can be surface treated with sodium-naphthalene [68], plasma [69-71], and molecular grafting [72]. The surface treated ePTFE based composite membranes showed higher Nafion resin uptake and lower gas permeability than hydrophobic ePTFE base membranes. Some researchers also tried to incorporate oxide nanoparticles and Pt nanoparticles into the ePTFE/Nafion structure [73-77].

Another group of PFSA membranes is called short-side-chain (SSC) PFSAs which have the same backbone structure as Nafion except relatively shorter ionic side chains. This group of membranes includes Dow Ionomer by Dow Chemical, GEFC by Golden Energy, and Hyflon Ion [78, 79] by Solvay Solexis. If the same cluster-network model [37] is applied to the SSC ionomers, it is reasonable to expect different ionic

cluster size because the difference in side chain length. And because the side chains are shorter, the thermal properties, such as glass transition temperature Tg, can also be different from that of Nafion [80]. The Hyflon Ion membranes with low EW showed higher water uptake and fuel cell performance than Nafion 112.

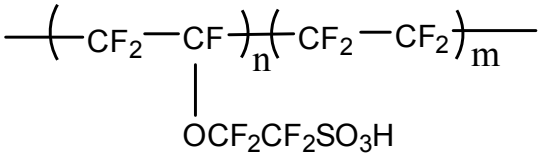

Fig 2-6. Chemical structure of Hyflon Ion [78]

Table 2-1. List of PFSA membrane materials [81, 82]

Manufacturer	Brand name	Side chain	EW ($g \cdot mol^{-1}$)	Conductivity ($S \cdot cm^{-1}$)	Life (h)	Water uptake (%)	Thickness (μm)	Price ($/m^2)
DuPont	Nafion	Long	1000-1200	0.05-0.20	>50000	34-37	50-260	500-800
Asahi Glass	Flemion	Long	800-1500	0.05-0.20	>50000	35	50-120	
Asahi Chemical	Aciplex	Long	800-1500	0.05-0.20	>50000	43	120	
Dow	Dow	Short	800-850	0.12-0.20	>10000	56	100	1700
Golden Energy	GEFC	Short	1000-1100	0.1(25ºC)		50	25.4-508	300-900
Gore and Associates	Gore-Select		900-1100	0.03-0.1	60000	32-43	12-20	

2.3.2 Hydrocarbon and aromatic membranes

Due to the drawbacks of PFSA membranes, a lot of effort has been focused on developing hydrocarbon based membranes. Compared to PFSA membranes, the hydrocarbon-based membranes are much less expensive and many polymers are already

commercially available. Because of the polar pendant groups, hydrocarbon-based membranes have higher water uptake, and they are more environmental friendly.

Hydrocarbon membranes lack thermal stability so aromatic groups are introduced into the backbone structure. As aromatic groups are more rigid than $-(CF_2)-$ groups which are found in PFSA membranes, aromatic membranes usually have much higher Tg than PFSA membranes [83]. The higher Tg value grants the possibility of working at higher temperatures, given with fair proton conductivity. The hydrocarbon polymers include SPEEK [84, 85], SPPESK[86, 87], Sulfonated polysulfone [88, 89], Sulfonated polystyrene [90, 91], Sulfonated polyimide [92-94], Sulfonated poly (arylene ether sulfone) [95-97], and Sulfonated polyacryls [98]. Some polymer structures are listed below:

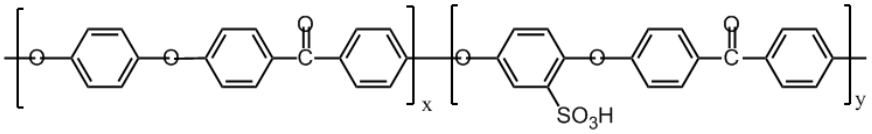

Fig 2-7. Chemical structure of SPEEK

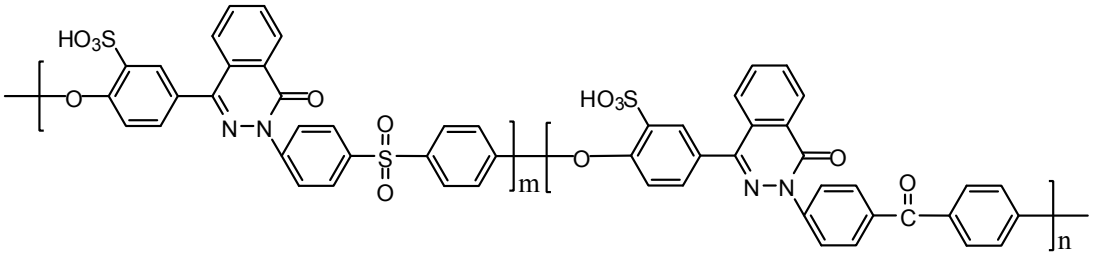

Fig 2-8. Chemical structure of SPPESK

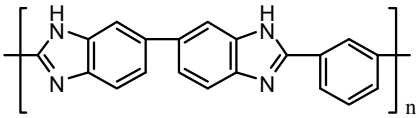

Fig 2-9. Chemical structure of PBI

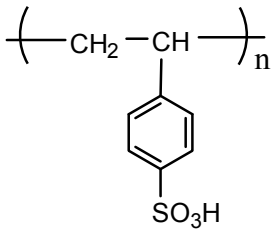

Fig 2-10. Chemical structure of Poly (styrene sulfonic acid)

The proton conductivity of hydrocarbon materials can be controlled by changing reaction parameters such as reaction time and temperature. Typically polymers with higher degree of sulfonation show higher proton conductivity, but the mechanical properties will be sacrificed and the polymer may even dissolve in water when the degree of sulfonation is too high. Kreuer's work [4] showed that hydrocarbon based membranes have narrower channels between polymer chains when compared to that of Nafion. The narrower channels can lead to lower fuel crossover, which is critical to direct methanol (DMFC) fuel cells. Most of the above mentioned hydrocarbon membranes heavily rely on water content to maintain proton conductivity.

In recent years, acid doped polybenzimidazole (PBI) has attracted more interest because of the ability to work at high temperature and low relative humidity conditions [99, 100]. PBI also has good mechanical strength and thermal stability which are necessary for high temperature proton conducting materials. The proton conductivity of PBI is related to the doping level and relative humidity. But unlike other low temperature PEM, the influence of relative humidity is not that critical and proton conductivity as high as 59mS/cm at 150ºC and 30% relative humidity has been reported on a PBI membrane with 630% doping level by Ma et al [100]. Li [101] claimed that the proton transfer inside an acid-doped PBI is mainly attributed to proton hopping between N-H

site and phosphoric acid. When the doping level is high, the proton hopping between phosphoric acid is also significant. Now some commercial PBI membranes have been available in the market. The main drawback of acid doped PBI is the leaching of H_3PO_4 at the presence of water, which will lead to the loss of conductivity.

2.4 Techniques for achieving higher working temperatures

Proton conductors can be roughly divided into two groups: (1) hydrous proton conductors, and (2) anhydrous proton conductors. Currently most proton conductors belong to hydrous proton conductors. Hydrous proton conductors rely on water for proton conduction and proton conduction can be explained by either Grotthuss mechanism [15, 16] or vehicle mechanism[17]. As most of these proton conductors lack the capability of holding water content at higher temperatures so the proton conductivity will decrease. For these materials, the proton conductivity at higher temperatures can be enhanced by adding hydrophilic filler materials. The water adsorbed on the fillers can help to keep proton conductivity level at higher temperatures. Anhydrous proton conductors do not rely on water for proton conduction so the working temperature could exceed 200ºC. The most extensively studied anhydrous proton conductor is H_3PO_4-doped PBI. The proton conductivity of H_3PO_4-doped PBI can be controlled by adjusting the acid doping level. PBI has a glass transition temperature up to 430ºC which makes it a superior candidate for high temperature applications. The main problem of H_3PO_4-doped PBI is acid leaching during fuel cell operation.

3. Nafion/silica composite membranes

3.1 Introduction

Based on the widely accepted Grotthuss mechanism [15, 16] and Vehicle mechanism [17], an effective way of promoting proton conduction is to increase water uptake. As many metal oxide nanoparticles are highly hydrophilic, some research work has been done to study the effect of adding metal oxide particles into Nafion and use the resulting composite membrane for fuel cell applications [50, 58, 102-104]. It was noticed that by incorporating silica and other oxide particles into PEM, the composite membranes showed higher water uptake and the better performance was observed on high temperature DMFCs. It is generally believed that the improvement in DMFC performance is caused by higher proton conductivity and lower methanol crossover. But, higher water uptake does not necessarily mean higher proton conductivity as not all the water absorbed by Nafion can take part in proton conduction [42]. While significant efforts have been made on developing different PEM/metal oxide composites for fuel cell applications, very few proton conductivity data is available on these membranes.

In order to achieve a comprehensive understanding of the effect of adding silica nanoparticles to the performance of Nafion membrane, both direct mixing method and in-situ reaction method were used in the present study. For the direct mixing method, the commercial hydrophilic fumed Aerosil 380 (Degussa) silica nanoparticles are used. The Aerosil 380 has very low particles size (7nm) and high specific surface area (BET surface

area = 380 m^2/g). Tetraethylorthsilicate is used in the sol-gel method to generate silica network in Nafion. The sol-gel reaction is:

$$Si(OC_2H_5)_4 + 2H_2O \rightarrow SiO_2 + 4C_2H_5OH$$

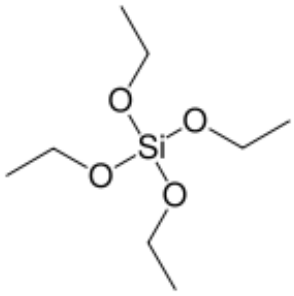

Fig 3-1 Structure of TEOS

3.2 Membrane preparation

3.2.1 Nafion/Aerosil 380 composite membrane

Firstly, 10% Nafion solution (Ion Powder) was mixed with a controlled amount of DMAc (N,N-Dimethylformamide, BASF). The amount of Aerosil 380 was controlled such that the silica weight in the three dry membrane samples are 1%, 3%, and 5% respectively. The mixture was heated to 50ºC with continuous stirring until the water and alcohol content in the original Nafion solution was evaporated and the original Nafion solution was changed to DMAc-based solution. The DMAc-based Nafion solution was then mixed with a predetermined amount of Aerosil 380 powder to form a suspension. The suspension was stirred at room temperature with a magnetic stir bar for 2 hours, followed by sonication in an ultrasonic bath for at least one hour. After that, the solution was poured onto a glass plate which was leveled inside a vacuum oven. The samples were dried in vacuum at 70ºC overnight and annealed at 140ºC for one hour to increase

the mechanical strength. The dry membranes were peeled off from the glass plates by soaking in distilled water for several minutes. The membrane samples were then treated in boiling 3% H_2O_2 (Fisher) for 1 hour to remove organic impurities and then treated in 0.5M H_2SO_4 solution (Fisher) for another hour to remove trace metal impurities and fully protonize the membrane. The treated membrane samples were then rinsed in boiling distilled water to remove the excess acid. After that, the membrane samples were stored in a plastic sample bag until use.

3.2.2 Nafion/TEOS composite membrane

To prepare Nafion/TEOS composite membranes, the 10% Nafion solution (Ion Power) was transferred into DMAc (BASF) based solution and the water and alcohol content were removed at 50ºC. The DMAc-based Nafion solution was then cooled to room temperature and a predetermined amount of TEOS (tetraethoxysilane, Alfa Aesar) was added such that the final silica contents in the dry membrane were 1%, 3%, and 5%, respectively. A few droplets of dilute hydrogen chloride solution were added to promote the hydrolysis ($SiOH_2^+ \underset{OH^-}{\overset{H_3O^+}{\rightleftarrows}} SiOH \underset{H_3O^+}{\overset{OH^-}{\rightleftarrows}} SiO^-$ [104]). The solution was stirred at room temperature for 1 hour and casted on a glass plate which was leveled inside a vacuum oven. The casted membranes were dried in vacuum at 70ºC overnight and then annealed at 140ºC for one hour. The dry membranes were peeled off from the glass plates by soaking in distilled water for a few minutes. Again, the membranes were boiled in 3% H_2O_2 and 0.5M H_2SO_4 for one hour respectively and rinsed with distilled water. The treated membranes were stored in plastic sample bags until testing.

3.3 Materials characterization

3.3.1 Proton conductivity and water uptake

A four-probe conductivity cell was used to measure the proton conductivity. The proton conductivity cell has four platinum electrode supported on a PTFE frame. During testing, the conductivity cell was placed in a humidity chamber (ESPEC, SH-241). A Keithley 2400 source meter was used to supply current and measure voltage. At each temperature/humidity level, the membrane was conditioned for at least 30 minutes or until equilibrium before measurement. Each conductivity data comes from a linear regression of several current/voltage data pairs. The dimension of the membrane samples used for conductivity calculation was measured at dry state.

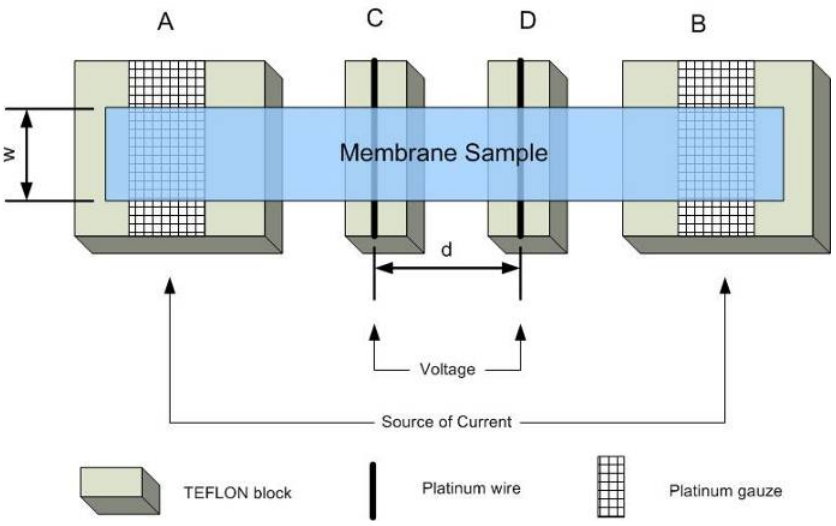

Fig 3-2. Four-point proton conductivity cell

The proton conductivity was calculated by

$$\sigma = \frac{1}{\rho} = \frac{d}{RS} = \frac{R}{R \cdot w \cdot t}$$

Where t is the average thickness of the membrane, R is the resistance which can be got by a linear fit of the U-I curve, w is the sample width, and d is the distance between two inter electrodes.

3.3.2 Single cell performance

The single cell performance was performed on a fuel cell test station (PD50, Asia Pacific Fuel Cell Technology) which is equipped with Chroma 63103 DC electronic load.

The membrane sample was first boiled in 3% H_2O_2 for one hour to remove organic impurities, followed by rinsing in DI water. After that, the membrane was boiled in 1M H_2SO_4 for another half an hour to remove metallic impurities and fully exchange the membranes into proton form.

A commercial gas diffusion electrode material (GDE, E-TEK Inc) with a Pt catalyst loading of 0.5mg/cm^2 was used to prepare the membrane electrode assembly (MEA). The electrode was impregnated with about 0.6mg/cm^2 Nafion (dry weight, 5% Nafion solution, Ion Power) and dried at 100ºC. The GDE and membrane were sandwiched between two PTFE sheets and hot pressed into a MEA at 130ºC under a pressure of 70kg/cm^2 for three minutes. The MEA was installed into a single cell (Fuel Cell Technologies) and the whole fixture was setup on the fuel cell test station. The MEA was conditioned by humidified H_2/O_2 at an open circuit state for 2 hours before testing.

3.3.3 Membrane surface morphology

The surface morphology of the prepared samples was examined by scanning electron microscopy (SEM, JEOL Field Emission Scanning Electron Microscopy, JSM-7401F).

3.3.4 Thermal properties

In order to study the thermal stability of the prepared composite membranes, thermalgravimetric analysis (TGA) was carried on a TA Instruments Q500 instrument. The dry membrane samples were heated from room temperature to 600ºC at a ramping rate of 10ºC/min under nitrogen atmosphere.

The glass transition temperature (Tg) and thermal expansion properties of the membranes were studied by a thermomechanical analyzer (TMA Q400, TA Instruments). The samples were cut into 1cm ×2cm pieces and tested using film/fiber probe with 0.075N force load. The samples were tested with a 10º/min heating rate and a nitrogen flow rate of 50ml/min.

3.4 Results and discussion

3.4.1 Proton conductivity and water uptake

It can be seen from the proton conductivity plot that by embedding Aerosil 380 silica nano-particles in a Nafion membrane, the proton conductivity of the membrane decreased. And, along with the increase in silica loading, the proton conductivity decreased accordingly. As water adsorbed on the surface of metal oxides can be hydrozylated [105], many metal oxides have an ion-exchange capability. It has been studied by Tamura et al that [106] the surface density of hydroxyl sites are similar for

different metal oxides, and the measured hydroxyl site density of SiO_2 was 0.954-1.80×10^{-5} mol·m^{-2}. The hydrozylation will somewhat contribute to the conductivity of the Nafion/silica composite membrane and the total contribution will depend on the total surface area of the silica particles or clusters. But, as metal oxides are themselves not proton conducive, so the total contribution of silica to conductivity could be negative. It can be seen from Fig 3-3 that, adding Aerosil 380 into Nafion leads to decreased proton conductivity. The proton conductivity decreases when the silica loading increases.

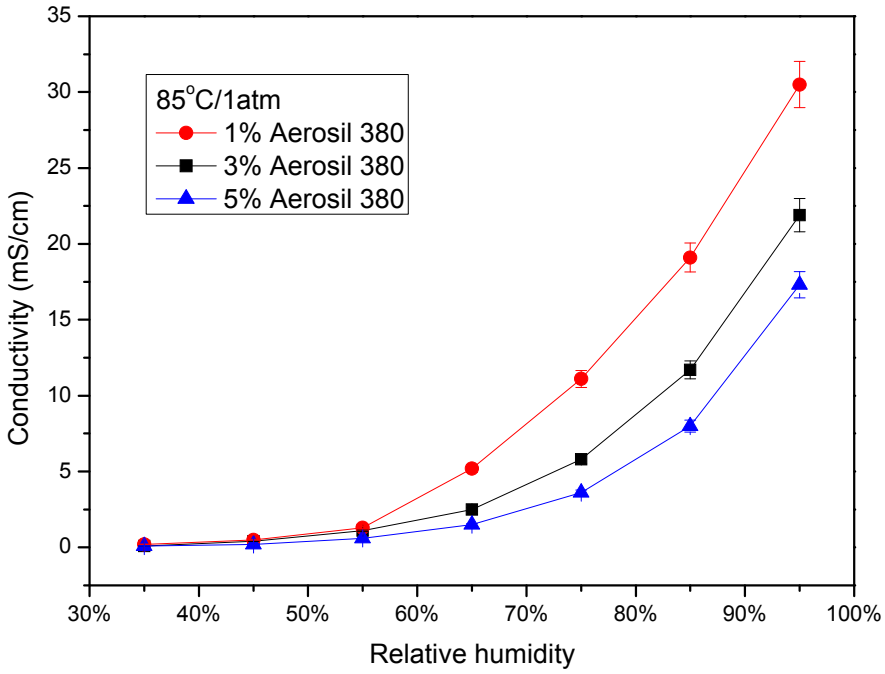

Fig 3-3. Proton conductivity of Nafion/Aerosil membranes at 85ºC

In order to solve the problem of silica agglomeration, recast membranes made from Nafion solution and TEOS were prepared. By using the sol-gel reaction, silica network was uniformly distributed throughout Nafion and no large clusters were observed on the surface under SEM. As for the proton conductivity, membranes with 1%, 3%, and 5% silica loadings showed about exactly the same proton conductivity at 60ºC.

However, when temperature was raised to 85ºC, membranes with higher silica loading showed better performance. The improved proton conductivity could be explained by the hydrophilic nature of well-dispersed silica nanoparticles generated by sol-gel reaction. Furthermore, from the conductivity data, the performance of water retention by silica nanoparticles is more effective at higher temperatures. Based on small angle X-ray scattering (SAXS), membranes with silica nanoparticles can support larger water clusters and lead to better proton conductivity at higher temperatures [107]. But Miyake [53] suggested that the water molecules in the membrane are likely to be attracted by silica and not taking part in the proton conduction. Due to instrument limitation, proton conductivity was not tested at temperatures higher than 85ºC. But better proton conductivity is expected for Nafion/TEOS membranes at elevated temperatures. It was reported elsewhere [49, 108] that the incorporated silica nanoparticles by sol-gel reaction can reduce methanol crossover, which is important for direct methanol fuel cells.

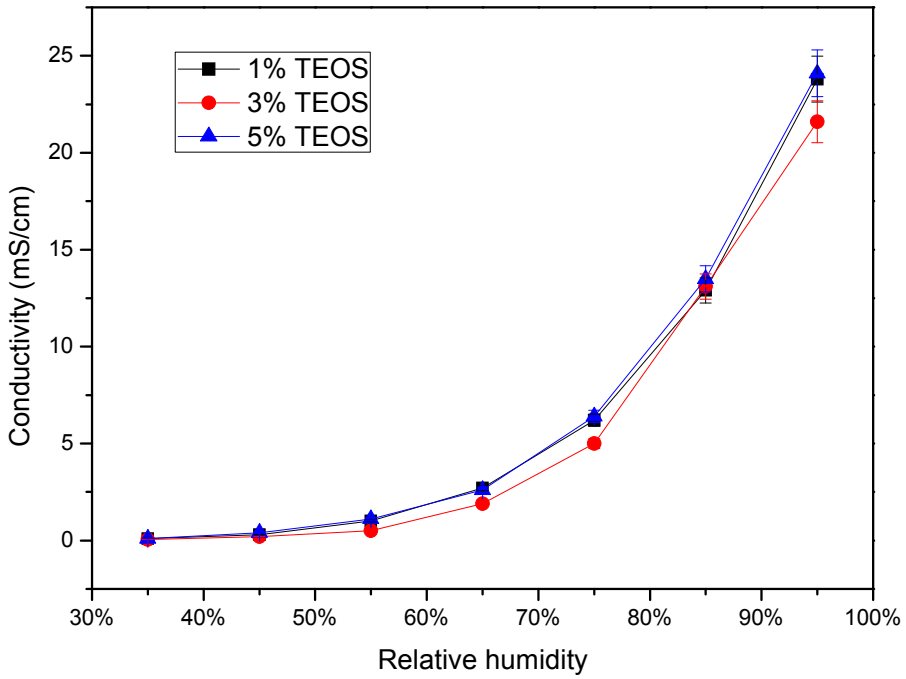

Fig 3-4. Proton conductivity of Nafion/TEOS membranes at 60ºC

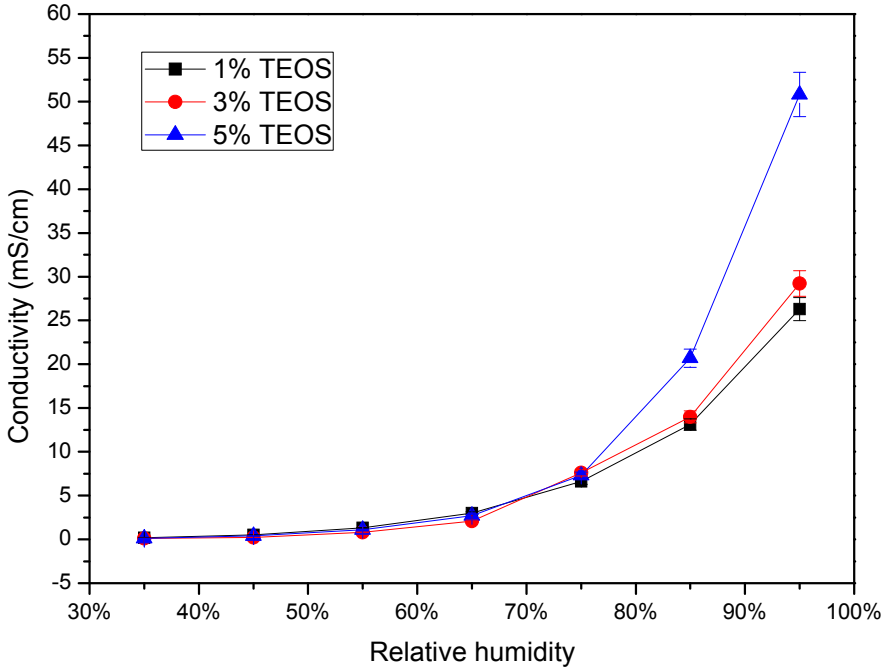

Fig 3-5. Proton conductivity of Nafion/TEOS membranes at 85ºC

3.4.2 Thermal properties

The TGA thermographs of recast Nafion and Nafion with Aerosil 380 are plotted in Fig 3-6. All the four membranes were thermally stable before 300ºC, and the slight weight loss was due to the loss of the absorbed water and solvent. The recast Nafion began to decompose from 300ºC and the degradation process possibly included desulfoanation, side-chain decomposition, and backbone decomposition [44, 109]. The decomposition was complete at about 600ºC. The other three membranes with different Aerosil 380 loading levels showed better thermal stability: the onset temperature of decomposition was raised to about 360ºC. Deng reported similar result on silica/Nafion membranes prepared from sol-gel reaction [49]. The shift of degradation onset temperature indicates incorporation of Aerosil 380 into Nafion makes the composite membrane work better under harsh working conditions. The TGA thermographs of

Nafion with TEOS are shown in Fig 3-7. The thermal stability of Nafion/TEOS membranes was also better than pure recast Nafion, though the improvement was not as significant as that of Nafion/Aerosil membranes.

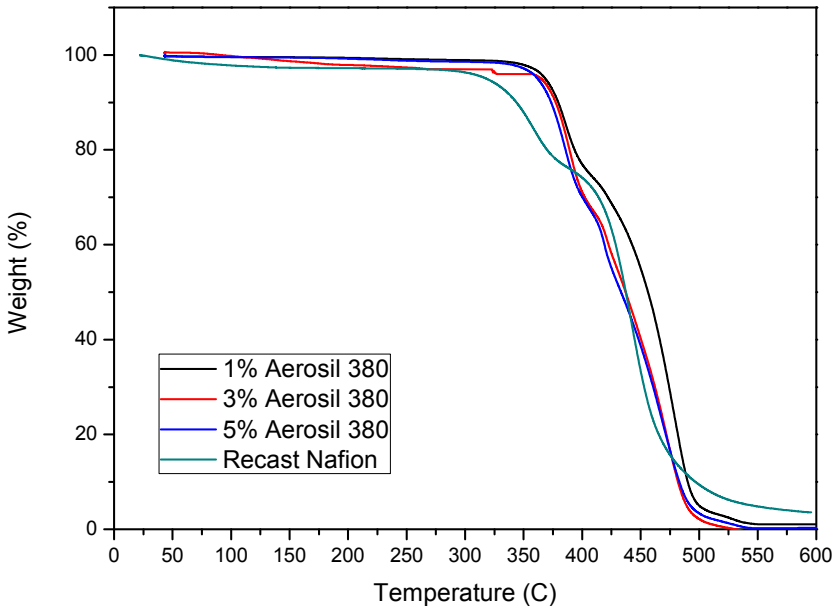

Fig 3-6 TGA plot of Nafion/Aerosil membranes

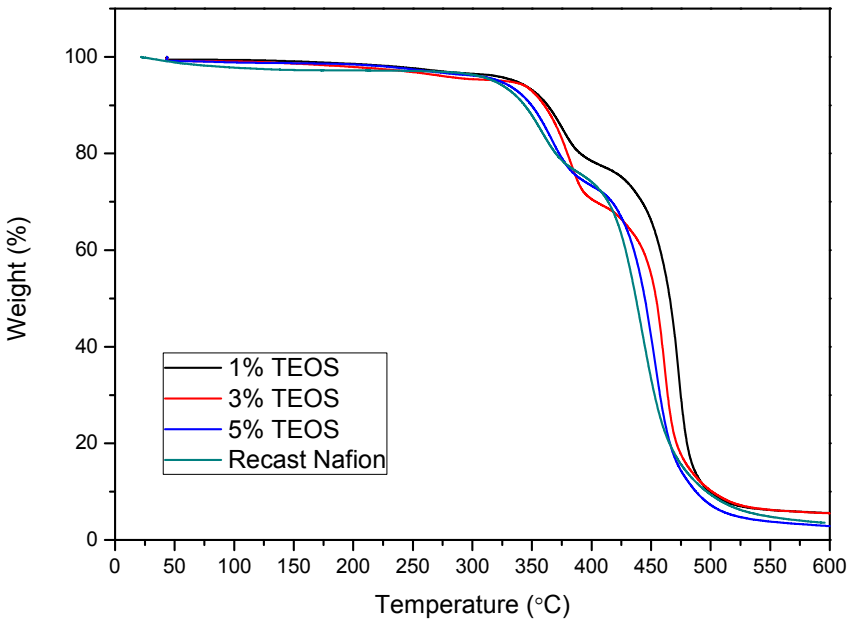

Fig 3-7. TGA plot of Nafion/TEOS membranes

The difference in thermal expansion coefficient between a proton exchange membrane and a carbon-based electrode could be an important factor for MEA degradation. The thermal expansion of polymers is orders of magnitude larger than that of carbon (~10^{-6}). Hence, it is reasonable to assume PEMs with lower thermal expansion coefficients have better thermal compatibility with carbon electrode. The thermo-mechanical analysis (TMA) result of Nafion/Aerosil 380 membranes was shown on Fig 3-8 and compared with that of recast Nafion. It can be seen that all three Nafion/Aerosil 380 membranes showed a lower thermal expansion at temperatures over 80ºC. The thermal expansion of Nafion/Aerosil 380 membranes was below 5% at a temperature as high as 125ºC. This implies that adding a small amount of silica into Nafion can improve MEA durability. The TMA result of Nafion/TEOS membranes is shown in Fig 3-9. Membranes with 1% and 3% TEOS showed similar thermal expansion behavior at all temperatures and the thermal expansion ratio was lower than recast Nafion below 150ºC. The thermal expansion ratio of Nafion with 5% TEOS loading was higher than that of the other two Nafion/TEOS membranes, but it was still lower than that of recast Nafion at temperatures below 140ºC. As 140ºC is close to the glass transition temperature of recast Nafion, it can be concluded that by adding silica into Nafion, the thermal expansion behavior of the composite membranes is better than recast Nafion in the "workable" temperature range.

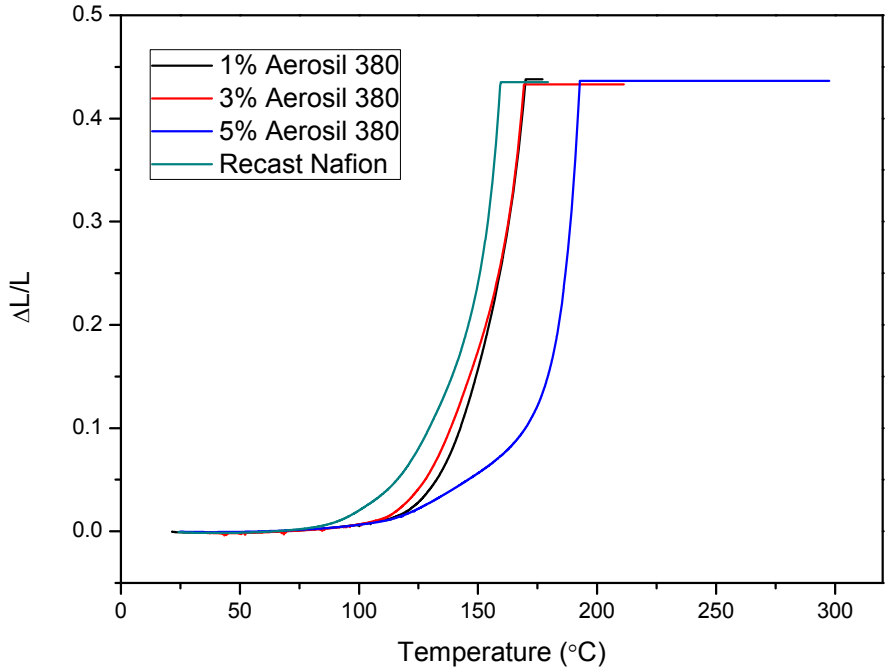

Fig 3-8. TMA plot of Nafion/Aerosil membranes

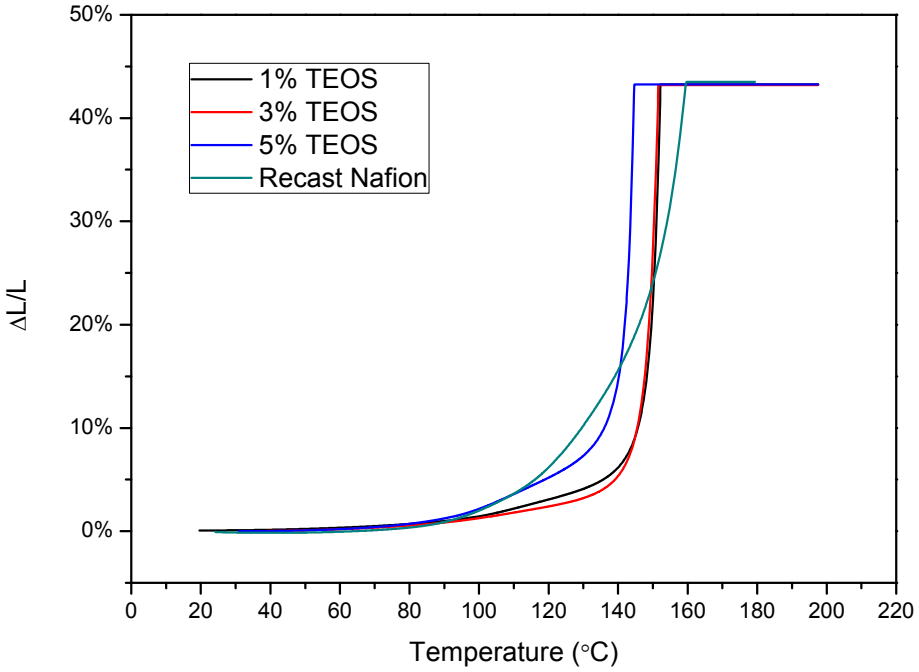

Fig 3-9. TMA plot of Nafion/TEOS membranes

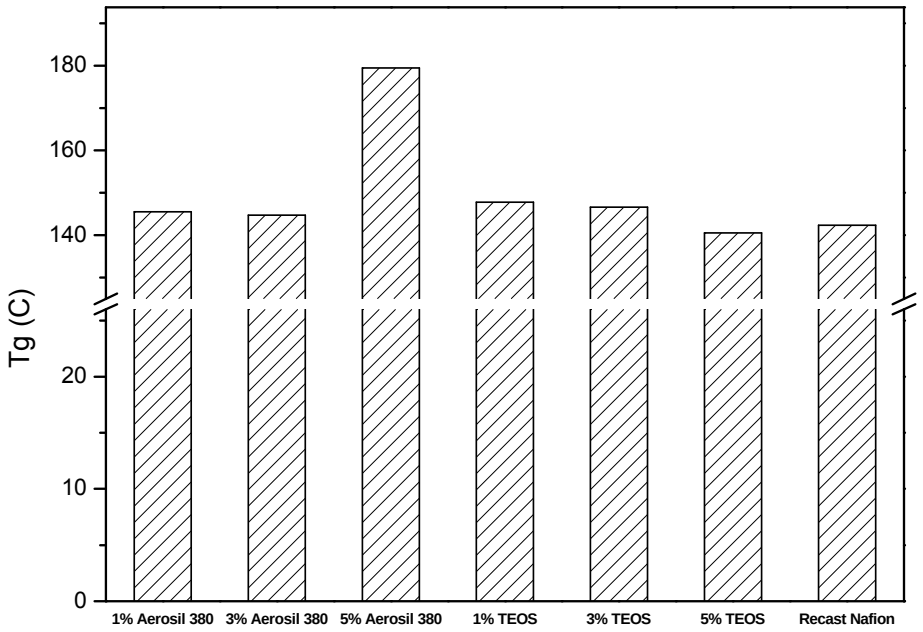

Fig 3-10. Glass transition temperature of Nafion/Silica composite membranes

3.4.3 Single cell performance

The polarization curves of three Nafion/TEOS MEAs with humidified H_2/O_2 are plotted in Fig 3-11 and Fig 3-12. The average thickness of the membranes was about 2.2-2.5 mils. The MEA with 5% TEOS showed slightly better performance than all the other three samples. Based on the conductivity data in this work, the proton conductivity of Nafion with 5% TEOS loading was close to that of recast Nafion. The better single cell performance of Nafion with 5% TEOS could be the result of reduced gas crossover. A similar conclusion was seen elsewhere [110] [111].

To explain the effect of reduced gas crossover on the fuel cell performance, the operational fuel cell voltage can be expressed by

$$E = E_0 - b\log\left(\frac{i+i_n}{i_0}\right) - Ri - m\exp(ni) \quad [5]$$

Where E is the operating voltage (actual cell voltage output), i is cell current, E_0 is the reversible open circuit voltage (OCV), i_n is the fuel crossover current, i_0 is the exchange current density, b is the Tafel slope, R is the Ohmic cell resistance, m and n are mass transport constants.

The OCV can be calculated by $E_0 = -\frac{-\Delta\bar{g}_f}{2F}$, where $\Delta\bar{g}_f$ is the Gibbs free energy change of the chemical reaction and F is Faraday constant (96485C). The OCV of the four MEAs are listed below:

Table 3-1 Open circuit voltage of Nafion/TEOS MEAs

Sample	OCV (V)
1% TEOS	0.98
3% TEOS	1.07
5% TEOS	1.13
Recast Nafion	0.94

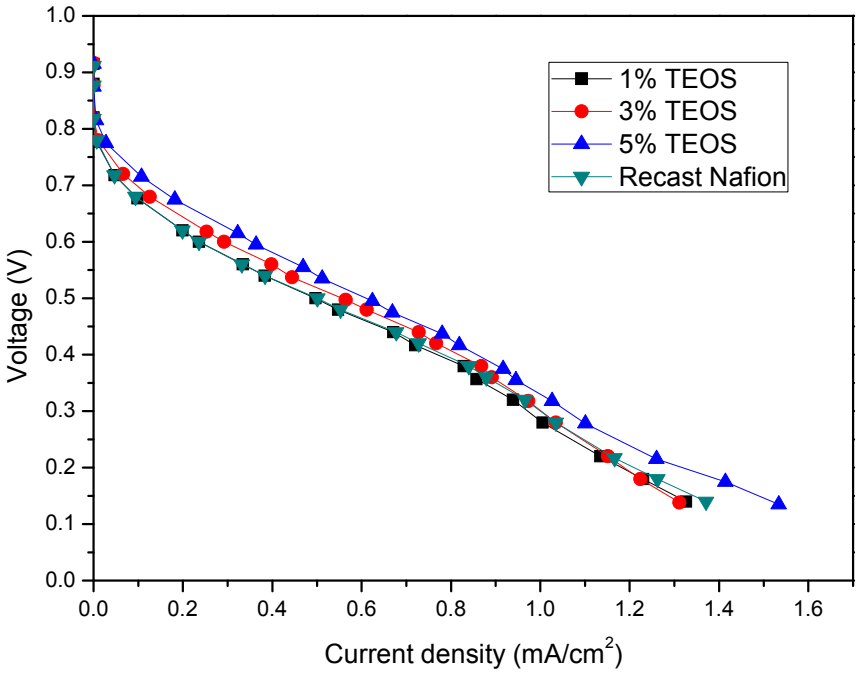

Fig 3-11. U-I curves of Nafion/TEOS MEAs at 85ºC and 1 atm

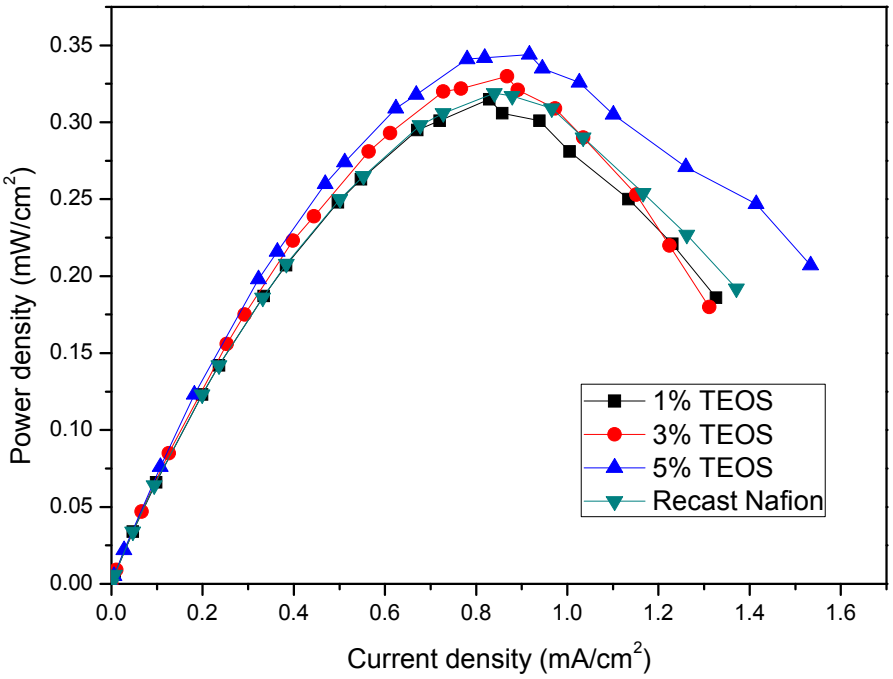

Fig 3-12. P-I curves of Nafion/TEOS MEAs at 85ºC and 1 atm

3.4.4 SEM

As nanoscale particles tend to agglomerate, it can be seen from the SEM micrograph that Aerosil 380 particles were not dispersed well in Nafion even after continuous agitation and unltrasonication. The silica particles form many clusters with about 0.1µm diameter. The formation of clusters will have an adverse effect on water retention of the composite membrane. At low silica loadings (1wt% & 3wt %), the clusters are isolated and dispersed in the polymer structure. While at the loading level of 5 wt%, the clusters are interconnected into a continuous network. In contrast, the silica generated by sol-gel reaction is uniformly distributed inside Nafion and no clusters were observed at ×30000 SEM micrograph.

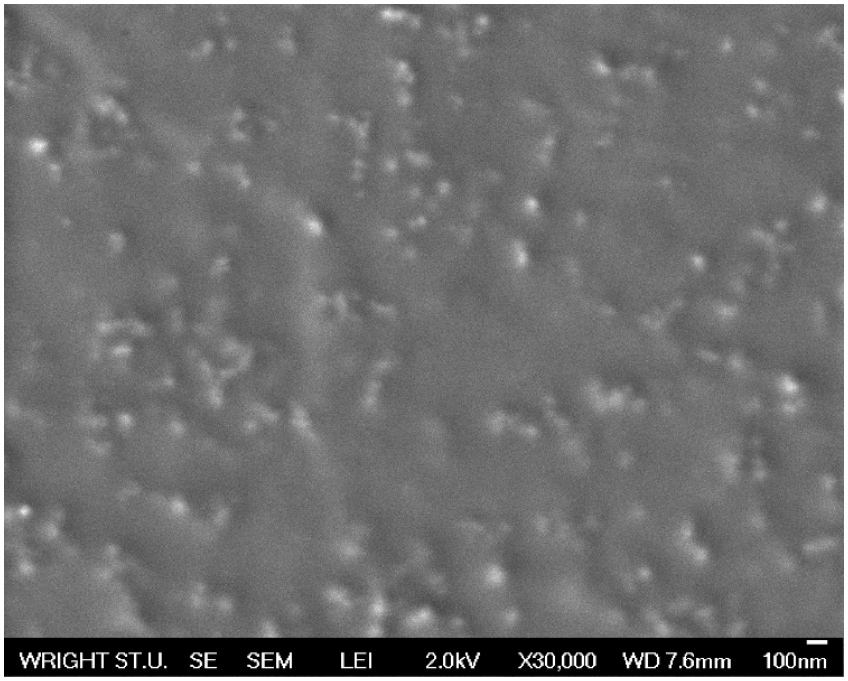

Fig 3-13. SEM micrograph of Nafion with 1wt% Aerosil 380

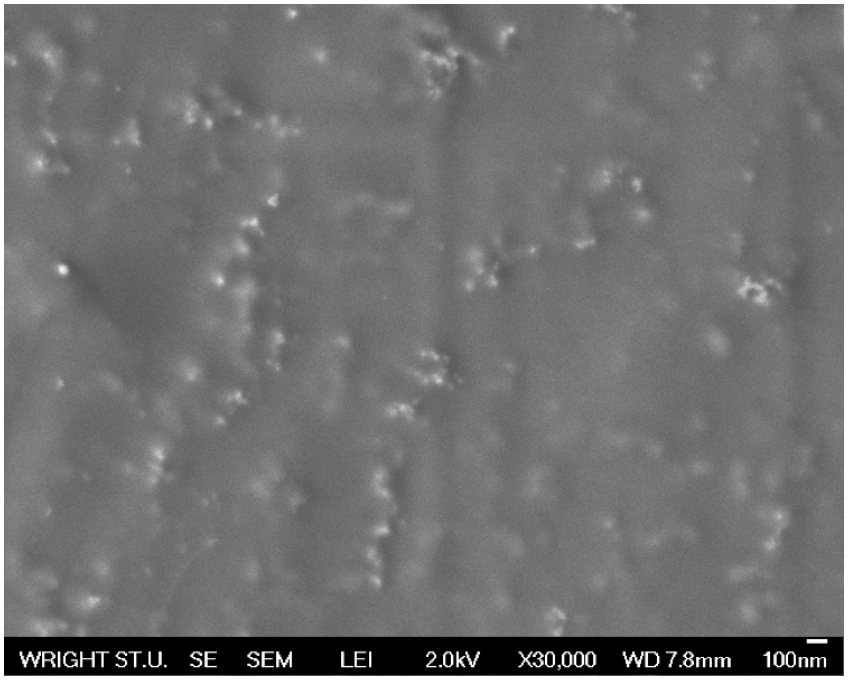

Fig 3-14.SEM micrograph of Nafion with 3wt% Aerosil 380

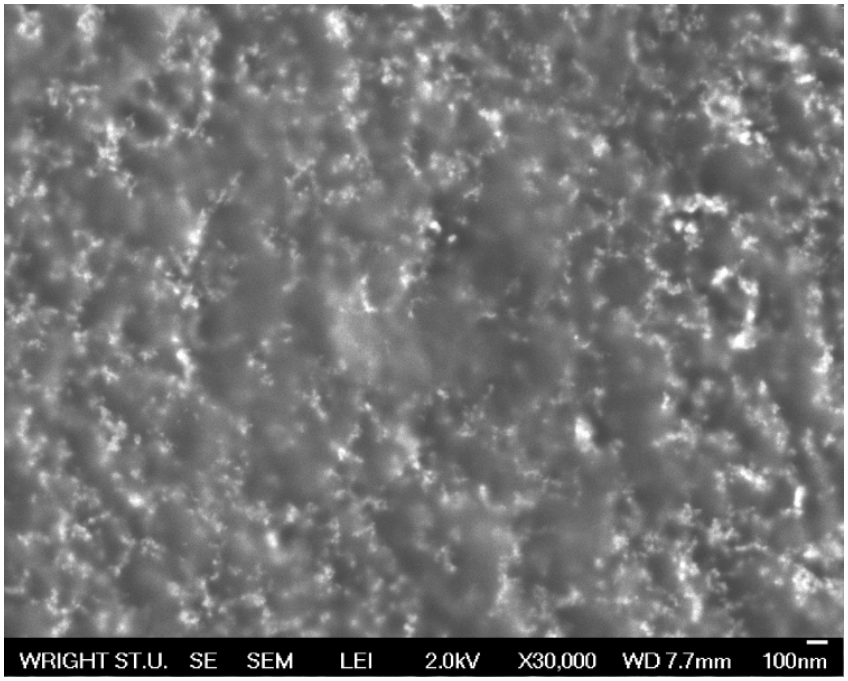

Fig 3-15. SEM micrograph of Nafion with 5wt% Aerosil 380

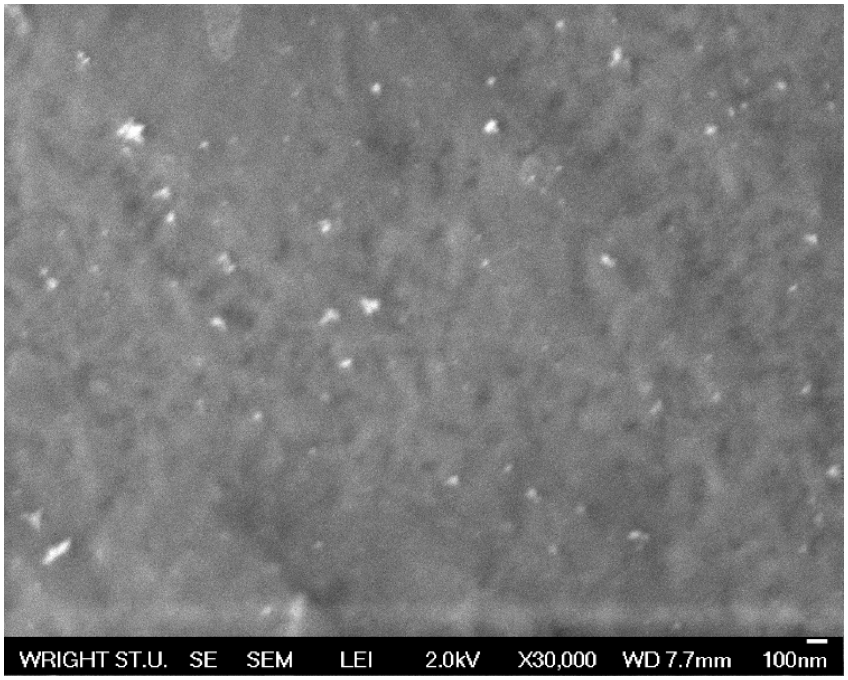

Fig 3-16. SEM micrograph of Nafion with 1wt% TEOS

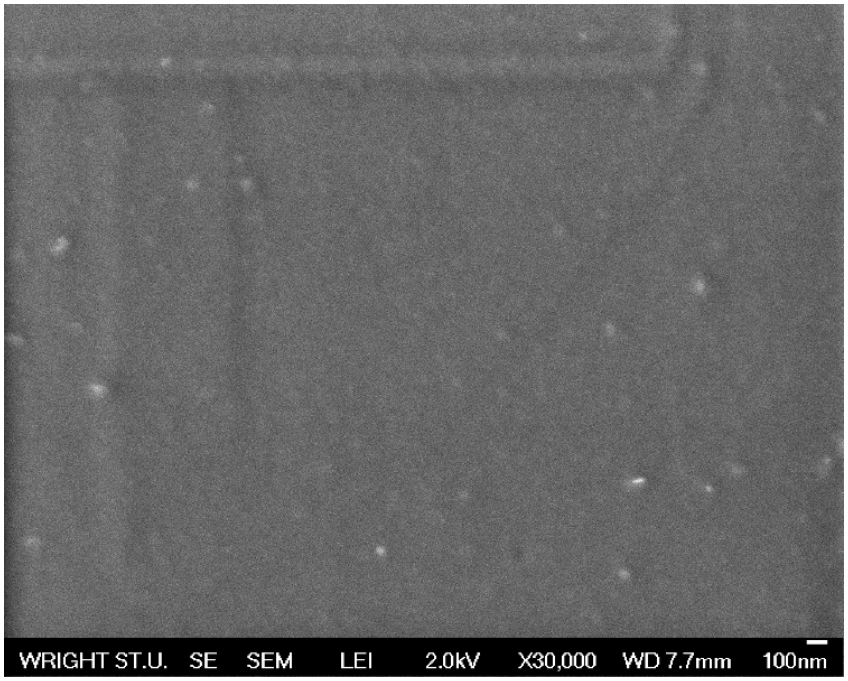

Fig 3-17. SEM micrograph of Nafion with 3wt% TEOS

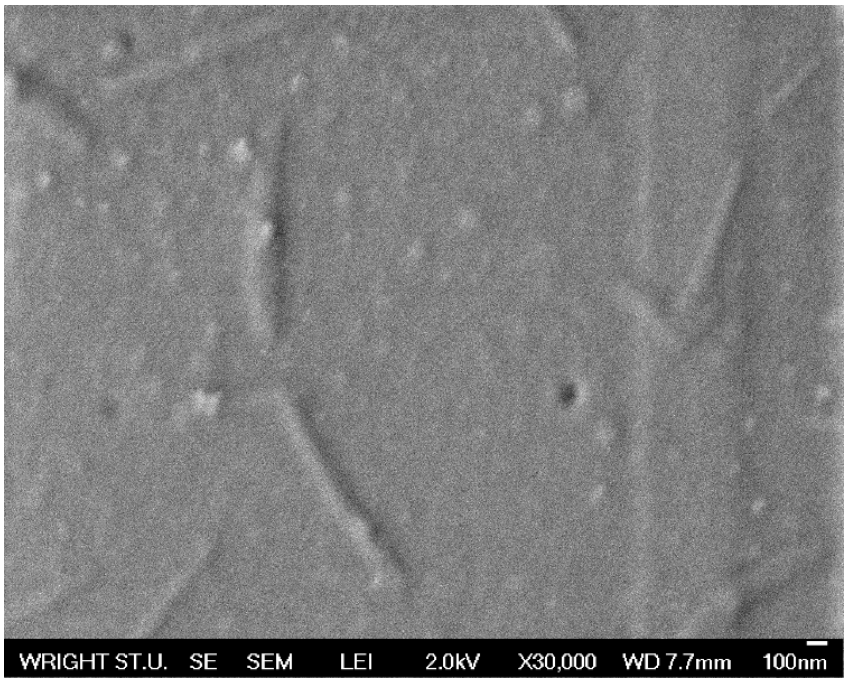

Fig 3-18. SEM micrograph of Nafion with 5% TEOS

3.5 Summary

Several Nafion/silica composite membranes with different silica loadings have been prepared by both direct mixing and sol-gel reaction. Based on SEM micrograph, it was observed that Aerosil 380 did not mix well in Nafion and formed many clusters with 0.1μm diameter. The agglomeration may prevent the formation of more hydroxyl groups on the surface of silica and reduce ionic conductive performance. Better dispersion of silica in Nafion can be realized by using sol-gel reaction. Incorporating silica in Nafion will reduce proton conductivity at temperature equal or below 85ºC. But the single cell performance of the Nafion/silica composite membranes is close or better than that of recast Nafion and the open circuit voltage (OCV) is also higher. This result indirectly indicates that the silica network inside Nafion can reduce reactant crossover and improve single cell performance. Two other benefits of incorporating silica are improved thermal stability and lowered thermal expansion, which are all beneficial for a longer life of the MEA.

4. Nafion/HPA composite membranes

4.1 Introduction

4.1.1 Heteropolyacid (HPA)

Heteropolyacids (HPAs) have been widely used for various catalysis applications due to their unique structural and chemical properties [112-120]. Three most common HPAs are silicotungstic acid (STA, $H_4SiW_{12}O_{40}.nH_2O$), phosphomolybdic acid hydrate (PMA, $H_3PMo_{12}O_{40}.nH_2O$), and phosphotungstic acid (PWA, $H_3PW_{12}O_{40}.nH_2O$).

HPAs are usually hydrophilic and they have several stable forms depending on temperature and relative humidity [121, 122]. The basic structural unit is called Keggin structure, which is shown in Fig 4-1. Keggin anions usually follow the formula of $(XM_{12}O_{40})^{n-}$ where X is the center atom (P, Si, or Ge), M is the addenda atom (Mo or W), which is surrounded by a group of oxygen ions [123].

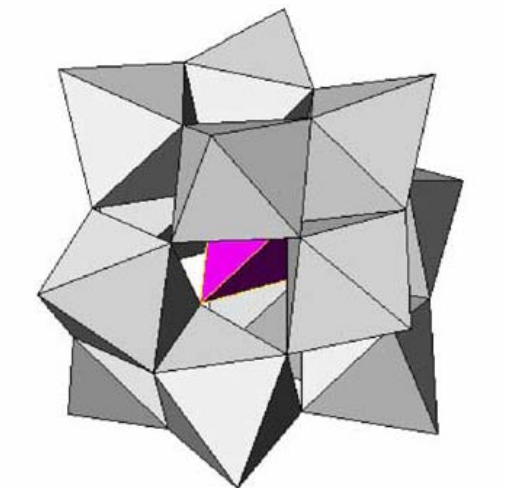

Fig 4-1. 3-D Keggin unit [124]

HPAs are the most proton conductive inorganic solid at ambient temperature [125]. Some HPA species can have a proton conductivity at up to 170 mS/cm at room temperature [121]. The extremely high proton conductivity and solid-type morphology make HPAs an ideal additive for proton exchange membranes (PEMs). The earliest study of HPAs as fuel cell electrolyte material can be traced back to 1979 by Nakamura [126] and many others have prepared composite proton exchange membranes for fuel cell applications [127-130]. By incorporating HPA into Nafion, the new composite membranes were observed to have better proton conductivity and a lower methanol crossover rate.

The surface morphology of Nafion membrane with 20 wt.% PMA loading is shown in Fig 4-2. It can be seen from the surface of NMA20 that PMA exhibited good retention in Nafion. Most PMA was well embedded inside the Nafion polymer matrix and only acid particles with diameter around 0.15 microns were observed on the surface of the membrane.

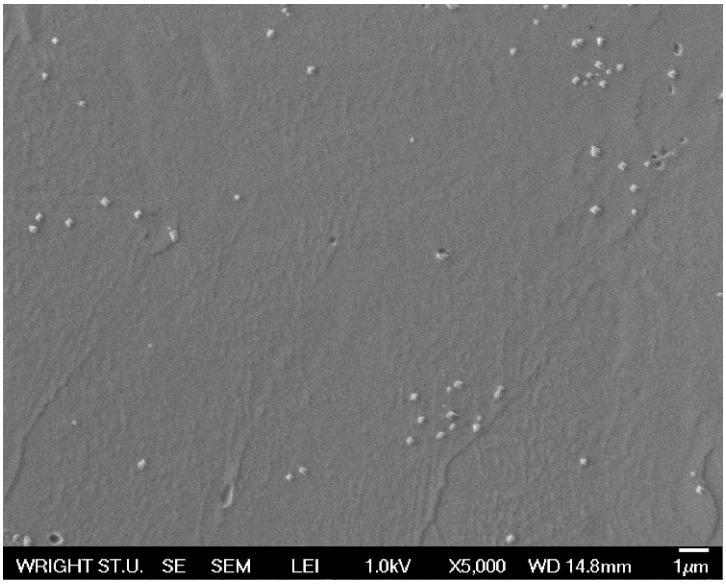

Fig 4-2. Surface of NMA20

However, as HPAs can easily dissolve in polar solvents, they are able to leach out of the composite membrane with the existence of water [131, 132]. The acid leeching can lead to a decrease in proton conductivity, and the tiny pores left behind can cause reactant crossover and even short circuit during the fuel cell operation.

To study the acid leaching with the existence of liquid water, a small piece was cut from the above NMA20 sample and soaked in distilled water at room temperature for 3 days. It was observed during the soaking period that the color of the membrane sample gradually changed from the original greenish to transparent, which looks alike pristine recast Nafion membrane. The fading in color indicates the acid loss during the soaking period.

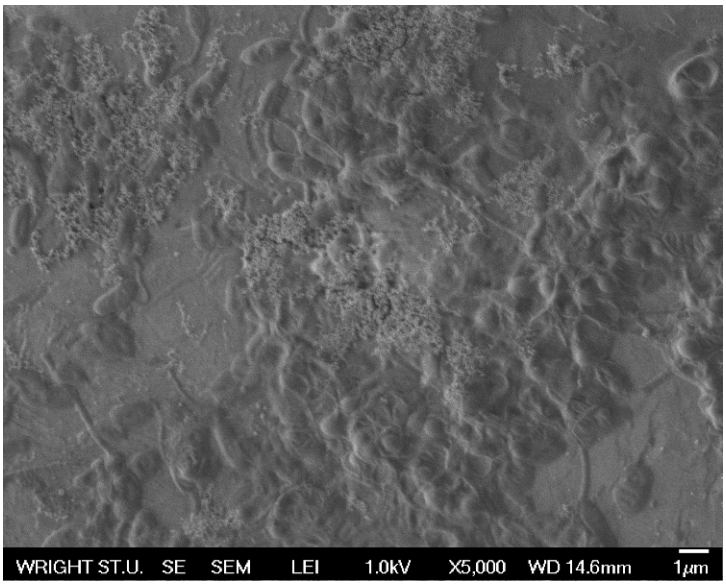

Fig 4-3. Surface of NMA20 (after soaking in water for 3 days)

It can be seen from the SEM micrograph that the surface morphology changed dramatically after soaking in water, which indirectly indicates the acid leaching in liquid

water. Some part of the surface exhibits a sponge-like structure which is left behind by the loss of acid. This porous structure can be a potential pathway for fuel crossover which will decrease fuel cell lifespan, not to mention the loss of proton conductivity.

In order for HPAs to be used in fuel cell membranes, several techniques were applied to prevent or reduce HPA leaching with the presence of water.

4.1.2 HPA trapping in silica

It was reported that some HPAs could be immobilized on the surface of mesoporous silica due to the chemical interaction between HPA and the Si-OH group, but the amount was very limited [133-135]. One good alternative choice of immobilizing HPA is to use silica from the sol-gel reaction. The silica prepared from sol-gel reaction has a large number of nano-scale pores inside the bulk structure, which makes its density much lower than natural silica. If HPA is trapped inside silica gel, the overall proton conductivity can also benefit from the large amount of silanol (Si-OH) groups [136, 137]. Silica gel network can be formed by hydrolyzing tetraethylorthosilicate (TEOS) in acidic environment. Shi [138] and He [135] have studied the effect of trapping TPA and PWA in silica, respectively. In Shi's and He's work, it was claimed that no apparent HPA leaching was observed and the majority of the catalysis capability of bulk HPA was kept in the Silica/HPA composite. It is reasonable to assume that by incorporating Silica/HPA particles, the proton conductivity will be at the same level of Nafion/HPA membranes. And the numerous tiny pores left behind by burning off the surfactant will increase the interface between Nafion and Silica/HPA particles. He's experimental method was followed in this work with slight modifications

4.1.3 HPA trapping in zeolite

Zeolites are microporous crystalline aluminosilicates which are composed of SiO_4 or AlO_4 tetrahedra with oxygen atoms connecting neighboring tetrahedral [139]. The first zeolite was discovered in 1756 by Axel Fredrik Cronstedt [140], a Swedish mineralogist. Up to now about 48 natural zeoites have been discovered and more than 150 zeolites have been synthesized. If there is no Al content, the whole structure is electrically charge neutral. When Al is introduced, the Al^{3+} makes the frame negatively charged, and thus requires the presence of extra-framework cations to keep the overall framework neutral. Zeolite composition can be described by the formula of $M_{n/m}^{m+} \cdot [Si_{1-n}Al_nO_2] \cdot nH_2O$, where M is extraframework cation. Zeolites are thermally stable material and depends on the silica/aluminum ratio, some high silica content zeolites are thermally stable up to 1300ºC [139].

Many interesting properties and applications of zeolites, such as adsorption capability, ion-exchange properties, catalytic activity, molecular separation, and serving as a host for nano-composite materials, come from their unique porous structure. International Zeolite Association classified zeolite structures based on three-letter codes, which are derived from the name of zeolites or "typical structure" [140]. Among all the zeolite structures, FAU (faujasite) structure possesses relatively large pore size because of the 12-ring pore openings. Two typical FAU-type zeolite are X and Y zeolites where Y zeolites have a higher Si/Al ratio.

Zeolites are widely known as "molecular sieves" which refers to pores of the size at molecular dimension scales. The pore size distribution of zeolites depends on their structural characteristics and ranges from about 0.35-1.25nm [141]. It has also been

reported that zeolite itself is a proton conductive material [121]. Kreuer [142] studied proton conduction mechanisms by AC-impedance at room temperature and a proton conductivity up to 2 mS/cm was observed on NH_4^+-zeolite Ahmad [143] studied several HPA/zeolite-based composite membranes for fuel cell applications. It was observed that ultrasonication of HPA and zeolite can prevent acid leaching. But theoretically HPA may not be able to enter the supercages of Y zeolite because of the geometry mismatch.

Zeolite has a unique supercage structure which is slightly larger than the anion of HPAs, and the windows of the supercages are smaller than the HPA anions. So zeolite could be an ideal host for HPAs even with the existence of water. Mukai [144] studied encaging 12-molybdophosphoric acid in Y zeolite and discussed several factors that might affect the encapsulation [145]. As HPA anions are larger than the windows of the zeolite supercages, practically the only way to embed HPA in zeolite is by in-situ generating HPAs inside the zeolite supercages. As Al_2O_3 shows basicity, which suppresses the generation of HPA, only zeolites with a high SiO_2/Al_2O_3 ratio can be used.

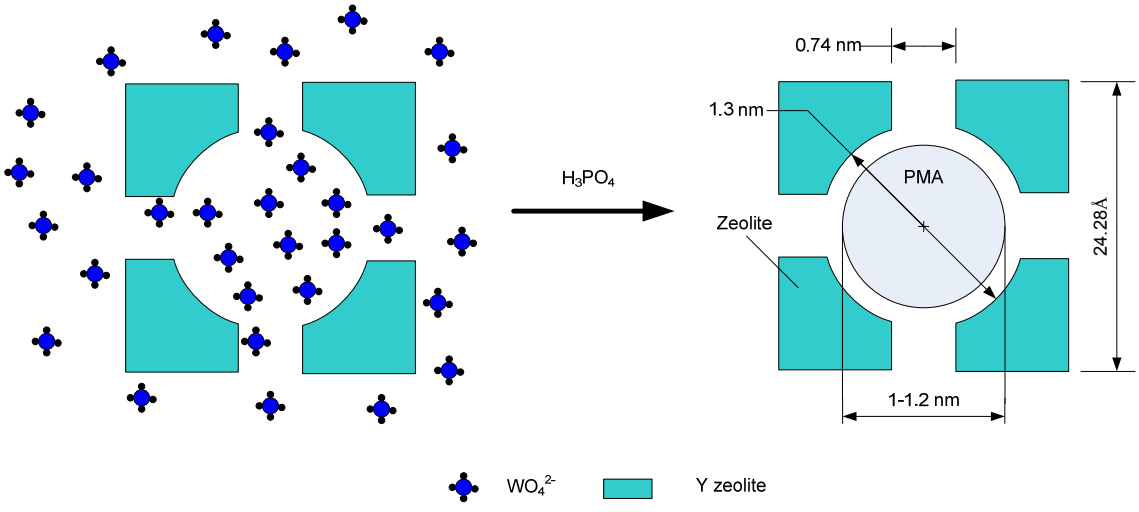

Fig 4-4. Process of PMA trapping in Y Zeolite

Mukai's method [144] was followed in this work to prepare encaged PMA and PWA in Y zeolite. The HPA/zeolite was processed into fine powders and used for proton exchange membrane filler materials. As the encaged HPA still shows high acidity, the new composite membranes are expected to have better proton conductivity and single cell performance than recast Nafion.

4.2 Experimental

4.2.1 Nafion/HPA composite membrane

The commercial 10% Nafion solution (Ion Powder) was first transferred to DMAc based solution at 50ºC under stirring. A certain amount of PMA (Sigma Aldrich) was mixed with DMAc-based Nafion solution so that the acid content in the dry membranes was controlled to be 10 wt% and 20 wt% respectively. The solution was stirred for half an hour and poured onto a leveled glass plate. The membrane samples were then dried at 70ºC overnight under vacuum. The dried membrane samples were peeled off from the glass plates by soaking in distilled water for a few minutes.

4.2.2 Nafion/Silica/HPA composite membrane

HPA-trapped mesoporous silica was prepared following the method proposed by He, etc [135]: 2g Pluronic 123 (BASF) was dissolved in 20g ethanol (Fisher). 0.6g PWA and 4.16g TEOS (Alfa Aesar) were added into the Pluronic/ethanol solution. The mixture was vigorously stirred at 45ºC for 30 minutes. The final solution was aged in open air for 3 days to finalize the hydrolysis reaction. After that, the sample was removed from the Petri dish and transferred into a crucible and calcinated at 300ºC for 3 hours. As P123 can

decompose at about 200ºC [146] while PWA is thermally stable up to over 400ºC [122], the calcination step removes P123 template while the ordered mesoporous silica/PWA structure is left. In a separate calcination experiment, it was observed that 98.8% of P123 decomposed by calcinating under 300ºC for 3 hours. After calcinations, the color of the samples changed from milky to black and the black color was supposed to come from the small amount of residue of P123 decomposition. The sample was then crushed in a mortar and then soaked in water for acid extraction. The water-extracted powder was used for composite membranes.

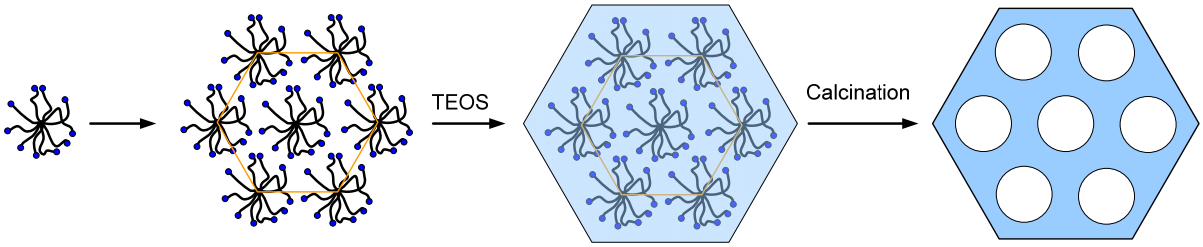

Fig 4-5. Templating mechanism for mesoporous structure growth [147]

As TEOS does not mix with water so ethanol was used to make TEOS/ethanol solution. The TEOS/ethanol solution was stirred for half an hour and premixed water/ethanol solution was added. The molar ratio of the three components is TEOS: ethanol: H_2O=1:3:4. The final solution was stirred at room temperature for another half an hour. After that, the PWA powder is added into the solution and the amount of PWA used was from the calculation that the weight between PWA and SiO_2 is 2:5. The sample was dried at 100ºC and then crushed into fine powders. The fine powder was screened using a 100-mesh sieve. The final powder was stored in a glass sample bottle until use.

4.2.3 Nafion/Zeolite/HPA composite membrane

The experiment followed Mukai's work [144, 145, 148] with slight modifications.

Zeolite Y with a SiO_2/Al_2O_3 mole ratio of 30 was purchased from Zeolyst International. According to Mukai's work [145], the SiO_2/Al_2O_3 ratio needs to be between 200-100 in order for HPA to be formed within the supercages of zeolite. The unit cell size of zeolite Y is 24.28Å and the surface area is 780 m^2/g.

Y zeolite was firstly exchanged to NH_4^+ form by soaking in 10% NH_4Cl solution for 30 min with continuous stirring. The PH value of the solution was changed to 3-4 after ion exchange. The purpose of the counter cation exchange was to promote the formation of polyanions from MoO_4^{2-} [145]. The zeolite powder was filtrated and dried at 105ºC. Two grams of cation-exchanged Y-zeolite, 7.2g MoO_3 (Sigma Aldrich) and 70g distilled water were mixed together and stirred at room temperature for 24 hours. After that, 0.48g H_3PO_4 (85%, Fisher) was added and the solution was stirred at 85ºC for 4 hours. The final product was dried at about 100ºC and crushed into fine powders in a mortar.

As the density of zeolite is higher than Nafion solution, it is important to make zeolite particles small in order to guarantee zeolite particles do not accumulate during membrane casting and lead to a homogeneous composite membrane. Before making the composite membrane, a 100-mesh sieve was used to remove large particles.

Reaction: $H_3PO_4 + 12MoO_3 \rightarrow H_3PMo_{12}O_{40}$

To prepare AZW10, 10 g 10% Nafion solution was firstly changed to DMAc based solution at 40ºC with continuous agitation. Then 0.11g PWA powder (NH4+

zeolite-trapped PWA, no washing) was added into the Nafion solution. The suspension was further stirred overnight.

To prepare AZM10, 10 g 10% Nafion solution was firstly changed to DMAc based solution at 40ºC with continuous agitation. Then, 0.11g PWA powder (NH_4^+ zeolite-trapped PWA, no washing) was added into the Nafion solution. The suspension was further stirred overnight.

The same steps were applied to make composite membranes which are zeolite/PWA encaged in Nafion.

Table 4-1. Abbreviations of membrane samples used in this work

Sample name	Description
NMA10	Nafion with 10 wt% PMA (dry weight)
NMA20	Nafion with 20 wt% PMA (dry weight)
NWA10	Nafion with 10 wt% PWA (dry weight)
NWA20	Nafion with 20 wt% PWA (dry weight)
AZW10	Nafion with 10 wt% PWA/Y zeolite (ammonia form)
AZM10	Nafion with 10 wt% PMA/Y zeolite (ammonia form)
PNWA10	Nafion with 10 wt% P123/PWA
TNWA10	Nafion with 10 wt% TEOS/PWA

4.3 Materials characterization

4.3.1 Proton conductivity and water uptake

The proton conductivity was measured by a 4-proble direct current (DC) method using a Keithley 2400 source meter and a Teflon-based conductivity cell. The membrane samples were cut into 3 mm by 30mm pieces and installed onto the four platinum

electrodes of the conductivity cell. Then, the thickness of the membranes sample was measured while dry at different points, and the average thickness value was used for conductivity calculation. The membrane sample with the conductivity cell was settled in an environmental chamber (ESPEC) which can accurately control temperature and relative humidity.

After the membrane sample was fully saturated at the set temperature and relative humidity level, current was scanned between 1-100 μA and the corresponding voltage output was measured. When current scan was complete, the U-I data pairs were processed by linear regression and the slope of the curve was used for conductivity calculation. In order to get reproducible results, it is important to fully "condition" the membrane at the preset temperature and relative humidity level. The duration of the conditioning depends on the intrinsic properties of the membrane. In this work, in was observed that HPA-incorporated composite membranes takes a much shorter time to get fully conditioned when compared with pristine Nafion. The shortened conditioning time of HPA/Nafion composite membranes could be caused by the hydrophilicity of the HPA particles. For practical consideration, it is desirable to have a proton exchange membrane getting fully hydrated in order to shorten the fuel cell cold starting time.

4.3.2 Acid leaching

The acid leaching experiments were performed to study how well the incorporated HPAs were secured inside the composite PEM with the existence of liquid water. The ability to keep HPAs from being lost is one of the basic requirements for the HPA-based composite membranes.

To test if the PMA is trapped inside the zeolite supercages, some dried PMA/Zeolite powders were soaked in DI water overnight. After that, the sample was filtrated and dried at 110ºC. It was observed that the color of the zeolite was still bright yellow, which means the PMA content was kept inside the zeolite supercage. The acid content was studied by a SEM (JEOL Field Emission Scanning Electron Microscopy, JSM-7401F) with an EDS detector. As PMA can easily dissolve in polar solvents such as water, any PMA not trapped inside the supercages of Y zeolite would be removed by washing in water. So the molybdenum element detected by EDS should be corresponding to the PMA trapped by Y zeolite.

The same testing procedure was also adapted to study PWA trapping in Y zeolite and silica.

4.3.3 Surface morphology

The morphology of the prepared samples was examined by scanning electron microscopy (SEM, JEOL Field Emission Scanning Electron Microscopy, JSM-7401F). As mentioned earlier, the acid-doped composite membranes had acid leaching problem so SEM was used to study the surface morphology change. SEM was also used to study the particle size of zeolite powder (both before and after HPA trapping) and the morphology change.

4.3.4 Single cell performance

Single cell performance was performed on a fuel cell test station (PD50, Asia Pacific Fuel Cell Technology Co.) with a Chroma 63103 DC electronic load. Voltage

scanning was used to measure the polarization curve and voltage scan range was between OCV and 0.1 volt. In order to parallel compare the performance of different composite membranes, the dry thickness of all the membranes before hot pressing was abut 100 microns.

Commercial carbon cloth supported gas diffusion electrode (GDE, E-TEK Inc) with Pt catalyst loading of 0.5 mg/cm^2 was used to guarantee the most reproducible results. In order to better utilize the Pt catalyst, the GDE was impregnated with 5% Nafion solution (Ion Power) and the dry Nafion loading was 0.6 mg/cm^2. The Nafion-impregnated GDE was then dried in air at 110ºC for 15 minutes. Two pieces of GDE and one piece of membrane were sandwiched between two PTFE sheets and hot pressed at 130ºC under 70 kg/cm^2 pressure for three minutes. After hot pressing, the two pieces of GDE were firmly attached onto the surface of the membrane and the MEA was ready for testing. After that, the MEA was installed into a single testing fuel cell (Fuel Cell Technologies) and conditioned by humidified H_2/O_2 at open circuit voltage for at least two hours before testing to fully activate the catalyst. This catalyst activation process is very important for low-temperature fuel cells to get the most power output [149, 150].

4.3.5 Thermal properties

In order to study the thermal stability of the prepared composite membranes, thermalgravimetric analysis (TGA) was carried out on a TA Instruments Q500 instrument. The dry membrane samples were heated from room temperature to 600ºC at a ramping rate of 10ºC/min under nitrogen atmosphere.

The glass transition temperature (Tg) and thermal expansion properties of the membranes were studied by a thermomechanical analyzer (TMA Q400, TA Instruments). The samples were cut into 1cm ×2cm pieces and tested using a film/fiber probe with 0.075N force load. The samples were tested with a 10º/min heating rate and a nitrogen flow rate of 50ml/min.

4.4 Results and discussion

4.4.1 Proton conductivity and water uptake

Ramani investigated the mechanism of using HPA to increase proton conductivity [151]. Based on Ramani's experiments, the water uptake (in water vapor) of HPA/Nafion composite membranes was at the same level as that of pure Nafion membranes. It was assumed that the improvement in conductivity was caused by a lowered activation energy for proton hopping (Grotthuss mechanism). Ramani's conclusion was very import in explaining the effect of HPA filler. Although HPA could absorb water molecules, it did not necessarily mean the absorbed water could exist like "vehicles" for proton conduction.

Bardin [123] suggested that heteropolyacid was essentially Bronsted acid in hydrated form, which led to high proton conductivity. Further, PWA was more acidic than PMA, which was also verified by the proton conductivity measurement in this work. The higher water uptake of the composite membranes can be attributed to incorporation of HPA because of its hydrophilic property. With a higher water content in the composite membranes, the proton conductivity is also higher than that of recast Nafion. It was also

reported by Zawodzinski that proton conductivity of Nafion had a linear relationship with the water content at 30ºC [21].

Ostrovskii [152] and Gruger [153] studied the state of water in the Nafion membrane and found that all the water molecules were involved in the OH-H bonding, rather than associated with $-CF_2-$ group. These study also supported Hsu's [37] cluster network model for Nafion structure. Falk [154] did an infrared study on Nafion membrane and concluded that, for high-EW Nafion, about 25% of the absorbed water did no involve hydrogen bonding and thus did not contribute to the proton conductivity. These research efforts led to the conclusion that in addition to providing more protonic sites and higher water uptake [155], lowing EW also led to better water "usage" in the proton conducting process.

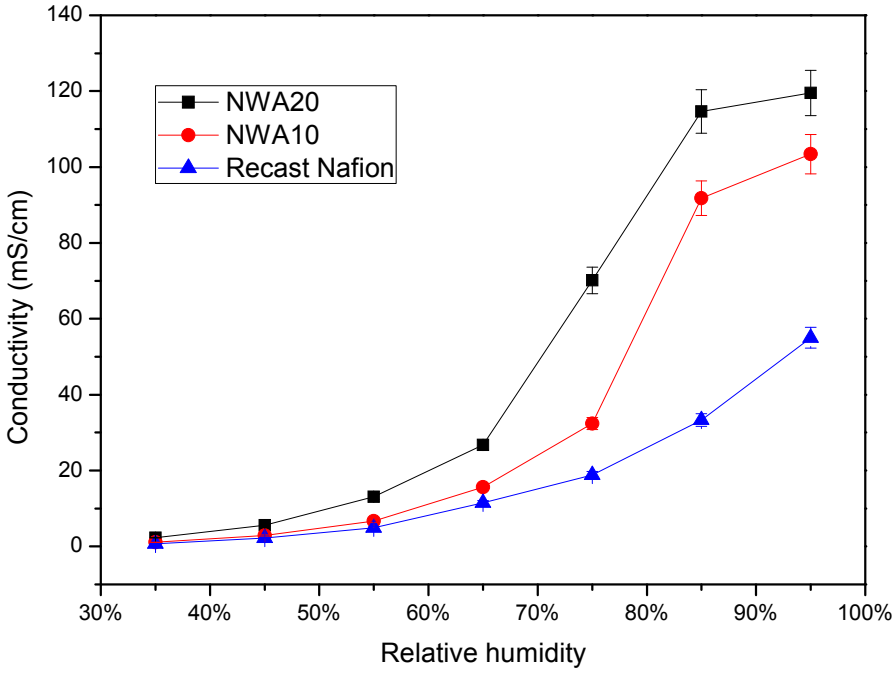

Fig 4-6. Proton conductivity of PWA/Nafion membranes at 85ºC

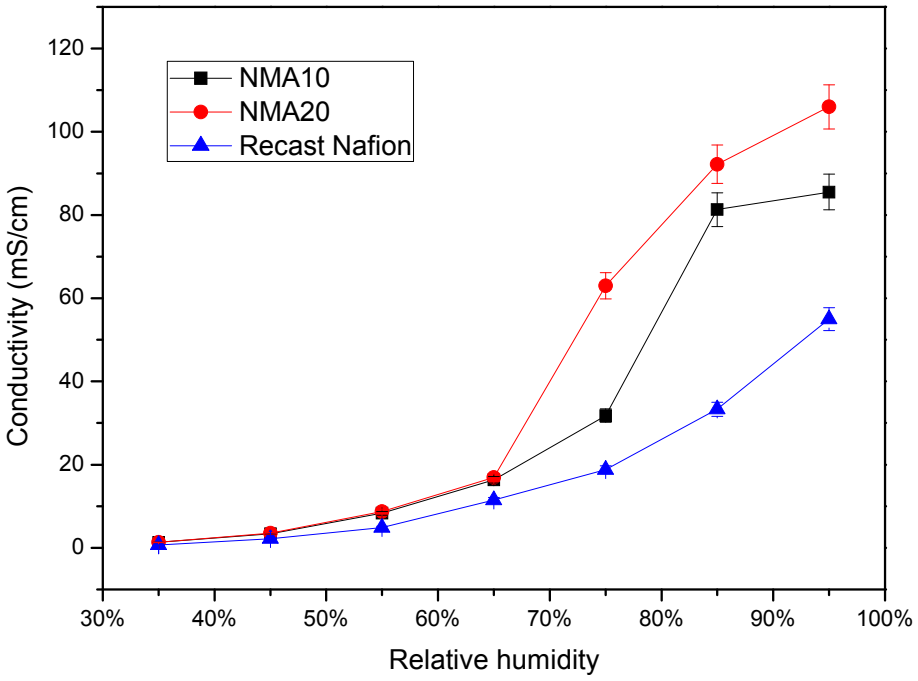

Fig 4-7. Proton conductivity of PMA/Nafion membranes at 85ºC

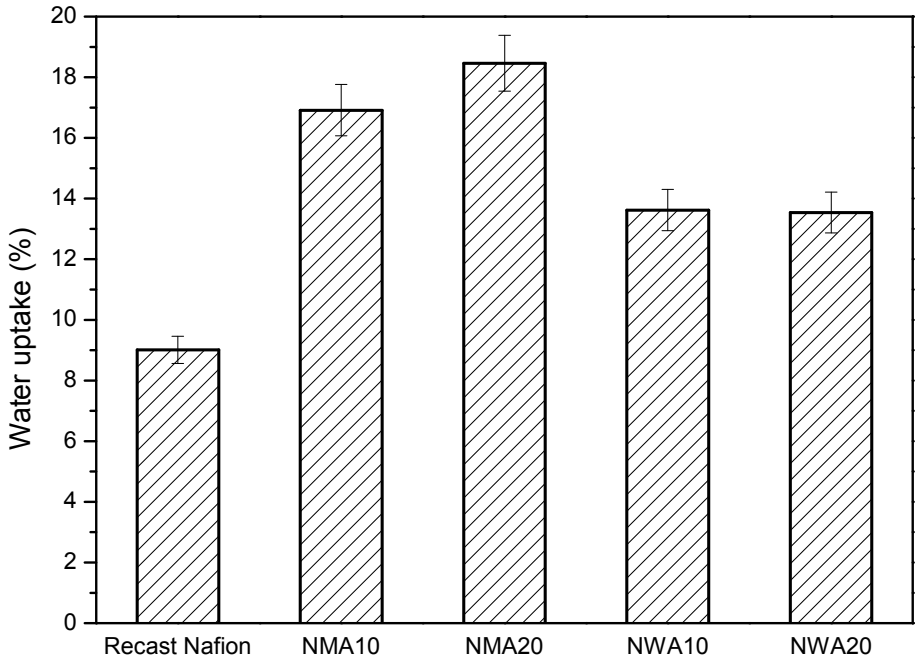

Fig 4-8. Water uptake of HPA/Nafion composite membranes and recast Nafion

It can be seen from Fig. 4-8 that the HPA-incorporated Nafion composite membranes have much higher water uptake than pure recast Nafion. Higher water uptake

is more desirable for proton exchange membranes as proton conductivity is linearly related to the proton conductivity of Nafion membranes [21]. The two most generally accepted mechanisms used to explain proton conductivity are the Grotthuss Mechanism [15, 16] and the Vehicle Mechanism [17]. The Grotthuss mechanism explains proton transport as a proton hopping between adjacent water molecules along with the rotational movement of the water molecules. While the vehicles mechanism explains the transport process as the moving of water molecules together with the proton. Based on both theories, water is an essential part in proton transportation. The exceptional water retention capability of the HPA-incorporated membranes comes from the hydrophilic properties of HPA. The stable form of PWA can take 29 water molecules per acid anion while PMA can take up to 30 molecules per acid anion [156]. By using TGA analysis, it was found that PWA could hold 6 water molecules at a temperature as high as 175ºC [122]. The water retention property makes HPAs very suitable for high temperature PEM fuel cell applications.

Staiti, et al. studied HPA/Silica/Nafion composite membranes for direct methanol fuel cells operating at up to 145ºC [55]. It was reported that the composite membranes exhibited a better V-I performance than Nafion membranes, and they concluded that the increase in cell performance was not caused by the increase in proton conductivity, but by the so-called "promoting behavior". As the polarization curves of the fuel cell MEA is greatly affected by the manufacturing process [157-160], it is more accurate to measure the membrane proton conductivity directly.

The proton conductivity of NWA10 and NWA20 at 85ºC and different relative humidity levels was shown in Fig. 4-6. It can be see that by incorporating PWA into

Nafion resin, the proton conductivity increased at all relative humidity levels and that a higher PEA loading led to better conductivity performance. At relative humidity higher than 50 percent, the proton conductivity of NWA20 was about twice or even higher than that of pure recast Nafion. The huge proton conductivity increase can greatly reduce the internal energy loss due to ohmic loss in the membranes, and more power output is expected. Compared to other electrical conductive components of a fuel cell, such as bipolar plates and gas diffusion layers, the ionic proton conductive membrane has much higher resistivity and energy loss. So increasing membrane conductivity can effectively improve the whole fuel cell performance.

HPAs are very good proton conductors and they are classified as "super ionic conductors" [121]. HPAs are by far the most proton conductive inorganic materials in solid form. By incorporating HPA into Nafion membrane, the crystals of HPAs are expected to be evenly distributed between polymer chains. Hsu et al. [36, 37] studied the structure of Nafion by small-angle X-Ray diffraction and proposed a cluster-network model. Based on the cluster-network model, the ionic side chains of hydrated Nafion form clusters with 4 nm diameter and the clusters are connected by short channels which are about 1 nm in diameter. Water molecules are only trapped within the ionic clusters. The cluster size changes along with the humidity level and certain cluster size is needed for the percolation conductivity threshold. The proton conductivity near or above the percolation threshold can be calculated by $\sigma = \sigma_0 \left(c - c_0\right)^n$ [37], where c is the volume of the aqueous phase, c_0 is 15%, n equals to 1.5, and σ_0 is related to polymer intrinsic properties. Based on this power law, it is evident that the higher water uptake of HPA-incorporated membranes leads to higher proton conductivity.

Because HPAs are themselves excellent proton conductors, the crystals of HPAs inside Nafion matrix form a separate proton exchange network, which can also conduct protons. Hopefully the HPA crystals can also enlarge the short channels that connect Nafion's ionic clusters. When the relative humidity level is low, the ionic clusters will shrink and some of them will be disconnected from the percolation network. With the help of doped HPA, the shrunk clusters can still be connected and contribute to proton conduction.

The activation energy of the HPA/Nafion composite membranes at 95% and 60% relative humidity was obtained from the Arrhenius plot. At 95% relative humidity level, the activation energy of NMA10, NMA20, NWA10, and NWA20 were 23.58 $kJ \cdot mol^{-1}$, 18.73 $kJ \cdot mol^{-1}$, 23.45 $kJ \cdot mol^{-1}$, and 19.09 $kJ \cdot mol^{-1}$, respectively. It can be seen that HPA-incorporated composite membranes have a lower activation energy than recast Nafion (30.74 $kJ \cdot mol^{-1}$) at 95% relative humidity. It was reported elsewhere that if Grotthuss mechanism dominates in the proton conduction, the activation should be within the range of 14-40kJ/mol^{-1} [121, 130]. So it can be concluded that the Grotthuss mechanism can be used to explain proton conduction of HPA/Nafion composite membranes at 95% relative humidity.

While at 60% relative humidity level, the activation energy of NMA10, NMA20, NWA10, and NWA20 was 62.77 $kJ \cdot mol^{-1}$, 18.73 $kJ \cdot mol^{-1}$, 23.45 $kJ \cdot mol^{-1}$, and 19.09 $kJ \cdot mol^{-1}$ respectively. They are also lower than the activation of energy of recast Nafion (67.66 $kJ \cdot mol^{-1}$) at 60% relative humidity. It can be concluded that doping HPA in

Nafion leads to a lowered proton conduction activation energy, and thus a better proton conductivity.

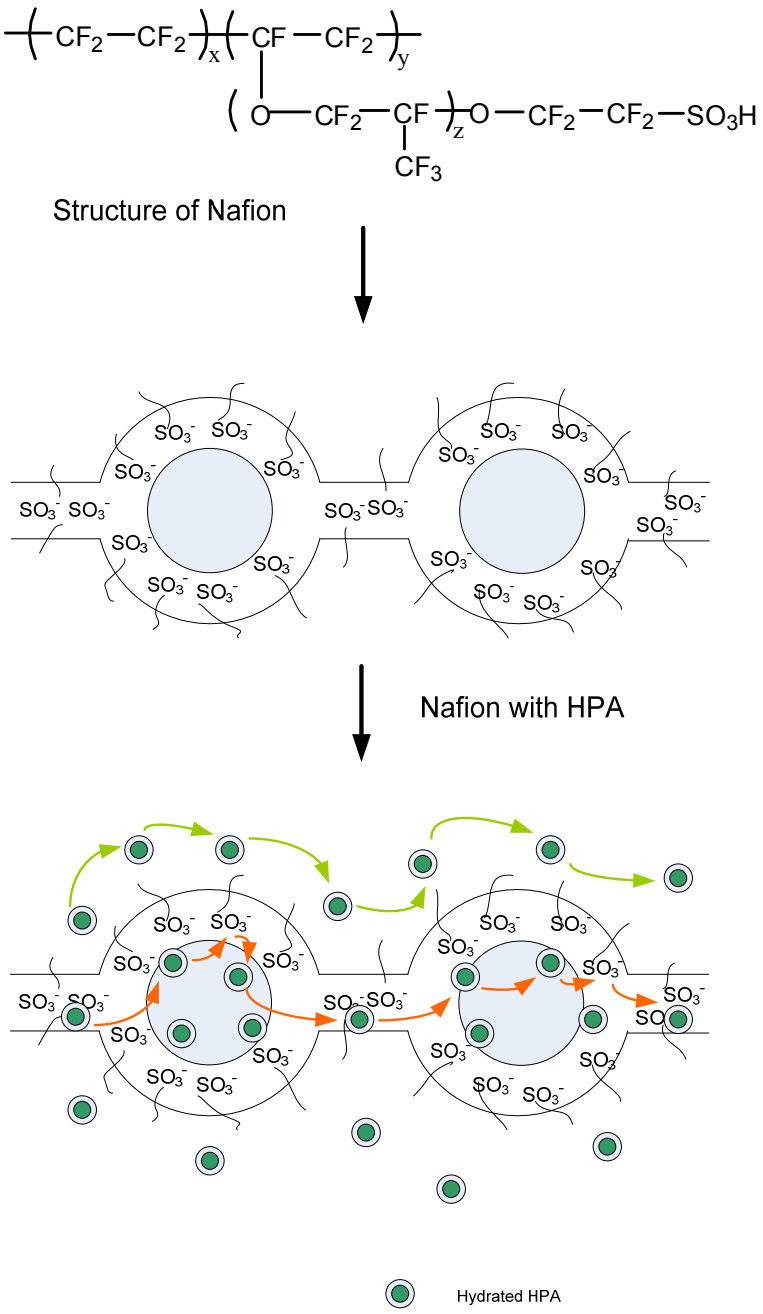

Fig 4-9. Schematic illustration of proton conduction in Nafion/HPA composite

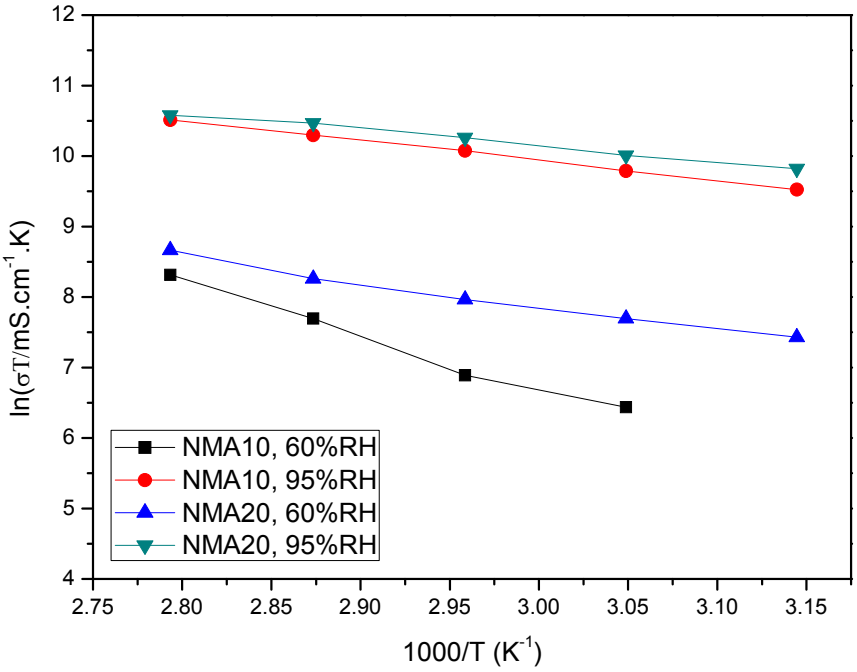

Fig 4-10. Arrhenius plot of NMA at different humidity levels

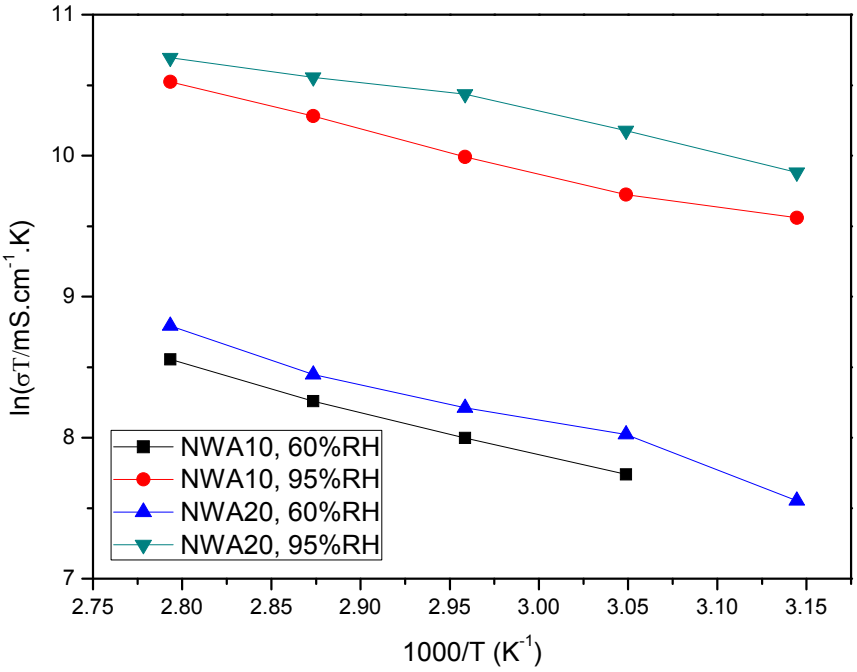

Fig 4-11. Arrhenius plot of NWA at different humidity levels

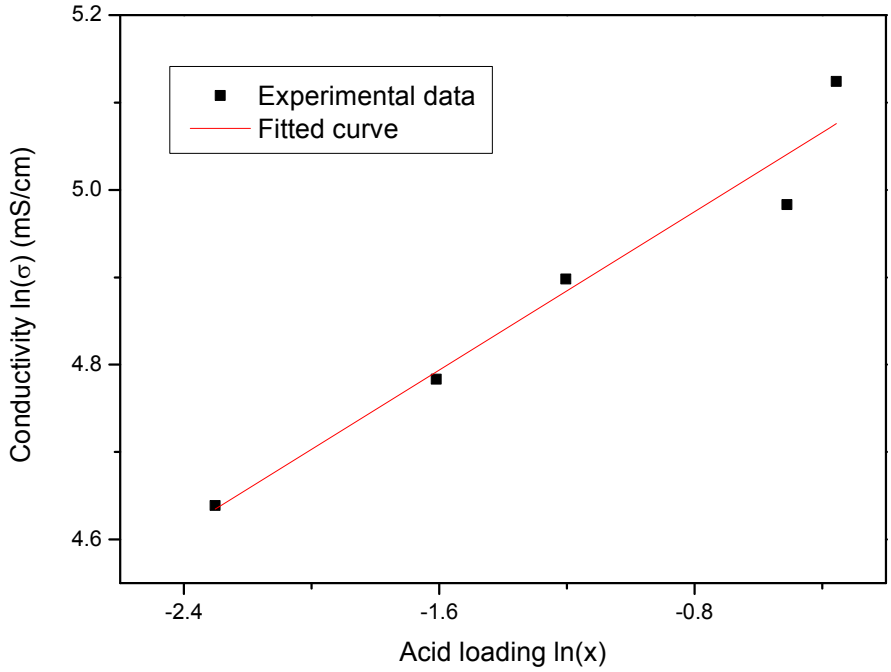

Fig 4-12. Curve fitting on conductivity data of Nafion/PWA membranes at 85ºC and 95% RH

To study the relationship between acid doping level and proton conductivity, the proton conductivity of several PWA/Nafion composite membranes with different doping levels was measured at 85ºC and 95% relative humidity. At acid-doping level higher than 70%, the composite membranes became mechanically very weak and it was difficult to perform the measurement. The power law of percolation theory is used to fit the experimental data:

$$\sigma_m = \sigma_0(\varphi - \varphi_c)^t$$

Where σ_m is the conductivity of the composite membrane, σ_0 is a prefactor, φ is the acid loading, φ_c is the threshold volume fraction of acid percolation, and t is a constant. Based on curve fitting on the conductivity data, σ_0 equals to 179.648 mS/cm and t equals to 0.227. The threshold volume fraction φ_c is ideally 0.15 for three dimensional random structure [37].

The proton conductivity of PNWA10 and TNW10 is shown in Fig 4-12. It can be seen that the proton conductivity is lower than that of HPA/Nafion membranes, but still much higher than that of recast Nafion. Because of the presence of silica, the actual acid doping level of PNWA10 and TNWA10 was lower than 10%. The exceptionally good proton conductivity could come from the hydrophilic nature of the nanoscale silica structure. Further, from the conductivity data, it can be seen that the mesoporous silica structure generated by the templating mechanism can lead to a much higher proton conductivity than that obtained by the direct sol-gel method. The mesopores in the silica structure may host water clusters and greatly increase the surface area of the silica/HPA structure.

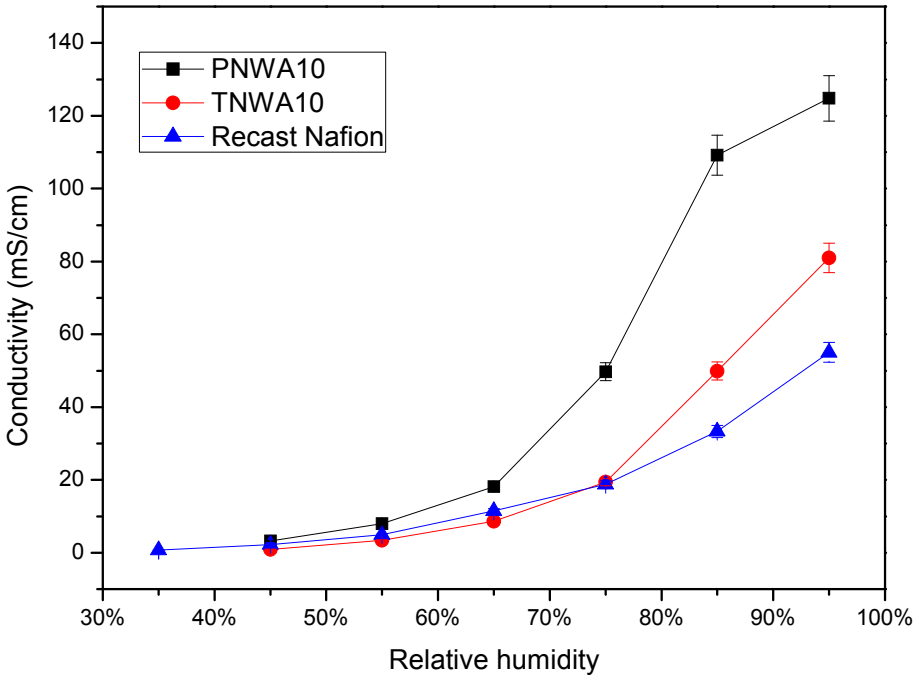

Fig 4-13. Proton conductivity of PNWAand TNWA at 85ºC

The proton conductivity data of AZW10 and AZM10 at 85ºC is plotted in (Fig 4-13). It can be seen that Y zeolite-trapped HPA still shows a good proton conductivity,

though somewhat lower than pure HPA. But, the Y zeolite-trapped HPA was secured inside the supercages of zeolite and did not leach out even with the presence of water. Due to the existence of Al_2O_3 in the zeolite structure, the reaction to generate HPA was not complete and a good portion of the supercages was actually not occupied by HPA anions. This can be used to explain the lower proton conductivity of AZW10 and AZM10 than that of PNWA10 and NWA10/NMA10. Kreuer [121] reported that zeolites were proton conductors but the proton conductivity was orders of magnitude lower than those of Nafion and HPA. Hence, the proton conductivity of AZW10 and AZM10 were mainly contributed by the HPA trapped in zeolite, but not from zeolite. Compared to the Nafion composite membranes doped with pure HPA, the zeolite/HPA-based membranes are expected to have a much longer service life as the acid leaching is no longer a problem.

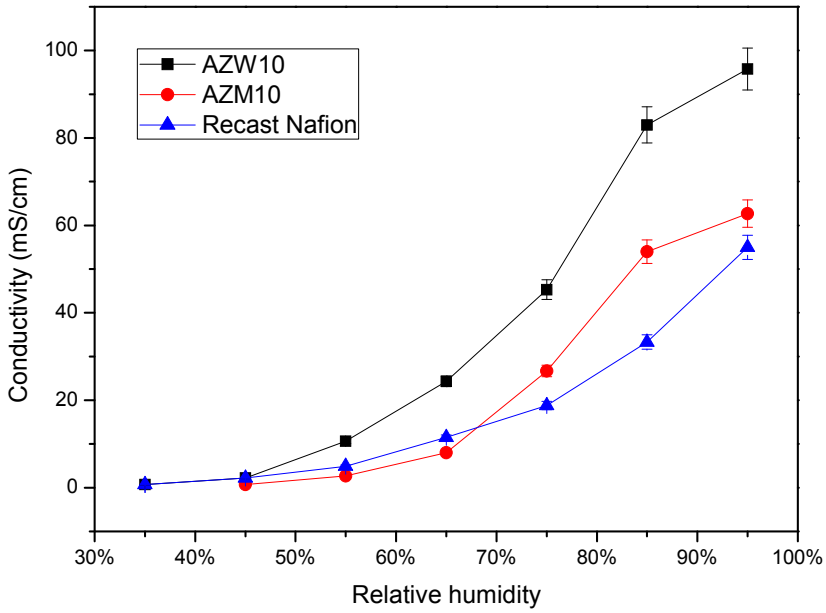

Fig 4-14. Proton conductivity of AZW10 and AZM10 at 85ºC

Table 4-2. Electrochemical parameters of Nfion/HPA membranes

Sample	OCV (V)	Activation energy ($KJ \cdot mol^{-1}$)		Tg (ºC)	Max power density (mW/cm^2)
		60% RH	95RH		
Recast Nafion	0.932	67.7	30.70	142.37	0.195
NMA10	0.873	62.80	23.60	129.06	0.254
NMA20	0.877	28.60	18.70	132.02	0.284
NWA10	0.955	27.50	23.40	123.85	0.249
NWA20	0.988	26.40	19.10	128.13	0.298

4.4.2 Acid leaching

The EDS result of Y zeolite-encaged PMA is shown in (Fig 4-14). As the zeolite/PMA powders were washed with distilled water before EDS scan, it is reasonable to assume that all the PWA not trapped in Y zeolite was washed away and any PWA detected should be within the supercages of Y zeolite. In a separate study, by directly mixing PWA with Y zeolite, all the PMA was lost after washing with water. The EDS spectrum indicates that a good amount of PMA was left behind after washing with water. The EDS result is a direct indication that PMA can be trapped in Y zeolite.

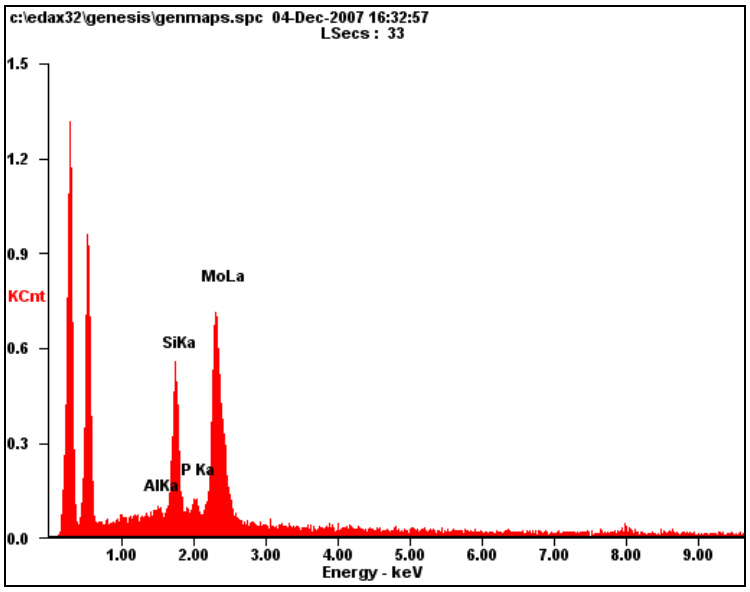

Fig 4-15. EDS element analysis of PMA trapping in Y zeolite

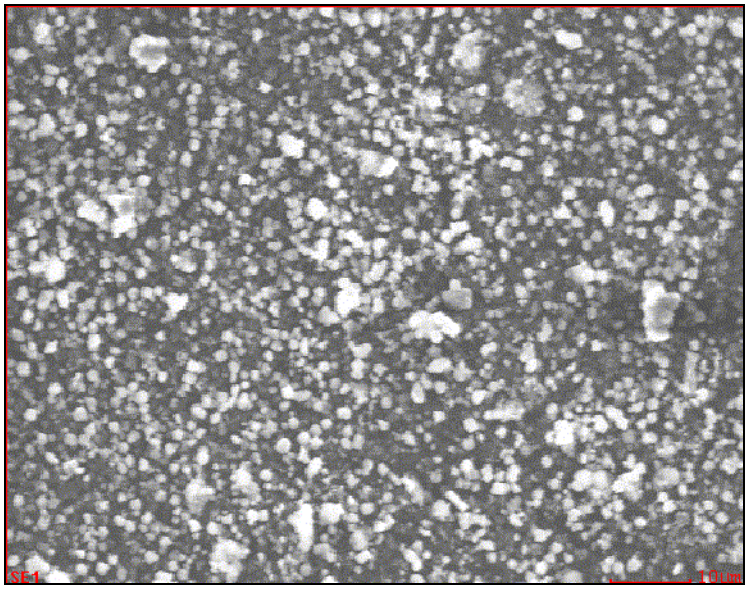

Fig 4-16. EDS element analysis region of PMA/Y zeolite

PWA trapping in Y zeolite was also studied by EDS and the result was shown in (Fig 4-16). It can be seen that the amount of PWA trapped in Y zeolite was less than that of PMA, which could be caused by the lower solubility of WO_3 in water than MO_3.

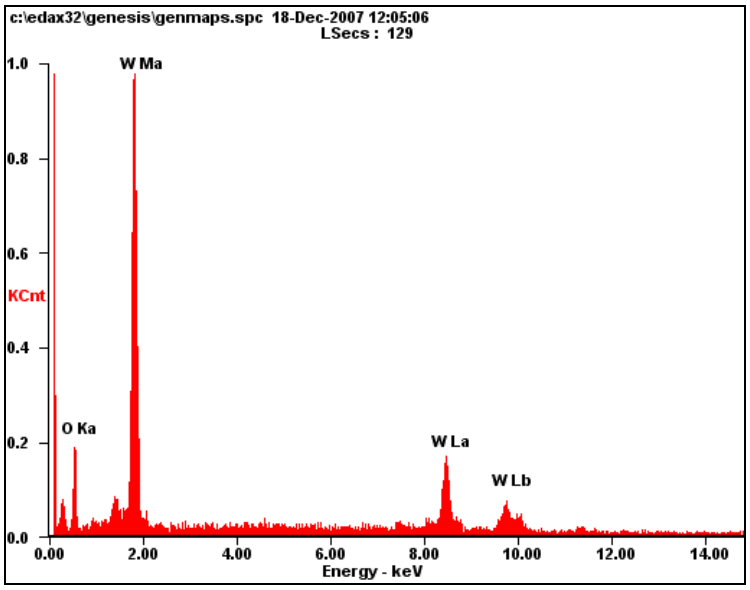

Fig 4-17. EDS element analysis of PWA trapping in Y zeolite

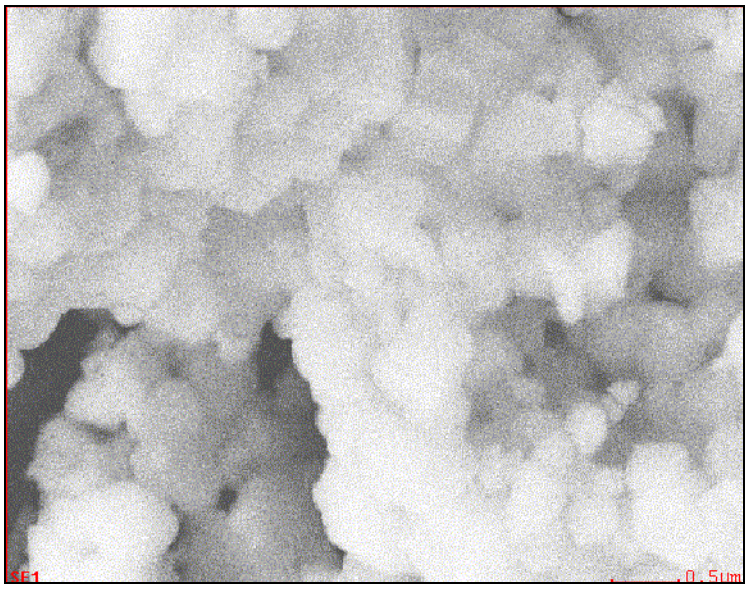

Fig 4-18. EDS element analysis region of PWA/Y zeolite

4.4.3 Morphology

The SEM morphology of Y zeolite and HPA-encaged Y zeoltie powders is shown in (figure 4-18 to figure 4-23). It can be seen that the average particle size of zeolites is about 0.5 microns which is somewhat large for preparing composite membranes. During

casting of the composite membranes, the concentration of the polymer solution and heating rate are important for making uniform zeolite/HPA/Nafion membranes. If the Nafion solution is too dilute or the heating rate is not high enough, the gravity of the zeolite powders will cause them to accumulate toward the glass plate and cause a layered structure. It can also be seen that zeolite particles tend to agglomerate and form larger clusters. The size of the larger clusters could be a few microns or even larger. Those larger clusters make uniformly dispersing zeolite particles in the final composite membranes very difficult.

After encapsulating the HPA molecules, the morphology of Y zeolite didn't change, which indicates that the supercages of Y zeolite did not collapse during HPA formation inside them.

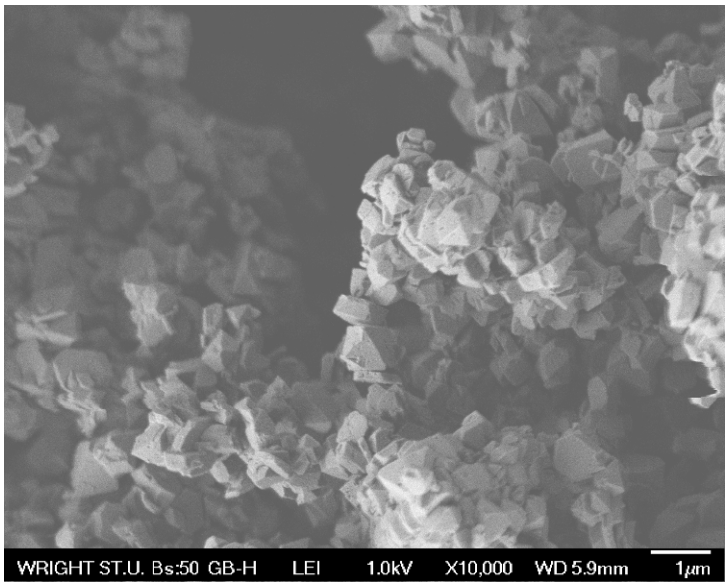

Fig 4-19. SEM micrograph of Y zeolite

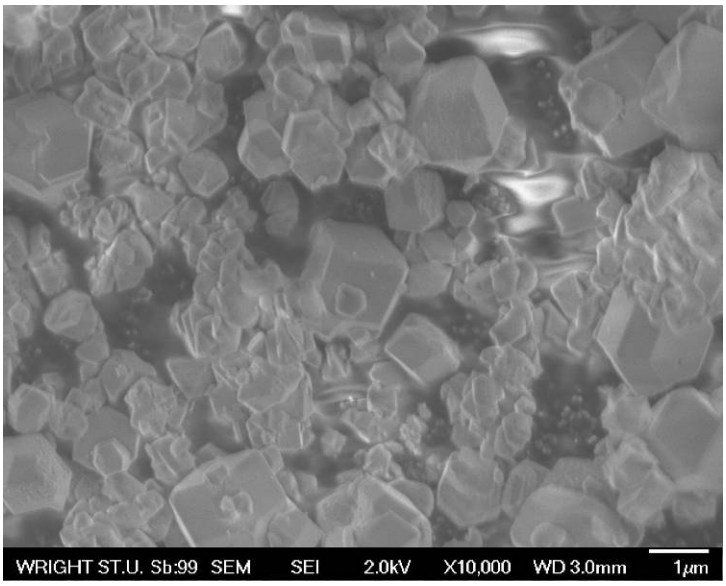

Fig 4-20. SEM micrograph of Y zeolite encaged with PWA

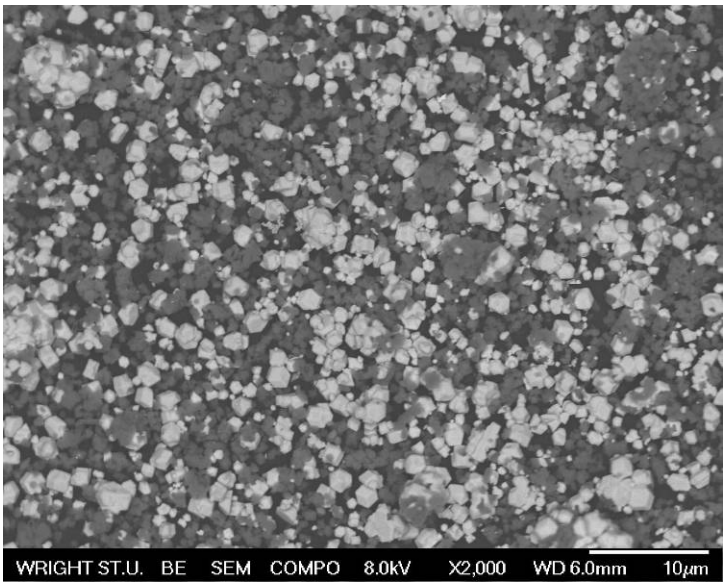

Fig 4-21. SEM micrograph of Y zeolite encaged with PWA (Low resolution)

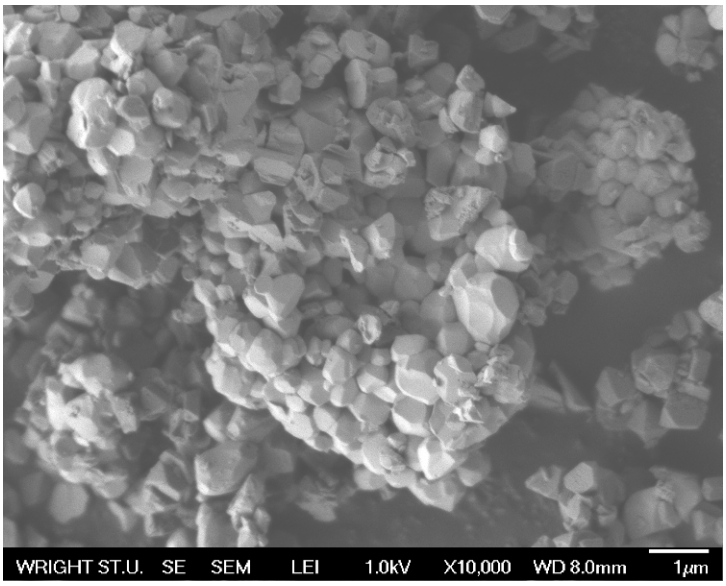

Fig 4-22. SEM micrograph of Y zeolite encaged with PWA (after wash)

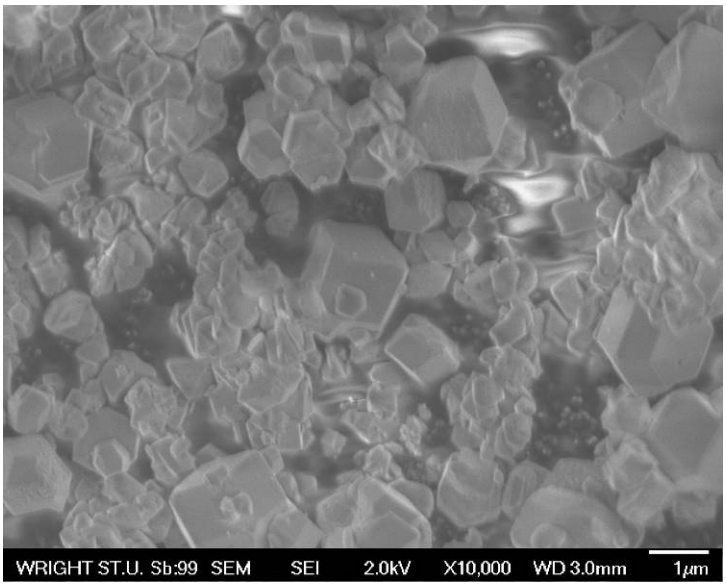

Fig 4-23. SEM micrograph of Y zeolite encaged with PMA (low magnification)

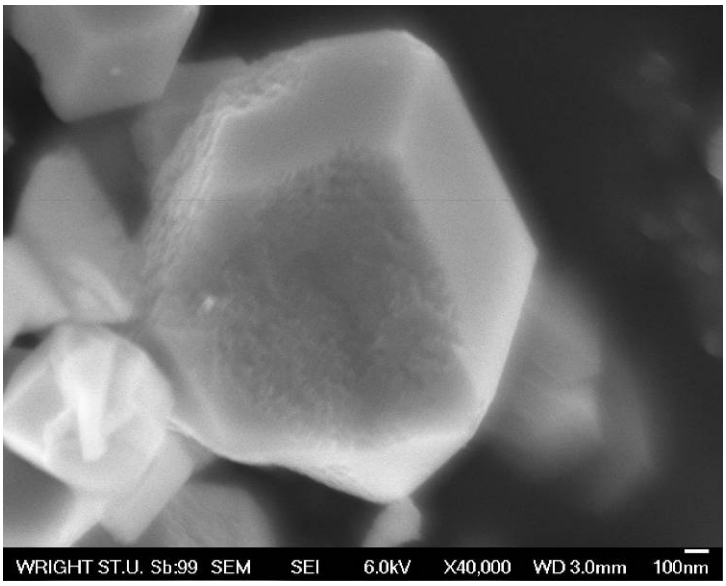

Fig 4-24. SEM micrograph of Y zeolite encaged with PMA (high magnification)

4.4.4 Thermal properties

Nafion has the same $-(CF_2)_n-$ backbone structure as PTFE which is thermally very stable. By incorporating ionic side groups, the thermal stability of Nafion decreases; but Nafion is till thermally stable up to 300ºC. When heated in air over 125ºC, the color of Nafion membranes will become dark brown which can be removed by boiling in dilute H_2SO_4 solution and the proton conductivity can be recovered.

The TGA curves of recast Nafion and HPA/Nafion composite membranes are shown in Fig 4-24. All five samples had no more than 5% weight loss before 320ºC, and the weight loss in this region was caused by evaporating the trapped moisture and solvent. After 320-350ºC, thermal decomposition of Nafion began. By studying the released gas at different temperature ranges, the process of Nafion degradation can be divided into desulfoanation, side-chain decomposition, and backbone decomposition [44, 109]. At temperatures over 600ºC, the decomposition of all the membranes was about

complete. By incorporating HPA into Nafion structure, the thermal stability of the composite membranes was still close to that of pure recast Nafion.

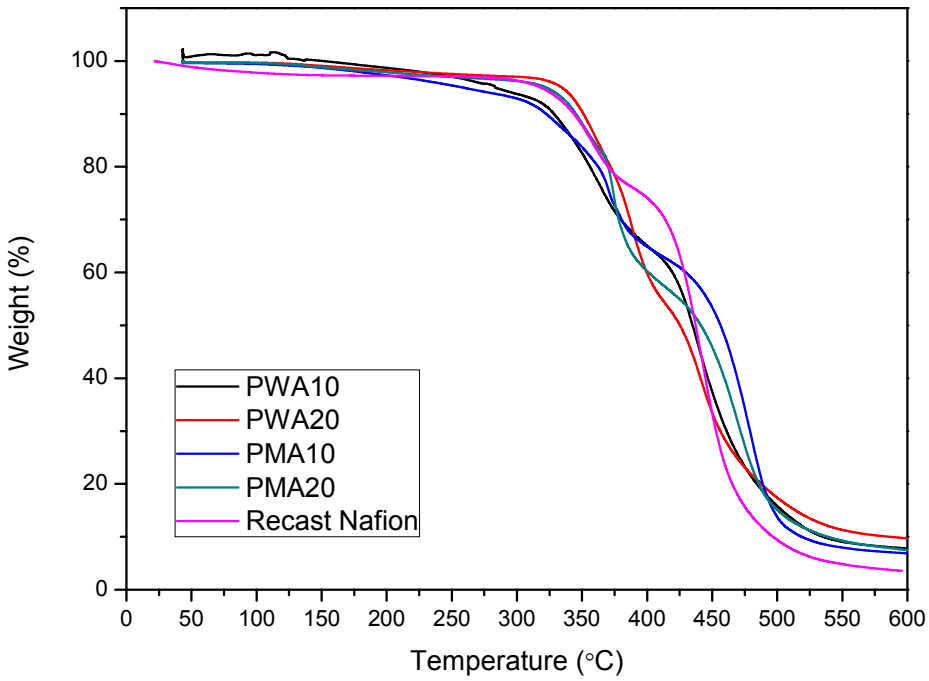

Fig 4-25. TGA plot of HPA/Nafion composite membranes

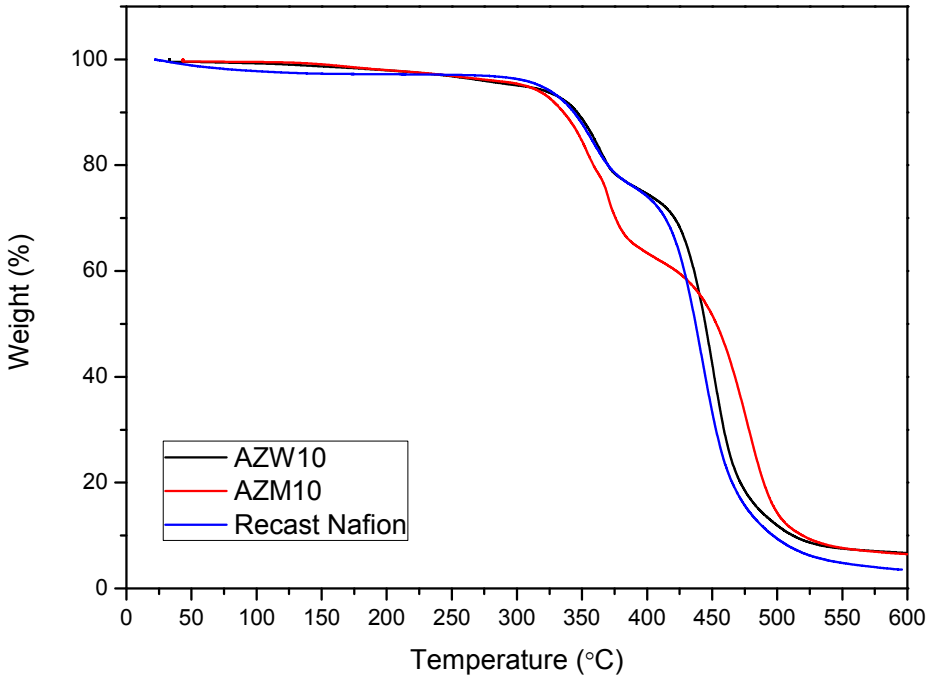

Fig 4-26. TGA plot of HPA/Zeolite/Nafion composite membranes

As no obvious transitions were observed from DSC curves, TMA was used to study the glass transition temperature (Tg) of the composite membranes. On a TMA plot, Tg is defined as the temperature of the change of thermal expansion coefficient. Although DSC is usually regarded as the official way to measure Tg, TMA is also widely used and the result from TMA is only about 5-10ºC different from the result of DSC. By incorporating PWA and PMA into Nafion, the glass transition temperature of the composite membranes decreased by about 10-18ºC compared to pure recast Nafion. The decrease in Tg indicates that HPA molecules do not have a strong interaction with Nafion polymer chains, and these acid molecules make the movement of polymer chains easier [80].

One reason for the degradation of a membrane electrode assembly (MEA) is the difference in thermal expansion coefficient between the carbon electrode and the polymer membrane. Usually the thermal expansion of polymers is much higher than that of carbon (10^{-6}). It can be seen from the TMA plot that at temperatures lower than 125˚C, Nafion with HPA additives shows almost the same thermal expansion coefficient as pure recast Nafion. When the temperature was over 125˚C, all four Nafion/HPA composite membranes showed much higher thermal expansion coefficients and the value quickly reached 43%. Considering the adverse effect of thermal expansion on the MEA, HPA-incorporated membranes are not suitable for operation at a temperature over 125˚C. By incorporating zeolite into Nafion, the thermal expansion coefficient of the composite membranes at temperatures between room temperature to 100ºC was almost the same as recast Nafion. At temperatures between 100ºC and 140ºC, AZM10 and AZW10 showed much less thermal expansion than recast Nafion. PNWA10 and TNW10 showed similar

thermal expansion behavior to that of AZM10 and AZW10. As zeolite is essentially a combination of Al_2O_3 and SiO_2, so it can be concluded that the thermal expansion of Nafion membranes can be reduced by incorporating oxide particles. This conclusion was further verified by TMA plot of PNWA10 and TNWA10.

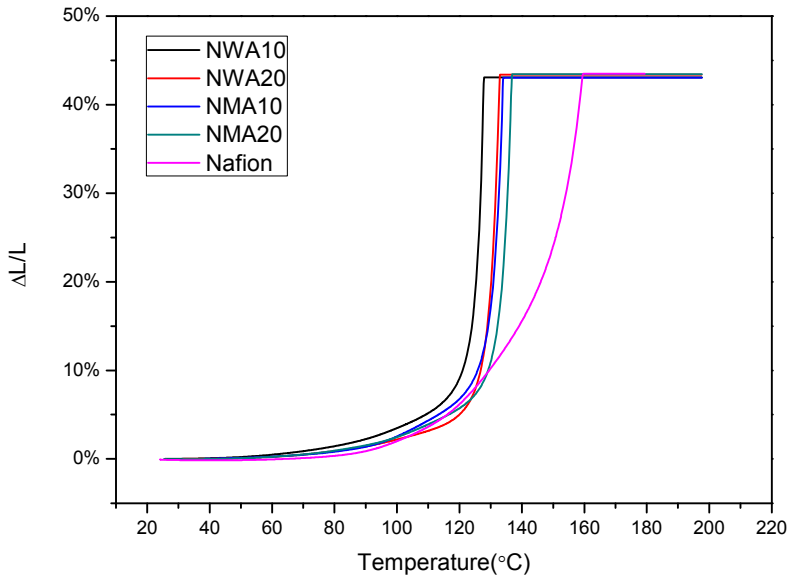

Fig 4-27. TMA plot of HPA/Nafion composite membranes

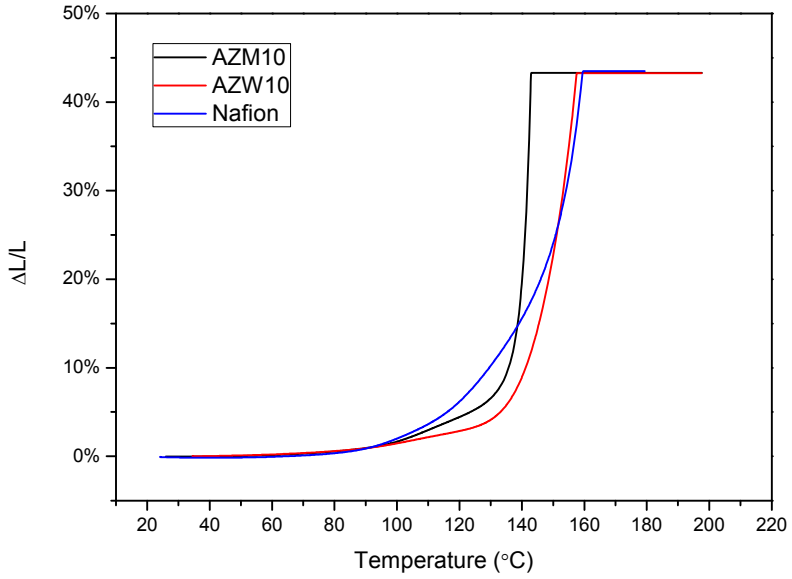

Fig 4-28. TMA result of zeolite/HPA/Nafion composite membranes

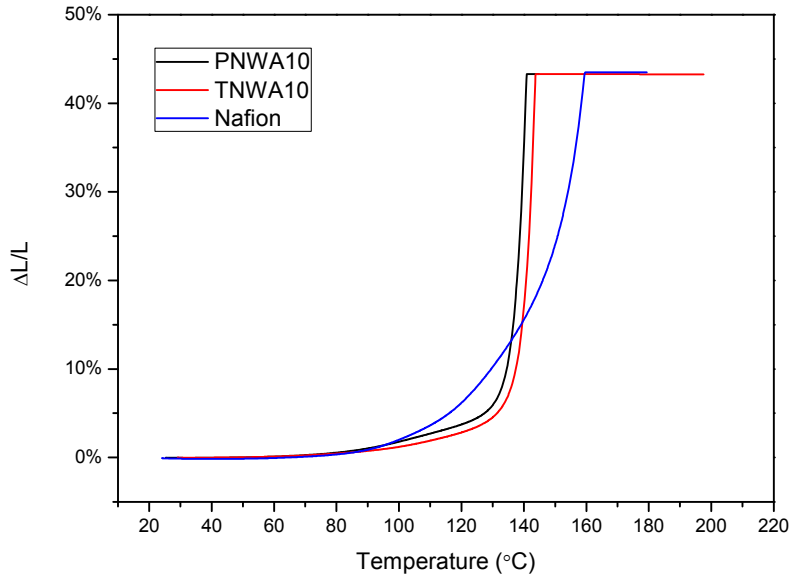

Fig 4-29. TMA result of SiO_2/HPA/Nafion composite membranes

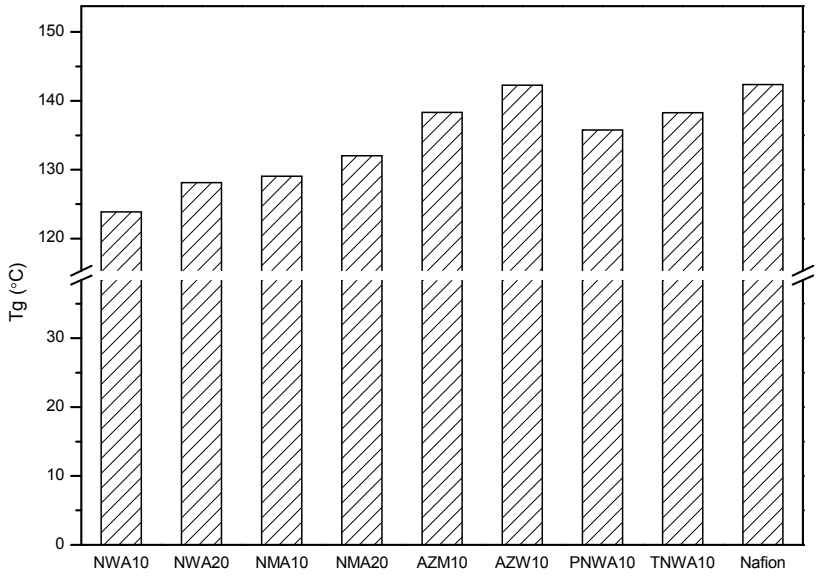

Fig 4-30. Glass transition temperature obtained by TMA

4.4.5 Single cell performance

The single cell performance of all the MEAs prepared from the composite membranes is shown on (Fig 4-30—Fig 4-35). The polarization curves were measured at 85˚C with no back pressure of humidified H_2/O_2 reactant. As the membranes used for

making MEAs were controlled to have the same thickness, the single cell performance is also an indication of the proton conductivity of the membranes. These data indicate that MEAs with HPA additives exhibit better performance than MEA made from recast Nafion. If reactant gas crossover is not considered, MEAs with lower resistance will have better single cell performance because of lower ohmic loss. In a previous conductivity study, proton conductivity of Nafion was increased by adding HPA additives. This effect can also be seen in the single cell performance: NWA20 showed better performance than NWA10, and recast Nafion has the lowers power output. The peak power output of NWA20 MEA had about 0.1W/cm^2 more power density output than recast Nafion MEA, which means a 50% performance increase. Similar single cell performance was observed on NMA20 and NMA10 MEAs.

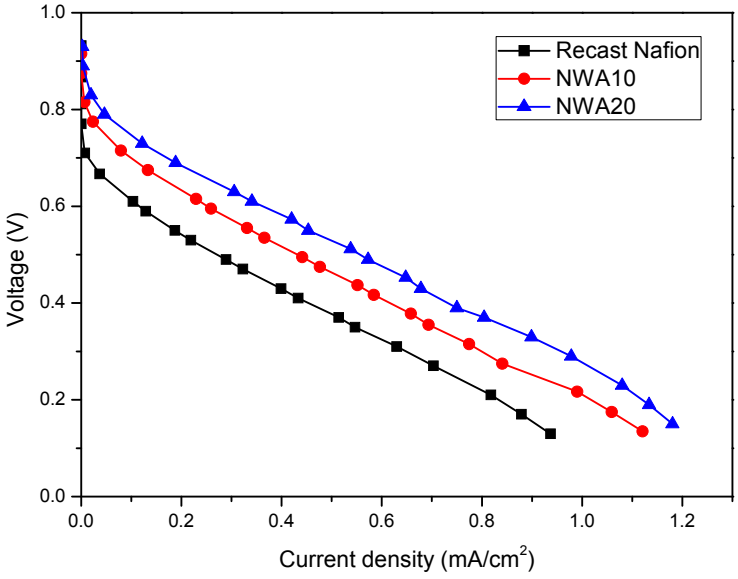

Fig 4-31. U-I curves of NWA20, NWA10, and recast Nafion MEAs at 85˚C and 1 atm

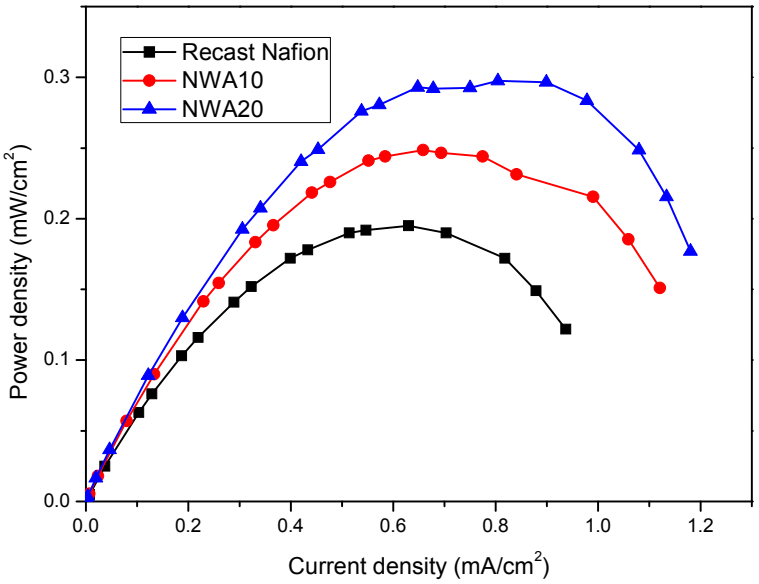

Fig 4-32. P-I curves of NWA20, NWA10, and recast Nafion MEAs at 85˚C and 1 atm

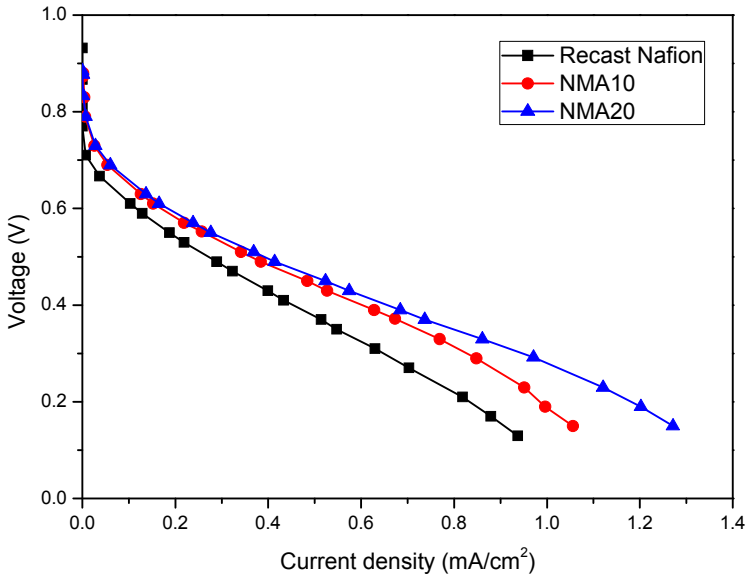

Fig 4-33. U-I curves of NMA20, NMA10, and recast Nafion MEAs at 85˚C and 1 atm

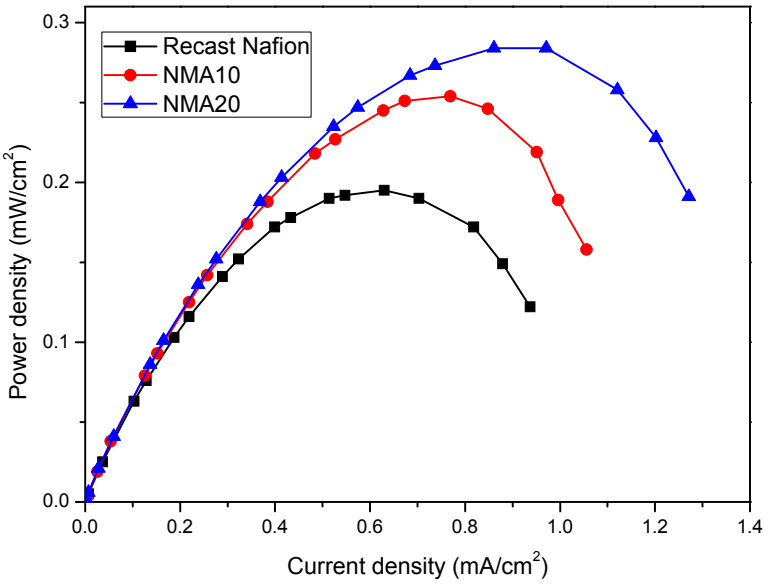

Fig 4-34. P-I curves of NMA20, NMA10, and recast Nafion MEAs at 85˚C and 1 atm

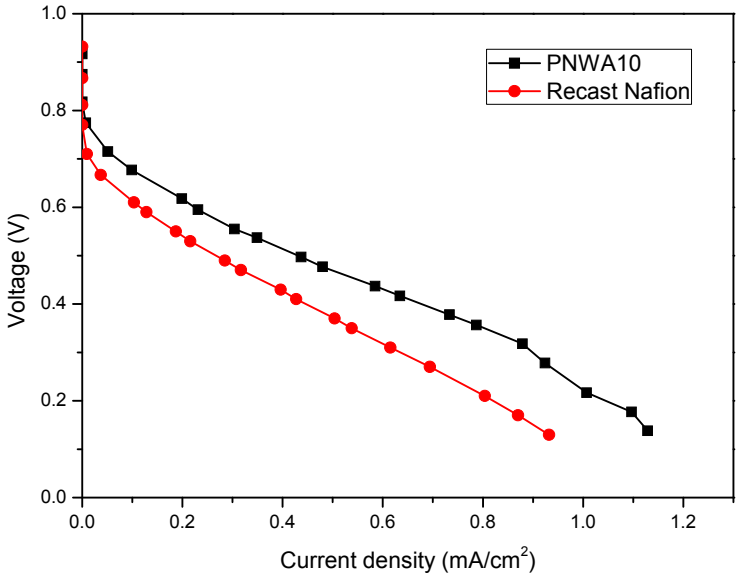

Fig 4-35. U-I curves of PNWA10 and recast Nafion MEAs at 85˚C and 1 atm

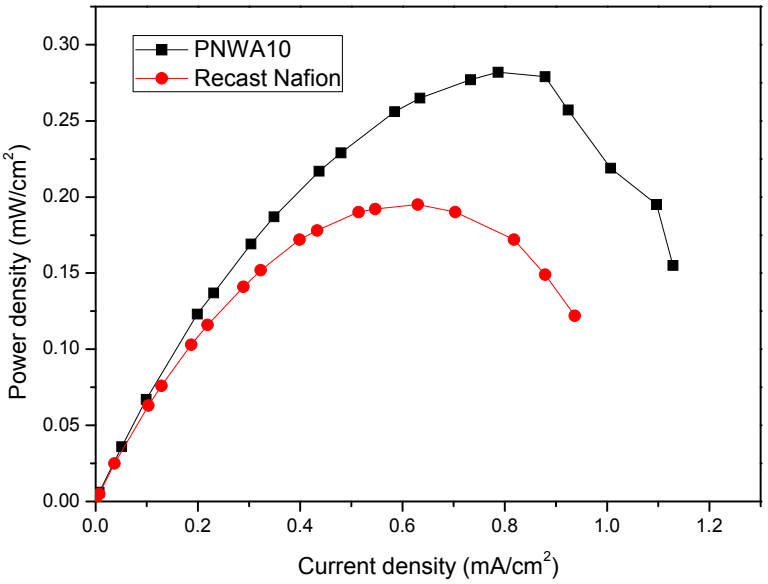

Fig 4-36. P-I curves of PNWA10 and recast Nafion MEAs at 85˚C and 1 atm

5. Hydrophilic ePTFE-based PEM

5.1 Introduction

Proton exchange membrane fuel cells (PEMFCs) have attracted ever increasing attention from the renewable energy research community in recent years because of their potential applications for vehicular transportation and portable electronics. Compared to other energy generating devices, fuel cells have the advantage of high power density, high efficiency, zero emission, and quite operation. One of the critical components of PEM fuel cells is the proton exchange membrane (PEM), which is used to separate the anode and cathode. The requirements for PEMs are high proton conductivity, high mechanical strength, good thermal stability, good dimension stability, and low fuel permeability. For several decades, Nafion® (DuPont de Nemours) has been the material of choice for proton exchange membranes. Although a tremendous amount of of research work has been performed to develop new proton exchange materials as a replacement for Nafion®, almost all of the current commercially available PEM fuel cells are still using Nafion® as the PEM material.

One of the limiting factors for the commercialization of fuel cells is the high cost. In order to reduce the loading of high-cost Nafion®, expanded PTFE (ePTFE) has been used for the supporting material for composite proton membranes [1-3]. ePTFE has very high mechanical strength, excellent chemical and thermal stability, and a much lower cost compared to Nafion®, which make it a very good candidate for the supporting matrix

materials of composite membranes. Further, because of the high mechanical strength of ePTFE, very thin membranes are practically possible. When the thickness of proton exchange membranes is greatly reduced, their resistance is also reduced accordingly. However, one great drawback of ePTFE is its high hydrophobicity, which can make the preparation of a very dense membrane very difficult [65, 67]. Additionally, the pinholes and voids left in the composite membrane can cause fuel crossover and electrical short circuit. Further, according to the Grotthuss Mechanism [15, 16] and the Vehicle Mechanism [17], lack of water can lead to a dramatic reduction in proton conductivity. Earlier studies indicate that the surface characteristics of the original hydrophobic ePTFE can be modified by exposure to plasma and ion beam, etching with sodium naphthalene, and molecular grafting [69, 70, 161-164]. These modifications only change the surface properties of ePTFE in a depth of nanometer scale, which means the majority of the mechanical strength is unchanged. The modified ePTFE (hydrophilic ePTFE) shows much a lower contact angle, improved wettability, and easier adhesion to other materials. Currently, the commercial hydrophilic ePTFE is generally used for liquid filtration.

In this work, we fabricated a composite membrane consisting of hydrophilic ePTFE- supported Nafion compared its performance with that of hydrophobic ePTFE-supported Nafion membrane and pristine recast Nafion membrane. These two composite membranes were compared in terms of their wettability, water uptake, proton conductivity, and single cell performance. Scanning electron microscopy (SEM) was conducted to study the morphology of the composite membranes. Thermogravimetry analysis and thermo-mechanical analysis were used to study thermal properties of the membrane samples.

5.2 Membrane preparation

The hydrophilic ePTFE membrane (0.2μm pore size, 71% porosity) was donated by Donaldson Company, Inc. The hydrophobic ePTFE (0.1 μm pore size, 71% porosity) was donated by Advantec MFS, Inc. The 5% Nafion® solution (equivalent weight=1000) was purchased from Ion Power. The as received Nafion solution was transferred into 5% DMAc (BASF) based solution before casting.

To make the comparison between hydrophilic- and hydrophobic- supported composite membranes more reasonable, the two composite membranes were prepared in the same manner: The ePTFE membranes were first soaked in anhydrous ethanol for half an hour, followed by rinsing in distilled water. The pretreated membranes were stretched in a leveled Petri dish, and 5% Nafion was applied onto the membrane. After that, the Petri dish containing the membrane samples was dried in an oven at 70ºC for half an hour. The same procedure was repeated for several times until the surface of ePTFE membrane was all covered by dry Nafion. After that, the membranes were dried in a vacuum oven overnight at 70ºC. The dried membranes were peeled off from the Petri dish and cut into several pieces for subsequent testing. The membranes for proton conductivity testing were boiled in 3% H_2O_2 for 30 min to remove organic impurities, followed by rinsing with distilled water and boiling in 1M H_2SO_4 for half an hour to remove trace metal impurities. Finally, the membranes were rinsed with distilled water continuously until the pH value was about 7. After that, the membranes were stored in distilled water until measurement.

5.3 Membrane characterization

The wettability test was performed by dropping distilled water on top of hydrophobic and hydrophilic ePTFE membrane and observing the interaction between water droplets and the membranes.

For the water uptake, the membrane samples were dried in a vacuum oven at 70ºC overnight and the initial weight (W_1) was recorded. After that, the membranes were soaked in distilled water at room temperature for two days. The water on the surface of the fully soaked membrane samples was quickly removed by Kimwipe™ and the wet weight was recorded (W_2). The water uptake was calculated by the following equation

$$\Delta W(\%) = \frac{W_2 - W_1}{W_1} \times 100\%$$

The cross-section of the composite membranes were examined by scanning electron microscopy (SEM, JEOL Field Emission Scanning Electron Microscopy, JSM-7401F)

A four-probe conductivity cell was used to measure the proton conductivity. The proton conductivity cell has four platinum electrode supported on a PTFE frame. During testing, the conductivity cell was placed in a humidity chamber (ESPEC, SH-241). A Keithley 2400 source meter was used to supplysource current and measure voltage. At each temperature/humidity level, the membrane was conditioned for at least 30 minutes or until equilibrium before measurement. Each conductivity data comes from a linear regression of several current/voltage data pairs. The dimension of the membrane samples used for conductivity calculation was measured at a dry state.

The proton conductivity was calculated by

$$\sigma = \frac{1}{\rho} = \frac{d}{RS} = \frac{R}{R \cdot w \cdot t} \quad (1)$$

where t is the average thickness of the membrane, R is the resistance which can be got by a linear fit of the VU-I curve, w is the sample width, and d is the distance between two inter electrodes.

A commercial gas diffusion electrode material (GDE, E-TEK Inc) with Pt catalyst loading of 0.5mg/cm^2 was used to make the membrane electrode assembly (MEA). The electrode was impregnated with about 0.6mg/cm^2 Nafion (dry weight, 5% Nafion solution, Ion Power). The GDE and membrane were sandwiched between two PTFE sheets and hot pressed into a MEA at 130ºC with a pressure of 70 kg/cm^2 for three minutes. The MEA was installed into a single cell and tested with a fuel cell test station (Asia Pacific Fuel Cell Technologies, Ltd., FCED-PD50). The MEA was conditioned by humidified H_2/O_2 at open circuit voltage for 2 hours before testing. The testing condition was 60ºC and 60% relative humidity.

Thermogravimetry analysis (TGA, TA Instruments, TGA Q500) was performed to study the thermal stability of the membranes. The TGA experiment was performed in a nitrogen atmosphere and a heating rate of 10ºC/min. The glass transition temperature (Tg) and thermal expansion coefficient of the samples was studied by Thermo-Mechanical Analysis (TMA, TA Instruments, TMA Q400).

5.4 Results and discussion

In the wettability test, it was observed that water droplets couldcan quickly entered the pores of hydrophilic ePTFE, which makes it much easier to avoid the formation of pinholes in the composite membrane. Further,And the hydrophilicity helps

to maintain water content inside the composite membrane, leading to a and thus better proton conductivity. In contrast,While for hydrophobic ePTFE, water droplets always stayed on top of the membrane because of the hydrophobic nature of pristine PTFE.

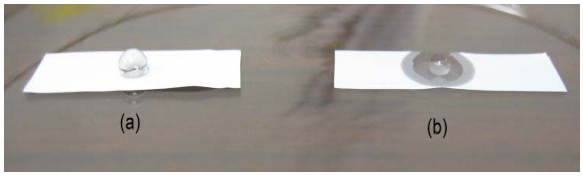

Fig 5-1. Wettability test of (a) hydrophobic ePTFE, and (b) hydrophilic ePTFE

The SEM micrographs (Figures 5-2 & 5-3) showed the micrograph of the cross sections of the composite membranes. In Fig.5-2, we can see the micro-pores of hydrophilic ePTFE were well impregnated with Nafion resin. A number of pinholes were observed at some locations in the hydrophobic ePTFE based composite membrane. These pinholes could be the pathway for gas crossover during the fuel cell operation, which can cause wastagee of fuels and lower the fuel cell operational voltage. The effect of a decrease in fuel cell operational voltage can be seen in the following equation [5]:

$$V = E - ir - A\ln\left(\frac{i + i_n}{i_0}\right) + m\exp(ni)$$

where E is the reversible OCV, i_n is the internal and fuel crossover equivalent current density, A is the slope of the Tafel line, i_0 is the exchange current density, m and n are the constants, and r is the area-specific resistance. It can been easily seen that hydrophilic ePTFE based membrane will have better polarization performance than hydrophobic ePTFE based membrane because of lower gas crossover.

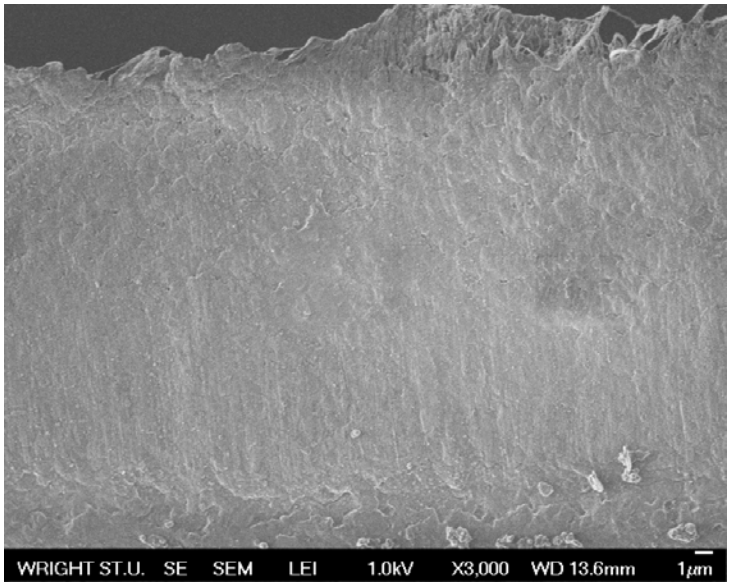

Fig 5-2. Cross section of hydrophilic ePTFE based composite membrane

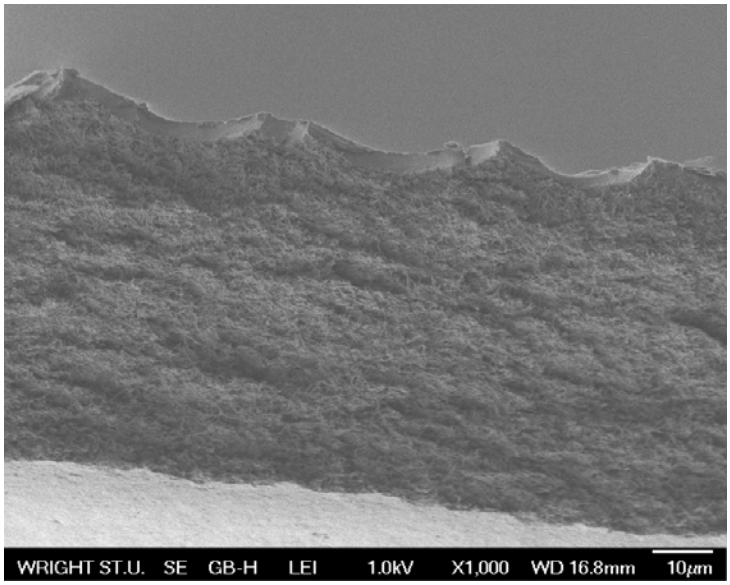

Fig 5-3 Cross section of hydrophobic ePTFE based composite membrane

Not surprisingly, the hydrophilic ePTFE based composite membrane has higher water uptake than the hydrophobic ePTFE based membrane, and that of recast Nafion membrane is somewhere in between. As water content in proton exchange membranes is directly related to proton conductivity [41], the subsequent proton conductivity study

verified that hydrophilic ePTFE based membrane has better proton conductivity than that of hydrophobic base membrane. Also,And both types of composite membranes have lower proton conductivity than pristine recast Nafion. This can be explained by the power law of percolation theory [37]:

$$\sigma = \sigma_0 (c - c_0)^n$$

where c is the volume fraction of the proton conductive phase, n is a universal constant (n=1.5 for a three-dimensional system), c_0 is the threshold volume fraction (15% for a 3D continuous random mixture), and σ_0 is a pre-factor. As the PTFE itself is not protonic conductive, the volume fraction of the proton conductive phase in both composite membranes is lower than that of recast Nafion, and, hence, thus thelower proton conductivity is lower as well. In fuel cell applications, ePTFE supported membranes could be made much thinner compared to pure Nafion membrane because of the high mechanical strength, and the actual area conductivity (S/cm^2) will be much higherlower than that of Nafion membrane.

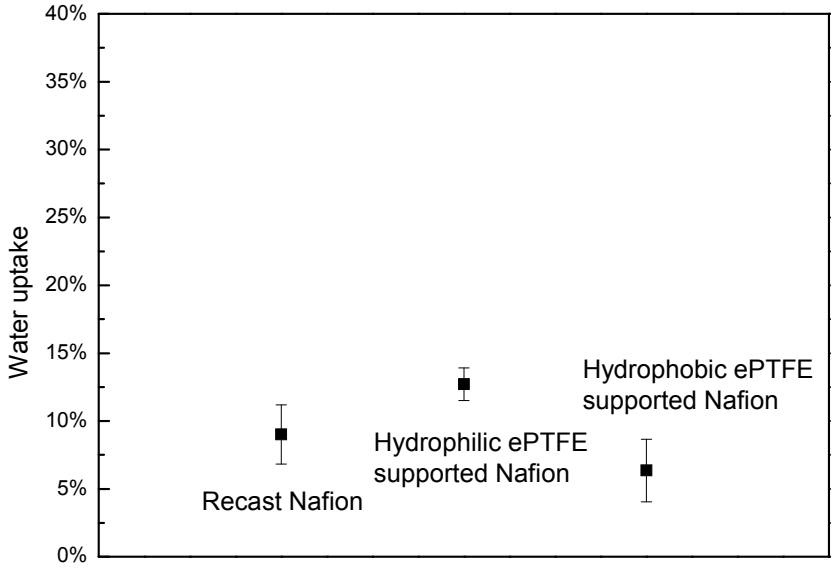

Fig 5-4 Water uptake of ePTFE membranes in liquid water

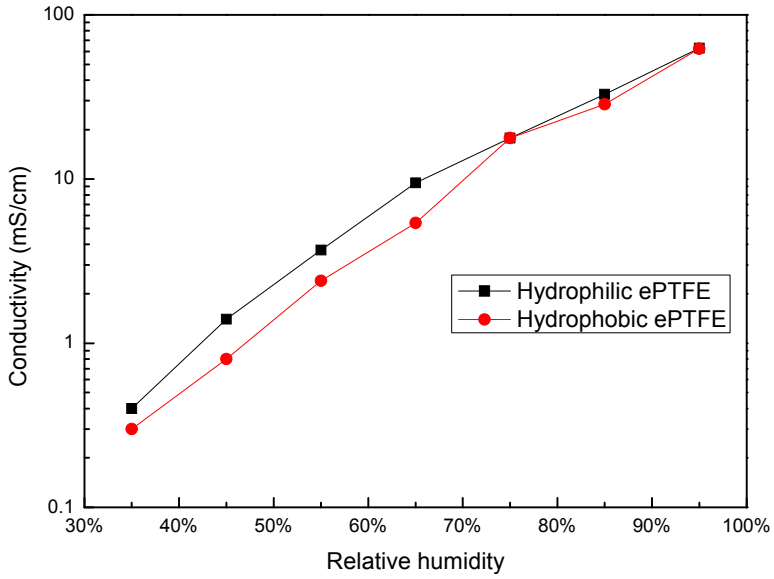

Fig 5-5. Proton conductivity of ePTFE membranes at 85ºC

The TGA thermograms are shown in Fig 6. All the three samples showed some weight loss below 300ºC, which could be ascribed to the vaporization of trapped solvent (DMAc) and water. The recast Nafion membrane began to decompose beyond 300ºC while the two ePTFE based composite membranes are thermally stable until 380ºC. Beginning from about 580ºC, all three membrane samples were completely decomposed and only very small amount of residue was left.

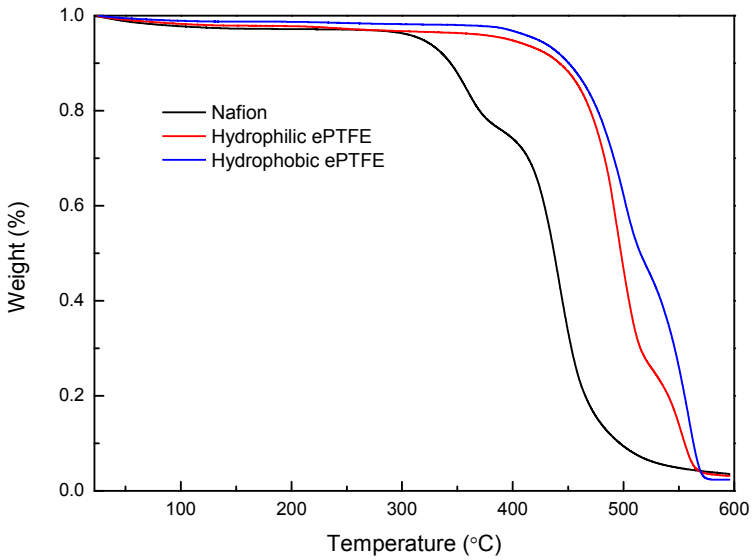

Fig 5-6 TGA curves of hydrophilic ePTFE based membrane, hydrophobic ePTFE supported membrane, and recast Nafion membrane

Both the hydrophilic & hydrophobic ePTFE supported membranes showed much higher glass transition temperature and low thermal expansion coefficient than did recast Nafion membrane. Generally speaking, PEMs have a much higher swelling ratio and thermal expansion rate than do carbon-based gas diffusion layers, which is detrimental to disadvantageous for longthe MEA life when frequently operating fuel cells are operated at frequently varying different humidity and temperature conditions. In this aspect, both ePTFE supported membranes are much superior than recast Nafion which make them very suitable for high temperature applications.

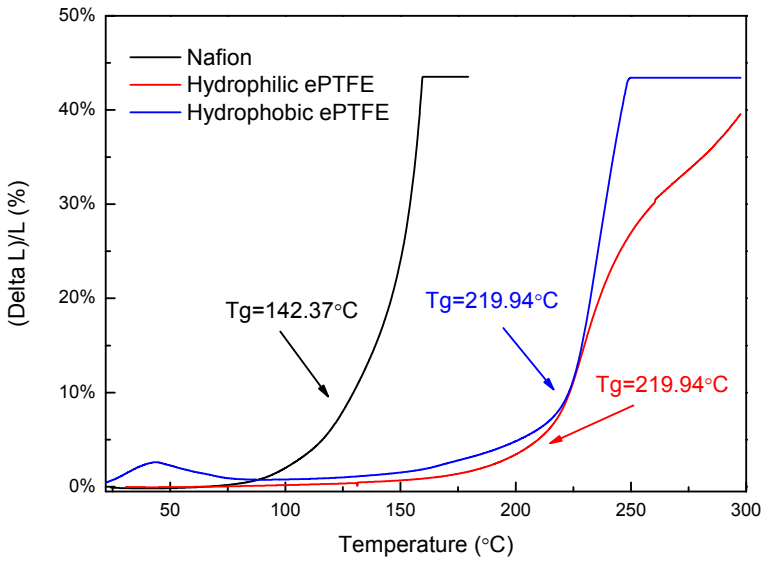

Fig 5-7. TMA curves of hydrophilic ePTFE based membrane, hydrophobic ePTFE supported membrane, and recast Nafion membrane

As mentioned earlier, ePTFE supported membranes are mechanically stronger than recast Nafion, which implies thinner composite membranes can be used without losing mechanical strength. The two ePTFE supported composite membranes (1.75 mils) used for single cell performance study are less than half the thickness of recast Nafion membranes (4.4 mils). Although hydrophilic ePTFE based membrane has lower proton conductivity than recast Naifon membrane as shown in Fig 5-5, the single cell performance of hydrophilic ePTFE based MEA showed the best performance. The low performance of hydrophobic supported membrane is likely due to be the fuel crossover caused by the pinholes left inside.

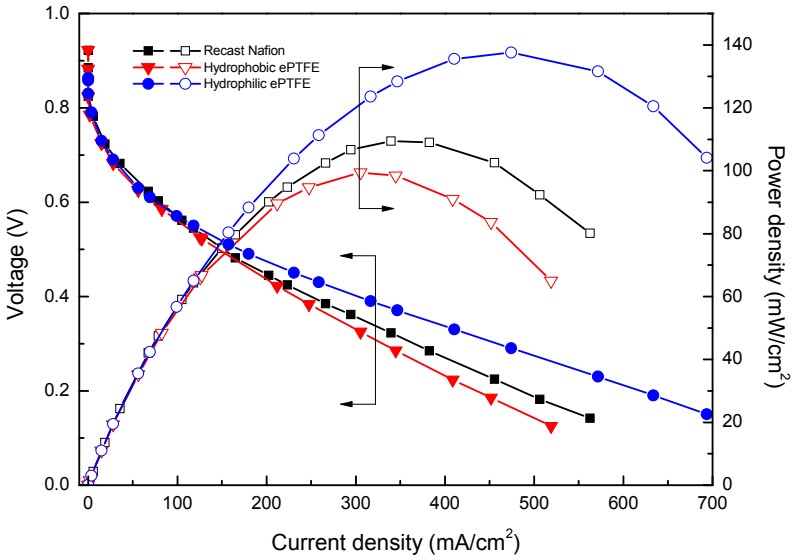

Fig 5-8 Single cell performance at 60ºC and 60% relative humidity

6. Conclusions

This work focused on developing and studying silica and heteropolyacid (HPA) based composite membranes for proton exchange membrane fuel cell applications. Proton conductivity was studied on the composite membranes at 85ºC and different humidity levels. The single cell performance, thermal properties, and other properties that may affect fuel cell performance were studied and compared to recast Nafion membrane. Mesoporous silica and Y zeolite were used to trap HPA from leaching out with the existence of liquid water. Hydrophilic ePTFE supported Nafion was developed and compared to hydrophobic ePTFE supported Nafion and recast Nafion.

Both direct mixing and sol-gel reaction were used to prepare Nafion/silica composite membranes. It was noticed that sol-gel reaction can lead to more uniform distribution of silica particles. Proton conductivity data showed adding silica into Nafion can decrease proton conductivity. But the higher open circuit voltage implied the embedded silica can decrease gas crossover and thus compensate the lowered conductivity. Nafion/silica composite membranes showed improved thermal stability and lower thermal expansion ratio.

Phosphomolybdic acid (PMA) and phosphotungstic acid (PWA) were used as filler materials to increase the proton conductivity of Nafion. It was observed that the

conductivity of PMA and PWA-based composite showed much higher proton conductivity than Nafion and the single cell performance was also better. In order to solve the acid leaching problem, mesoporous silica and Y zeolite was used to trap HPA molecules. EDX result showed HPA was successfully trapped even after washed with water.

In order to improve the mechanical properties and thermal stability, porous hydrophilic ePTFE was used as the supporting material for PEM. Compared to pristine ePTFE, the surface modified hydrophilic ePTFE leads to higher water uptake and better quality membranes. Hydrophilic ePTFE-based composite membranes showed much higher glass transition temperature and lower thermal expansion ratio, which makes them ideal for high temperature applications. Due to the exceptional strength, hydrophilic ePTFE is believed to be an ideal supporting structure for high proton conductive materials.

7. Recommendations for future work

Based on the results showed in this study, adding silica does not significantly improve the performance of Nafion, though lowered fuel crossover was observed. The results showed that the extra water adsorbed by the hydrophilic silica may not take part in proton conduction under the testing conditions. Extra work may be focused on studying the interaction between embedded silica and Nafion polymer chains, and how the silica affect the "pore structure" of hydrated Nafion. It is suggested to study the proton conductivity and single cell performance at temperatures higher than 100ºC. Composite membranes with higher silica loading should be developed and used to verify the fitted percolation equation obtained by fitting Nafion/PWA conductivity data.

Y zeolite and mesoporous were shown to be able to trap HPA, but no quantitative data is available at this point. It is suggested to study the total percentage of the zeolite supercages that could be filled with HPA. The factors that could affect generating HPA inside zolite should be studied and optimized. Many other types of zeolite can also be studied for HPA trapping. The particles size of the Y zeolite was in micron scale which was too big to cast uniform composite membranes. Future study should focus on using zeolite with smaller particle size. It is also suggested to test the composite membranes and MEAs at temperatures above 100 ºC.

More work can be focused on studying the optimum MEA preparation conditions, such as hot pressing temperature, pressure, duration, and Nafion loading. Each membrane

may have its own optimum preparation conditions which are related to it mechanical and thermal conditions. Accelerated testing can be used to test the life time of the composite membranes.

8. References

1. Grove, W.R., *On Voltaic Series and the Combination of Gases by Platinum.* Phil. Mag., 1839. **XIV**: p. 127-130.
2. Mond, L. and C. Langer. *A New Form of Gas Battery*. in *Proceedings of the Royal Society of London*. 1889.
3. Mehta, V. and J.S. Cooper, *Review and analysis of PEM fuel cell design and manufacturing.* Journal of Power Sources, 2003. **114**(1): p. 32-53.
4. Mauritz, K.A. and R.B. Moore, *State of understanding of Nafion.* CHEMICAL REVIEWS, 2004. **104**(10): p. 4535-4585.
5. Larmine, J., *Fuel Cell Systems Explained*. 2 ed. 2003: SAE International.
6. Thomas, S., *Fuel Cells, Green Power*. 1999: United States Department of Energy.
7. Barbir, F., *PEM Fuel Cells: Theory and Practice* 2005: Academic Press.
8. Shiraishi, M., et al., *Hydrogen storage in single-walled carbon nanotube bundles and peapods.* Chemical Physics Letters, 2002. **358**(3-4): p. 213-218.
9. Wang, Q.K., et al., *Hydrogen storage by carbon nanotube and their films under ambient pressure.* International Journal of Hydrogen Energy, 2002. **27**(5): p. 497-500.
10. Zhang, X.R., D.P. Cao, and J.F. Chen, *Hydrogen adsorption storage on single-walled carbon nanotube arrays by a combination of classical potential and density functional theory.* Journal of Physical Chemistry B, 2003. **107**(21): p. 4942-4950.

11. Anani, A., et al., *ALLOYS FOR HYDROGEN STORAGE IN NICKEL-HYDROGEN AND NICKEL METAL HYDRIDE BATTERIES.* Journal of Power Sources, 1994. **47**(3): p. 261-275.

12. Sakai, T., et al., *HYDROGEN STORAGE ALLOYS FOR NICKEL METAL HYDRIDE BATTERY.* Zeitschrift Fur Physikalische Chemie-International Journal of Research in Physical Chemistry & Chemical Physics, 1994. **183**: p. 333-346.

13. Chen, J., et al., *Hydrogen storage alloys with PuNi3-Type structure as metal hydride electrodes.* ELECTROCHEMICAL AND SOLID STATE LETTERS, 2000. **3**(6): p. 249-252.

14. Bogdanovic, B. and M. Schwickardi, *Ti-doped NaAlH4 as a hydrogen-storage material - preparation by Ti-catalyzed hydrogenation of aluminum powder in conjunction with sodium hydride.* Applied Physics a-Materials Science & Processing, 2001. **72**(2): p. 221-223.

15. Grotthuss, C.J.D.v., Ann. Chim., 1806. **LVIII**(54).

16. Agmon, N., *The Grotthuss Mechanism.* Chemical Physics Letters, 1995. **244**(5-6): p. 456-462.

17. Kreuer, K.D., A. Rabenau, and W. Weppner, *Vehicle Mechanism, a New Model for the Interpretation of the Conductivity of Fast Proton Conductors.* Angewandte Chemie-International Edition in English, 1982. **21**(3): p. 208-209.

18. Yi, B., *Fuel cells-Theory, Techniques, and Applications (in Chinese)*. 2003: Chemical Industry Press.

19. Zhang, J.L., et al., *High temperature PEM fuel cells.* Journal of Power Sources, 2006. **160**(2): p. 872-891.

20. Bai, Z.W., M.F. Durstock, and T.D. Dang, *Proton conductivity and properties of sulfonated polyarylenethioether sulfones as proton exchange membranes in fuel cells.* Journal of Membrane Science, 2006. **281**(1-2): p. 508-516.

21. Zawodzinski, T.A., et al., *Water-Uptake by and Transport through Nafion(R) 117 Membranes.* Journal of the Electrochemical Society, 1993. **140**(4): p. 1041-1047.

22. Hakenjos, A., et al., *A PEM fuel cell for combined measurement of current and temperature distribution, and flow field flooding.* Journal of Power Sources, 2004. **131**(1-2): p. 213-216.

23. Natarajan, D. and T. Van Nguyen, *Three-dimensional effects of liquid water flooding in the cathode of a PEM fuel cell.* Journal of Power Sources, 2003. **115**(1): p. 66-80.

24. Dhar, H.P., et al., *PERFORMANCE STUDY OF A FUEL-CELL PT-ON-C ANODE IN PRESENCE OF CO AND CO2, AND CALCULATION OF ADSORPTION PARAMETERS FOR CO POISONING.* JOURNAL OF THE ELECTROCHEMICAL SOCIETY, 1986. **133**(8): p. 1574-1582.

25. Yang, C., et al., *Approaches and technical challenges to high temperature operation of proton exchange membrane fuel cells.* Journal of Power Sources, 2001. **103**(1): p. 1-9.

26. Adjemian, K.T., et al., *Silicon oxide Nafion composite membranes for proton-exchange membrane fuel cell operation at 80-140 degrees C.* JOURNAL OF THE ELECTROCHEMICAL SOCIETY, 2002. **149**(3): p. A256-A261.

27. Springer, T.E., T.A. Zawodzinski, and S. Gottesfeld, *POLYMER ELECTROLYTE FUEL-CELL MODEL.* JOURNAL OF THE ELECTROCHEMICAL SOCIETY, 1991. **138**(8): p. 2334-2342.

28. Gierke, T.D., G.E. Munn, and F.C. Wilson, *The Morphology in Nafion Perfluorinated Membrane Products, as Determined by Wide-Angle and Small-Angle X-Ray Studies.* Journal of Polymer Science Part B-Polymer Physics, 1981. **19**(11): p. 1687-1704.

29. Blake, N.P., et al., *Structure of hydrated Na-Nafion polymer membranes.* Journal of Physical Chemistry B, 2005. **109**(51): p. 24244-24253.

30. Seeliger, D., C. Hartnig, and E. Spohr, *Aqueous pore structure and proton dynamics in solvated Nafion membranes.* Electrochimica Acta, 2005. **50**(21): p. 4234-4240.

31. Haubold, H.G., et al., *Nano structure of NAFION: a SAXS study.* Electrochimica Acta, 2001. **46**(10-11): p. 1559-1563.

32. Rubatat, L., et al., *Characterization of ionomer membrane structure (NAFION) by small-angle X-ray scattering.* Journal De Physique Iv, 2002. **12**(PR6): p. 197-205.

33. Rollet, A.L., O. Diat, and G. Gebel, *A new insight into Nafion structure.* Journal of Physical Chemistry B, 2002. **106**(12): p. 3033-3036.

34. Divisek, J., et al., *A study of capillary porous structure and sorption properties of Nafion proton-exchange membranes swollen in water.* Journal of the Electrochemical Society, 1998. **145**(8): p. 2677-2683.

35. Cahan, B.D. and J.S. Wainright, *Ac-Impedance Investigations of Proton Conduction in Nafion(Tm).* Journal of the Electrochemical Society, 1993. **140**(12): p. L185-L186.

36. Hsu, W.Y., J.R. Barkley, and P. Meakin, *Ion Percolation and Insulator-to-Conductor Transition in Nafion Perfluorosulfonic Acid Membranes.* Macromolecules, 1980. **13**(1): p. 198-200.

37. Hsu, W.Y. and T.D. Gierke, *Ion-Transport and Clustering in Nafion Perfluorinated Membranes.* Journal of Membrane Science, 1983. **13**(3): p. 307-326.

38. Slade, R.C.T., A. Hardwick, and P.G. Dickens, *Investigation of H+ Motion in Nafion Film by Pulsed H-1-Nmr and Ac Conductivity Measurements.* Solid State Ionics, 1983. **9-10**(DEC): p. 1093-1098.

39. Yeo, R.S., *Ion Clustering and Proton Transport in Nafion Membranes and Its Applications as Solid Polymer Electrolyte.* JOURNAL OF THE ELECTROCHEMICAL SOCIETY, 1983. **130**(3): p. 533-538.

40. Wodzki, R., A. Narebska, and W.K. Nioch, *Percolation Conductivity in Nafion Membranes.* Journal of Applied Polymer Science, 1985. **30**(2): p. 769-780.

41. Cappadonia, M., et al., *Conductance of Nafion-117 Membranes as a Function of Temperature and Water-Content.* Solid State Ionics, 1995. **77**: p. 65-69.

42. Falk, M., *An infrared study of water in perfluorosulfonate (Nafion) membranes.* Canadian Journal of Chemistry, 1980. **58**(14): p. 1495-1501.

43. Deng, Q., et al., *TGA-FTi.r investigation of the thermal degradation of Nafion(R) and Nafion(R)/[silicon oxide]-based nanocomposites.* Polymer, 1998. **39**(24): p. 5961-5972.

44. de Almeida, S.H. and Y. Kawano, *Thermal behavior of Nafion membranes.* Journal of Thermal Analysis and Calorimetry, 1999. **58**(3): p. 569-577.

45. Schulze, M., et al., *XPS analysis of the degradation of Nafion.* Fresenius Journal of Analytical Chemistry, 1999. **365**(1-3): p. 106-113.

46. Paddison, S.J. and T.A. Zawodzinski Jr, *Molecular modeling of the pendant chain in Nafion(R).* Solid State Ionics, 1998. **113-115**: p. 333-340.

47. Paddison, S.J., R. Paul, and T.A. Zawodzinski, *A statistical mechanical model of proton and water transport in a proton exchange membrane.* Journal of the Electrochemical Society, 2000. **147**(2): p. 617-626.

48. Zhen, Y., et al., *Modeling of ion conductivity in Nafion membranes.* Front. Energy Power Eng. China, 2007. **1**(1): p. 58-66.

49. Deng, Q., R.B. Moore, and K.A. Mauritz, *Nafion (R) (SiO2, ORMOSIL, and dimethylsiloxane) hybrids via in situ sol-gel reactions: Characterization of fundamental properties.* Journal of Applied Polymer Science, 1998. **68**(5): p. 747-763.

50. Zoppi, R.A., I.V.P. Yoshida, and S.P. Nunes, *Hybrids of perfluorosulfonic acid ionomer and silicon oxide by sol-gel reaction from solution: Morphology and thermal analysis.* Polymer, 1998. **39**(6-7): p. 1309-1315.

51. Antonucci, P.L., et al., *Investigation of a direct methanol fuel cell based on a composite Nafion (R)-silica electrolyte for high temperature operation.* Solid State Ionics, 1999. **125**(1-4): p. 431-437.

52. Doyle, M., S.K. Choi, and G. Proulx, *High-temperature proton conducting membranes based on perfluorinated ionomer membrane-ionic liquid composites.* Journal of the Electrochemical Society, 2000. **147**(1): p. 34-37.

53. Miyake, N., J.S. Wainright, and R.F. Savinell, *Evaluation of a sol-gel derived Nafion/silica hybrid membrane for polymer electrolyte membrane fuel cell applications - II. Methanol uptake and methanol permeability.* Journal of the Electrochemical Society, 2001. **148**(8): p. A905-A909.

54. Miyake, N., J.S. Wainright, and R.F. Savinell, *Evaluation of a sol-gel derived Nafion/silica hybrid membrane for proton electrolyte membrane fuel cell applications - I. Proton conductivity and water content.* Journal of the Electrochemical Society, 2001. **148**(8): p. A898-A904.

55. Staiti, P., et al., *Hybrid Nafion-silica membranes doped with heteropolyacids for application in direct methanol fuel cells.* Solid State Ionics, 2001. **145**(1-4): p. 101-107.

56. Gierke, T.D. and W.Y. Hsu, *The Cluster-Network Model of Ion Clustering in Perfluorosulfonated Membranes*, in *Perfluorinated Ionomer Membranes*, A. Eisenberg and H.L. Yeager, Editors. 1982, American Chemical Society: Washington, D. C.

57. Choi, P., N.H. Jalani, and R. Datta, *Thermodynamics and proton transport in Nafion - II. Proton diffusion mechanisms and conductivity.* JOURNAL OF THE ELECTROCHEMICAL SOCIETY, 2005. **152**(3): p. E123-E130.

58. Watanabe, M., et al., *Self-humidifying polymer electrolyte membranes for fuel cells.* JOURNAL OF THE ELECTROCHEMICAL SOCIETY, 1996. **143**(12): p. 3847-3852.

59. Watanabe, M., H. Uchida, and M. Emori, *Polymer electrolyte membranes incorporated with nanometer-size particles of Pt and/or metal-oxides: Experimental analysis of the self-humidification and suppression of gas-crossover in fuel cells.* Journal of Physical Chemistry B, 1998. **102**(17): p. 3129-3137.

60. Watanabe, M., H. Uchida, and M. Emori, *Analyses of self-humidification and suppression of gas crossover in Pt-dispersed polymer electrolyte membranes for fuel cells.* JOURNAL OF THE ELECTROCHEMICAL SOCIETY, 1998. **145**(4): p. 1137-1141.

61. Mauritz, K.A. and R.M. Warren, *MICROSTRUCTURAL EVOLUTION OF A SILICON-OXIDE PHASE IN A PERFLUOROSULFONIC ACID IONOMER BY AN INSITU SOL-GEL REACTION .1. INFRARED SPECTROSCOPIC STUDIES.* MACROMOLECULES, 1989. **22**(4): p. 1730-1734.

62. Mauritz, K.A. and I.D. Stefanithis, *MICROSTRUCTURAL EVOLUTION OF A SILICON-OXIDE PHASE IN A PERFLUOROSULFONIC ACID IONOMER BY AN INSITU SOL-GEL REACTION .2. DIELECTRIC-RELAXATION STUDIES.* MACROMOLECULES, 1990. **23**(5): p. 1380-1388.

63. Tian, H. and O. Savadogo, *Silicotungstic Acid Nafion Composite membrane for proton-exchange membrane fuel cell operation at high temperature.* Journal of New Materials for Electrochemical Systems, 2006. **9**(1): p. 61-71.

64. Penner, R.M. and C.R. Martin, *Ion Transporting Composite Membranes .1. Nafion-Impregnated Gore-Tex.* Journal of the Electrochemical Society, 1985. **132**(2): p. 514-515.

65. Nouel, K.M. and P.S. Fedkiw, *Nafion (R)-based composite polymer electrolyte membranes.* Electrochimica Acta, 1998. **43**(16-17): p. 2381-2387.

66. Yu, *Nafion/PTFE composite membranes for fuel cell applications.* JOURNAL OF POLYMER RESEARCH-TAIWAN, 2004. **11**(3): p. 217-224.

67. Ahn, S.Y., et al., *Properties of the reinforced composite membranes formed by melt soluble ion conducting polymer resins for PEMFCs.* Electrochimica Acta, 2004. **50**(2-3): p. 571-575.

68. Tang, H.L., et al., *Fabrication and characterization of PFSI/ePTFE composite proton exchange membranes of polymer electrolyte fuel cells.* Electrochimica Acta, 2007. **52**(16): p. 5304-5311.

69. Jardine, S. and J.I.B. Wilson, *Plasma surface modification of ePTFE vascular grafts.* Plasma Processes and Polymers, 2005. **2**(4): p. 328-333.

70. Njatawidjaja, E., et al., *Hydrophilic modification of expanded polytetrafluoroethylene (ePTFE) by atmospheric pressure glow discharge (APG) treatment.* Surface & Coatings Technology, 2006. **201**(3-4): p. 699-706.

71. Tu, C.Y., et al., *Expanded poly(tetrafluoroethylene) membrane surface modification using acetylene/nitrogen plasma treatment.* European Polymer Journal, 2005. **41**(10): p. 2343-2353.

72. Kang, E.T. and Y. Zhang, *Surface modification of fluoropolymers via molecular design.* Advanced Materials, 2000. **12**(20): p. 1481-1494.

73. Huang, L.N., et al., *Nafion/PTFE/silicate composite membranes for direct methanol fuel cells.* Journal of Power Sources, 2006. **161**(2): p. 1096-1105.

74. Zhu, X.B., et al., *A novel PTFE-reinforced multilayer self-humidifying composite membrane for PEM fuel cells.* ELECTROCHEMICAL AND SOLID STATE LETTERS, 2006. **9**(2): p. A49-A52.

75. Wang, L., et al., *Pt/SiO2 catalyst as an addition to Nafion/PTFE self-humidifying composite membrane.* Journal of Power Sources, 2006. **161**(1): p. 61-67.

76. Zhang, Y., et al., *Fabrication and characterization of a PTFE-reinforced integral composite membrane for self-humidifying PEMFC.* Journal of Power Sources, 2007. **165**(2): p. 786-792.

77. Liu, F., et al., *Development of novel self-humidifying composite membranes for fuel cells.* Journal of Power Sources, 2003. **124**(1): p. 81-89.

78. Arcella, V., C. Troglia, and A. Ghielmi, *Hyflon ion membranes for fuel cells.* Industrial & Engineering Chemistry Research, 2005. **44**(20): p. 7646-7651.

79. Gordano, A., V. Arcella, and E. Drioli, *New HYFLON AD composite membranes and AFM characterization.* Desalination, 2004. **163**(1-3): p. 127-136.

80. Sperling, L.H., *Introduction to Physical Polymer Science*. 4 ed. 2005: Wiley-Interscience.

81. Smitha, B., S. Sridhar, and A.A. Khan, *Solid polymer electrolyte membranes for fuel cell applications - a review.* Journal of Membrane Science, 2005. **259**(1-2): p. 10-26.

82. Yang, H., X. Qian, and J. Suo, *Proton exchange membranes for fuel cells.* Chinese chemical society, 2003. **66**.

83. Rikukawa, M. and K. Sanui, *Proton-conducting polymer electrolyte membranes based on hydrocarbon polymers.* Progress in Polymer Science, 2000. **25**(10): p. 1463-1502.

84. Alberti, G., et al., *Polymeric proton conducting membranes for medium temperature fuel cells (110-160[deg]C).* Journal of Membrane Science, 2001. **185**(1): p. 73-81.

85. Kaliaguine, S., *Properties of SPEEK based PEMs for fuel cell application.* CATALYSIS TODAY, 2003. **82**(1-4): p. 213-222.

86. Dai, Y., et al., *Thin film composite (TFC) membranes with improved thermal stability from sulfonated poly(phthalazinone ether sulfone ketone) (SPPESK).* Journal of Membrane Science, 2002. **207**(2): p. 189-197.

87. Kim, D.S., et al., *Preparation and characterization of sulfonated poly(phthalazinone ether sulfone ketone) (SPPESK)/Silica hybrid membranes for direct methanol fuel cell applications.* Macromolecular Research, 2004. **12**(4): p. 413-421.

88. Genova-Dimitrova, P., et al., *Ionomeric membranes for proton exchange membrane fuel cell (PEMFC): sulfonated polysulfone associated with phosphatoantimonic acid.* Journal of Membrane Science, 2001. **185**(1): p. 59-71.

89. Manea, C. and M. Mulder, *Characterization of polymer blends of polyethersulfone/sulfonated polysulfone and polyethersulfone/sulfonated polyetheretherketone for direct methanol fuel cell applications.* Journal of Membrane Science, 2002. **206**(1-2): p. 443-453.

90. Ericson, H., et al., *Confocal Raman spectroscopic investigations of fuel cell tested sulfonated styrene grafted poly(vinylidene fluoride) membranes.* JOURNAL OF THE ELECTROCHEMICAL SOCIETY, 2002. **149**(2): p. A206-A211.

91. Saxena, A., B.P. Tripathi, and V.K. Shahi, *Sulfonated poly(styrene-co-maleic anhydride)-poly(ethylene glycol)-silica nanocomposite polyelectrolyte membranes for fuel cell applications.* Journal of Physical Chemistry B, 2007. **111**(43): p. 12454-12461.

92. Aoki, M., et al., *Durability of sulfonated polyimide membrane evaluated by long-term polymer electrolyte fuel cell operation.* JOURNAL OF THE ELECTROCHEMICAL SOCIETY, 2006. **153**(6): p. A1154-A1158.

93. Meyer, G., et al., *Degradation of sulfonated polyimide membranes in fuel cell conditions.* Journal of Power Sources, 2006. **157**(1): p. 293-301.

94. Woo, Y., et al., *Synthesis and characterization of sulfonated polyimide membranes for direct methanol fuel cell.* Journal of Membrane Science, 2003. **220**(1-2): p. 31-45.

95. Kim, Y.S., et al., *Fabrication and characterization of heteropolyacid (H3PW12O40)/directly polymerized sulfonated poly(arylene ether sulfone) copolymer composite membranes for higher temperature fuel cell applications.* Journal of Membrane Science, 2003. **212**(1-2): p. 263-282.

96. Krishnan, N.N., et al., *Synthesis and characterization of sulfonated poly(ether sulfone) copolymer membranes for fuel cell applications.* Journal of Power Sources, 2006. **158**(2): p. 1246-1250.

97. Li, X.F., H. Na, and H. Lu, *Synthesis of a novel sulfonated poly(ether ether sulfone)s used as proton exchange membrane fuel cell (PEMFC).* CHEMICAL JOURNAL OF CHINESE UNIVERSITIES-CHINESE, 2004. **25**(11): p. 2157-2160.

98. Kreuer, K.D., *On the development of proton conducting polymer membranes for hydrogen and methanol fuel cells.* Journal of Membrane Science, 2001. **185**(1): p. 29-39.

99. Li, Q., et al., *PBI-Based Polymer Membranes for High Temperature Fuel Cells – Preparation, Characterization and Fuel Cell Demonstration* Fuel Cells, 2004. **4**(3): p. 147-159.

100. Ma, Y.L., et al., *Conductivity of PBI membranes for high-temperature polymer electrolyte fuel cells.* Journal of the Electrochemical Society, 2004. **151**(1): p. A8-A16.

101. Li, Q., et al. *Proton Conductivity and Operational Features of PBI-based Membranes*. in *Proceedings of the 26th Risø International Symposium on Materials Science: Solid State Electrochemistry*. 2005. Roskilde, Denmark.

102. Dimitrova, P., et al., *Transport properties of ionomer composite membranes for direct methanol fuel cells.* Journal of Electroanalytical Chemistry, 2002. **532**(1-2): p. 75-83.

103. Arico, A.S., et al., *FTIR spectroscopic investigation of inorganic fillers for composite DMFC membranes.* Electrochemistry Communications, 2003. **5**(10): p. 862-866.

104. Tang, H., et al., *Self-assembled Nafion-silica nanoparticles for elevated-high temperature polymer electrolyte membrane fuel cells.* Electrochemistry Communications, 2007. **9**(8): p. 2003-2008.

105. Shaw, D.J., *Introduction to colloid & surface chemistry*. 1992: Butterworth-Heinemann.

106. Tamura, H., et al., *Surface hydroxyl site densities on metal oxides as a measure for the ion-exchange capacity.* Journal of Colloid and Interface Science, 1999. **209**(1): p. 225-231.

107. Krishnan, L., *Composite membranes for high temperature and low relative humidity operation in proton exchange membrane fuel cells*, in *Department of chemistry*. 2005, Princeton university.

108. Mauritz, K.A., *Organic-inorganic hybrid materials: perfluorinated ionomers as sol-gel polymerization templates for inorganic alkoxides.* Materials Science and Engineering: C, 1998. **6**(2-3): p. 121-133.

109. Wilkie, C.A., J.R. Thomsen, and M.L. Mittleman, *INTERACTION OF POLY (METHYL-METHACRYLATE) AND NAFIONS.* Journal of Applied Polymer Science, 1991. **42**(4): p. 901-909.

110. Sahu, A.K., et al., *A sol-gel modified alternative nafion-silica composite membrane for polymer electrolyte fuel cells.* JOURNAL OF THE ELECTROCHEMICAL SOCIETY, 2007. **154**(2): p. B123-B132.

111. Jiang, R.C., H.R. Kunz, and J.M. Fenton, *Composite silica/Nafion (R) membranes prepared by tetraethylorthosilicate sol-gel reaction and solution casting for direct methanol fuel cells.* Journal of Membrane Science, 2006. **272**(1-2): p. 116-124.

112. Baronetti, G., et al., *Heteropolyacid-based catalysis. Dawson acid for MTBE synthesis in gas phase.* Applied Catalysis a-General, 1998. **172**(2): p. 265-272.

113. Izumi, Y., K. Hisano, and T. Hida, *Acid catalysis of silica-included heteropolyacid in polar reaction media.* Applied Catalysis a-General, 1999. **181**(2): p. 277-282.

114. Jansen, R.J.J., et al., *RECENT (1987-1993) DEVELOPMENTS IN HETEROPOLYACID CATALYSTS IN ACID-CATALYZED REACTIONS AND OXIDATION CATALYSIS.* Recueil Des Travaux Chimiques Des Pays-Bas-Journal of the Royal Netherlands Chemical Society, 1994. **113**(3): p. 115-135.

115. Nomiya, K., M. Miwa, and Y. Sugaya, *CATALYSIS BY HETEROPOLYACID .7. CATALYTIC-OXIDATION OF CYCLOHEXANOL BY DODECAMOLYBDATE.* Polyhedron, 1984. **3**(5): p. 607-610.

116. Nomiya, K., M. Miwa, and Y. Sugaya, *CATALYSIS BY HETEROPOLYACID .6. ASYMMETRIC POLYCONDENSATION OF BENZYL ALCOHOL TO OPTICALLY-ACTIVE POLYBENZYL INITIATED BY BRUCINE-INDUCED CHIRAL DIPHOSPHOOCTADECAMOLYBDIC ACID.* Polyhedron, 1984. **3**(3): p. 381-383.

117. Nomiya, K., H. Saijoh, and M. Miwa, *CATALYSIS BY HETEROPOLYACID .5. CATALYTIC ALKYLATION OF TOLUENE BY MIXED-COORDINATION TYPE,*

H4[SIMO12-NWNO40], HETEROPOLYACID. Bulletin of the Chemical Society of Japan, 1980. **53**(12): p. 3719-3720.

118. Nomiya, K., S. Sasa, and M. Miwa, *CATALYSIS BY HETEROPOLYACID .4. REACTIVE FORM OF 12-MOLYBDOSILICATE CATALYST ON FRIEDEL-CRAFTS-TYPE REACTION.* Chemistry Letters, 1980(9): p. 1075-1076.

119. Nomiya, K., Y. Sugaya, and M. Miwa, *CATALYSIS BY HETEROPOLYACID .3. ACYLATION AND SULFONYLATION OF AROMATIC-COMPOUNDS CATALYZED BY KEGGIN-STRUCTURE HETEROPOLYACIDS.* Bulletin of the Chemical Society of Japan, 1980. **53**(11): p. 3389-3390.

120. Nomiya, K., T. Ueno, and M. Miwa, *CATALYSIS BY HETEROPOLYACID .1. POLYMERIZATION REACTION OF BENZYL ALCOHOLS.* Bulletin of the Chemical Society of Japan, 1980. **53**(3): p. 827-828.

121. Colomban, P., *Proton conductors: solids, membranes, and gels: materials and devices*. 1992: Cambridge University Press.

122. Mioc, U.B., et al., *Thermally-Induced Phase-Transformations of 12-Tungstophosphoric Acid 29-Hydrate - Synthesis and Characterization of Pw8o26-Type Bronzes.* Journal of Materials Science, 1994. **29**(14): p. 3705-3718.

123. Bardin, B.B., et al., *Acidity of Keggin-type heteropolycompounds evaluated by catalytic probe reactions, sorption microcalorimetry, and density functional quantum chemical calculations.* Journal of Physical Chemistry B, 1998. **102**(52): p. 10817-10825.

124. Gomez-Romero, P., J.A. Asensio, and S. Borros, *Hybrid proton-conducting membranes for polymer electrolyte fuel cells phosphomolybdic acid doped*

poly(2,5-benzimidazole)-(ABPBI-H3PMo12O40). Electrochimica Acta, 2005. **50**(24): p. 4715-4720.

125. Kreuer, K.D., *Proton conductivity: Materials and applications.* Chemistry of Materials, 1996. **8**(3): p. 610-641.

126. Nakamura, O., et al., *HIGH-CONDUCTIVITY SOLID PROTON CONDUCTORS - DODECAMOLYBDOPHOSPHORIC ACID AND DODECATUNGSTOPHOSPHORIC ACID CRYSTALS.* Chemistry Letters, 1979(1): p. 17-18.

127. Tazi, B. and O. Savadogo, *Parameters of PEM fuel-cells based on new membranes fabricated from Nafion(R), silicotungstic acid and thiophene.* Electrochimica Acta, 2000. **45**(25-26): p. 4329-4339.

128. Kim, H.J., Y.G. Shul, and H. Han, *Synthesis of heteropolyacid (H3PW12O40)/SiO2 nanoparticles and their catalytic properties.* Applied Catalysis a-General, 2006. **299**: p. 46-51.

129. Ponce, M.L., et al., *Reduction of methanol permeability in polyetherketone-heteropolyacid membranes.* Journal of Membrane Science, 2003. **217**(1-2): p. 5-15.

130. Shao, Z.-G., P. Joghee, and I.M. Hsing, *Preparation and characterization of hybrid Nafion-silica membrane doped with phosphotungstic acid for high temperature operation of proton exchange membrane fuel cells.* Journal of Membrane Science, 2004. **229**(1-2): p. 43-51.

131. Park, M.W., et al., *Heteropolyacid (H3PW12O40) incorporated solid polymer electrolyte for PEMFC.* Denki Kagaku, 1996. **64**(6): p. 743-748.

132. Stangar, U.L., et al., *Proton-conducting sol-gel hybrids containing heteropoly acids.* Solid State Ionics, 2001. **145**(1-4): p. 109-118.

133. Kozhevnikov, I.V., *Catalysis by heteropoly acids and multicomponent polyoxometalates in liquid-phase reactions.* CHEMICAL REVIEWS, 1998. **98**(1): p. 171-198.

134. Ghanbari-Siahkali, A., et al., *The acidity and catalytic activity of heteropoly acid on MCM-41 investigated by MAS NMR, FTIR and catalytic tests.* Applied Catalysis a-General, 2000. **192**(1): p. 57-69.

135. He, N.Y., et al., *Immobilization of tungstophosphoric acid in mesoporous silica*, in *Nanoporous Materials Iv*. 2005. p. 177-182.

136. Tatsumisago, M., K. Kishida, and T. Minami, *PREPARATION AND PROTON-CONDUCTION OF SILICA-GELS CONTAINING HETEROPOLY ACIDS.* Solid State Ionics, 1993. **59**(3-4): p. 171-174.

137. Mioc, U.B., et al., *Structure and proton conductivity of 12-tungstophosphoric acid doped silica.* Solid State Ionics, 1997. **97**(1-4): p. 239-246.

138. Shi, C.F., et al., *Synthesis, characterization, and catalytic properties of SiPW-X mesoporous silica with heteropolyacid encapsulated into their framework.* European Journal of Inorganic Chemistry, 2005(23): p. 4801-4807.

139. *Handbook of Zeolite Science and Technology*, ed. S.M. Auerbach, K.A. Carrado, and P.K. Dutta. 2003, New York: CRC Press.

140. Cronstedt, A.A.F., *Handl. Stockholm.* 1756. **18**: p. 120-130.

141. *Introduction to Zeolite Science and Technology*, ed. H.v. Bekkum, et al. 2001, Amsterdam: Elsevier.

142. Kreuer, K.D., W. Weppner, and A. Rabenau, *Proton Conduction in Zeolites.* Materials Research Bulletin, 1982. **17**(4): p. 501-509.

143. Ahmad, M.I., et al., *Synthesis and proton conductivity of heteropolyacids loaded Y-zeolite as solid proton conductors for fuel cell applications.* Microporous and Mesoporous Materials, 2006. **91**(1-3): p. 296-304.

144. Mukai, S.R., et al., *Preparation of encaged heteropoly acid catalyst by synthesizing 12-molybdophosphoric acid in the supercages of Y-type zeolite.* Applied Catalysis a-General, 1997. **165**(1-2): p. 219-226.

145. Mukai, S.R., et al., *Key factors for the encapsulation of Keggin-type heteropoly acids in the supercages of Y-type zeolite.* Chemical Engineering Science, 2001. **56**(3): p. 799-804.

146. Zhao, D.Y., et al., *Nonionic triblock and star diblock copolymer and oligomeric surfactant syntheses of highly ordered, hydrothermally stable, mesoporous silica structures.* Journal of the American Chemical Society, 1998. **120**(24): p. 6024-6036.

147. Beck, J.S., et al., *A NEW FAMILY OF MESOPOROUS MOLECULAR-SIEVES PREPARED WITH LIQUID-CRYSTAL TEMPLATES.* Journal of the American Chemical Society, 1992. **114**(27): p. 10834-10843.

148. Mukai, S.R., et al., *Improvement of the preparation method of "ship-in-the-bottle" type 12-molybdophosphoric acid encaged Y-type zeolite catalysts.* Applied Catalysis a-General, 2003. **256**(1-2): p. 107-113.

149. Qi, Z.G. and A. Kaufman, *Activation of low temperature PEM fuel cells.* Journal of Power Sources, 2002. **111**(1): p. 181-184.

150. Qi, Z.G. and A. Kaufman, *Quick and effective activation of proton-exchange membrane fuel cells.* Journal of Power Sources, 2003. **114**(1): p. 21-31.

151. Ramani, V., H.R. Kunz, and J.M. Fenton, *Investigation of Nafion (R)/HPA composite membranes for high temperature/low relative humidity PEMFC operation.* Journal of Membrane Science, 2004. **232**(1-2): p. 31-44.

152. Ostrovskii, D.I., A.M. Brodin, and L.M. Torell, *Raman study of water in Nafion-117 membranes.* Solid State Ionics, 1996. **85**(1-4): p. 323-327.

153. Gruger, A., et al., *Nanostructure of Nafion (R) membranes at different states of hydration - An IR and Raman study.* Vibrational Spectroscopy, 2001. **26**(2): p. 215-225.

154. Falk, M., *AN INFRARED STUDY OF WATER IN PERFLUOROSULFONATE (NAFION) MEMBRANES.* Canadian Journal of Chemistry-Revue Canadienne De Chimie, 1980. **58**(14): p. 1495-1501.

155. Hinatsu, J.T., M. Mizuhata, and H. Takenaka, *Water uptake of perfluorosulfonic acid membranes from liquid water and water vapor.* Journal of the Electrochemical Society, 1994. **141**(6): p. 1493-1498.

156. Davidovic, M. and U.B. Mioc, *Heteropolyacids as protonic conductors*, in *Advanced Materials for High Technology Applications*. 1996. p. 99-108.

157. Song, S., et al., *The effect of the MEA preparation procedure on both ethanol crossover and DEFC performance.* Journal of Power Sources, 2005. **140**(1): p. 103-110.

158. Nakrumpai, B., K. Pruksathorn, and P. Piumsomboon, *Optimum condition of membrane electrode assembly fabrication for PEM fuel cells.* Korean Journal of Chemical Engineering, 2006. **23**(4): p. 570-575.

159. Frey, T. and M. Linardi, *Effects of membrane electrode assembly preparation on the polymer electrolyte membrane fuel cell performance.* Electrochimica Acta, 2004. **50**(1): p. 99-105.

160. Zhang, J., et al., *Effects of hot pressing conditions on the performances of MEAs for direct methanol fuel cells.* Journal of Power Sources, 2007. **165**(1): p. 73-81.

161. Tu, C.Y., et al., *Hydrophilic surface-grafted poly(tetrafluoroethylene) membranes using in pervaporation dehydration processes.* Journal of Membrane Science, 2006. **274**(1-2): p. 47-55.

162. Kim, S.R., *Surface modification of poly(tetrafluoroethylene) film by chemical etching, plasma, and ion beam treatments.* Journal of Applied Polymer Science, 2000. **77**(9): p. 1913-1920.

163. Ji, L.Y., et al., *Surface modification of poly(tetrafluoroethylene) film by consecutive graft copolymerization with 4-vinylaniline and aniline.* Macromolecules, 1999. **32**(24): p. 8183-8188.

164. Inagaki, N., S. Tasaka, and Y. Goto, *Surface modification of poly(tetrafluoroethylene) film by plasma graft polymerization of sodium vinylsulfonate.* Journal of Applied Polymer Science, 1997. **66**(1): p. 77-84.